АУТОМАТИКА
/
AUTOMATION

(АУ/AUI)

Ublažavanje četeringa digitalnog regulatora promenljive strukture za linearne sisteme

Boban Veselić, *Senior Member, IEEE*, Čedomir Milosavljević, Branislava Peruničić-Draženović, *Senior Member, IEEE*, Senad Huseinbegović, *Member, IEEE*, Milutin Petronijević, *Member, IEEE*

***Apstrakt*—U radu se ispituje mogućnost smanjenja četeringa u kliznom režimu jednog digitalnog regulatora promenljive strukture namenjenog za linearne sisteme sa ograničenim upravljačkim ulazom. Nelinearna diskontinualna funkcija relejnog tipa, koja je sastivni deo originalnog zakona upravljanja, zamenjena je adekvatnom kontinualnom aproksimacijom. Analizirana je stabilnost modifikovanog sistema i istaknute su uočene osobine sistema. Dobijeni teorijski zaključci su potvrđeni simulacionom proverom na numeričkom primeru.**

***Ključne reči*—Sistemi upravljanja promenljive strukture, diskretni klizni režimi, četering, kompenzacija poremećaja.**

I. Uvod

Sistemi upravljanja promenljive strukture (SUPS) [1] u radnom kliznom režimu (KR) [2] su jedna od popularnih robusnih nelinearnih tehnika upravljanja, teorijski invarijantni, u idealnom KR, na parametarske i spoljne poremećaje koji deluju u kanalu upravljanja [3]. Za ovu osobinu je potrebno diskontinualno upravljanje na kliznoj površi sa mogućnošću ostvarivanja beskonačne frekvencije preključivanja upravljačkih struktura. Iz tih razloga, zakoni upravljanja u KR sadrže diskontinualnu komponentu, najčešće relejnog tipa. U praktičnim realizacijama se osobina invarijantnosti redukuje u veliku robusnost sistema, upravo zbog realno ostvarljive visoke, ali konačne frekvencije preključivanja usled neidealnosti prekidačkih elemenata.

Glavna prepreka široke primene SUPS sa KR je pojava visokofrekvencijskih oscilacija u KR, poznatih kao četering, što je neprihvatljivo u nekim sistemima poput mehaničkih. Ovaj neželjeni efekat nastaje usled diskontinualne prirode upravljanja i postojanja neizbežne nemodelovane (parazitne) dinamike, koja se pobuđuje takvim upravljanjem i generiše četering.

U literaturi su predložene različite metode za ublažavanje četeringa u KR. Jedan od prvih pristupa [4] podrazumeva da se diskontinualna signum funkcija u upravljanju zameni kontinualnom nelinearnošću tipa zasićenja sa velikim pojačanjem, što za posledicu ima smanjenje robusnosti budući da pojačanje u sistemu postaje konačno. Drugi pristup je uvođenje opservera stanja [5], preko koga se zatvara petlja u kojoj ne egzistira četering. Petlja sa opserverom je idealna (nema nemodelovanu dinamiku) te nema četeringa u njoj pa služi kao bajpas za četering. Međutim, varijacije parametara sistema narušavaju robusnost i performanse sistema. Klizni režimi višeg reda (KRVR) [6], noviji pristup dosta popularan poslednju deceniju, su nastali u nastojanju rešavanja problema četeringa. Za nastanak KR r-tog reda potreno je da relativni red sistema u odnosu na kliznu promenljivu bude r, pa se tek u r-tom izvodu klizne promenljive javlja diskontinualno upravljanje. Naročitu pažnju je privukao tzv. super-twisting algoritam (STA) [6], razvijen za kontinualne sisteme sa jednim ulazom, koji ostvaruje KR drugog reda. Međutim, na osnovu analiza sprovedenim u [7-9] može se zaključiti da KRVR mogu ostvariti manji četering u odnosu na konvencionalne KR samo u sistemima sa dovoljno brzim aktuatorima. Dodatna redukcija četeringa se može ostvariti adekvatnim podešavanjem kontinualne aproksimacije signum funkcije u regulatorima promenljive strukture [10].

Digitalna implementacija upravljačkih algoritama uz pomoć mikroprocesora je otvorila analizu KR u vremenski diskretnom domenu [11]-[15]. Pokazano je da je samo u nominalnom sistemu moguće ostvariti diskretni KR, i pri tome upravljanje ne mora biti diskontinualno. U svim ostalim slučajevima moguće je ostvariti samo tzv. kvazi-KR (KKR), gde se kretanje sistema odvija u nekoj bliskoj okolini oko klizne površi. Kako vremenski diskretno upravljanje unosi dodatno kašnjenje u sistem, četering je izraženiji u slučaju diskretnih KR. Jedan od načina da se eliminiše ova pojava je da se u okolini klizne površi primeni linearno upravljanje [16], što će naravno dovesti do gubitka robusnosti sistema u toj zoni. U slučaju primene ove strategije, potrebno je izvršiti eventualnu kompenzaciju poremećaja u sistemu u cilju povećanja tačnosti. Za sporopromenljive poremećaje, kompenzaciona upravljanja su predložena u [17-19], koja imaju linearni karakter. U radu [20] je predložen digitalni regulator promenljive strukture sa nelinearnim kompezatorom poremećaja za linearne sisteme sa ograničem upravljačkim signalom. Predložena upravljačka struktura podseća na diskretizovanu varijantu STA upravljanja [21], ali indukuje manji četering.

U ovom radu se upravo polazi od digitalnog regulatora promenljive strukture [20], čije je upravljanje u okolini klizne

Boban Veselić i Milutin Petronijević – Elektronski fakultet, Univerzitet u Nišu, Niš, Srbija (e-mail: boban.veselic@elfak.ni.ac.rs, milutin.petronijevic@elfak.ni.ac.rs).

Čedomir Milosavljević – Elektrotehnički fakultet, Univerzitet u Istočnom Sarajevu, Istočno Sarajevo, Bosna i Hercegovina (e-mail: cedomir.milosavljevic@elfak.ni.ac.rs).

Branislava Peruničić-Draženović i Senad Huseinbegović – Elektrotehnički fakultet, Univerzitet u Sarajevu, Sarajevo, Bosna i Hercegovina (e-mails: brana_p@hotmail.com, shuseinbegovic@etf.unsa.ba).

Ovaj rad je podržan od strane Ministarstva prosvete, nauke i tehnološkog razvoja Republike Srbije.

površi linearno i potpomognuto je kompenzacionim članom. Dopunska kompenzaciona upravljačka komponenta se formira nelinearnom estimacijom poremećaja, koja se dobija integracijom signuma klizne promenljive. Kako kompenzacioni deo regulatora ipak sadrži diskontinualnu funkciju, može doći do indukovanja četeringa. Iz tih razloga, u ovom radu se ispituje primena određene kontinualne aproksimacije signum funkcije sa ciljem ublažavanja četeringa, kao i njeni efekti na performanse sistema u pogledu stabilnosti i tačnosti. Određena je oblast konvergencije modifikovanog upravljačkog sistema i pokazano da se adekvatnim izborom parametra kontinualne aproksimacije može suziti širina kvazi-klizne oblasti u slučaju sporopromenljivih poremećaja u odnosu na originalni algoritam. Dobijeni teorijski rezultati su verifikovani simulacionim ispitivanjima.

II. Opis digitalnog regulatora promenljive strukture

Posmatra se linearni kontinualni sistem upravljanja koji je opisan modelom u prostoru stanja

$$\dot{x}(t) = Ax(t) + b(u(t) + d(t)), \quad (1)$$

gde je $x \in \mathbb{R}^n$ vektor stanja, $u \in \mathbb{R}$ je upravljački signal, $A \in \mathbb{R}^{n\times n}$ i $b \in \mathbb{R}^{n\times 1}$ su matrice stanja i ulaza, respektivno. Na sistem deluje ograničeni poremećaj d, $|d(t)| \le d_0 < \infty$, koji zadovoljava uslove poklapanja, tj. deluje u prostoru upravljanja. Za realizaciju digitalnog regulatora potrebno je izvršiti vremensku diskretizaciju modela (1). Vremenski diskretni model sistema je oblika

$$x_{k+1} = A_d x_k + b_d(u_k + d_k), \quad (2)$$

$$A_d = e^{AT},\ b_d = \int_0^T e^{At} B dt, \quad (3)$$

pod pretpostavkom da je perioda diskretizacije T dovoljno mala i da su poremećaji u sistemu sporopromenljivi. Tada se poremećaj može smatrati konstantnim između dva uzastopna trenutka odabiranja, što za posledicu ima očuvanje uslova poklapanja u diskretnom domenu.

Da bi se ostvario KR željene dinamike potrebno je da se najpre dizajnira odgovarajuća klizna površ, a da se potom nađe upravljanje koje uspostavlja KR. Kretanje sistema se tada može dekomponovati na dve faze: fazu dosezanja klizne površi i fazu klizanja po datoj površi. Za svaku od ovih faza vezana je odgovarajuća upravljačka komponenta.

Pristup koji omogućava jasno razdvajanje komponenti upravljanja za dosezanje i klizanje bazira se na korišćenju diskretnog modela sistema koji je dobijen primenom δ-transformacije, [16]. Matematički model sistema (1) u δ-domenu se dobija korišćenjem modela (2) na sledeći način.

$$\delta x_k = \frac{x_{k+1}-x_k}{T} = A_\delta x_k + b_\delta(u_k + d_k), \quad (4)$$

$$A_\delta = (A_d - I_n)/T,\ b_\delta = b_d/T. \quad (5)$$

KR treba organizovati po površi $s_{\delta,k} = 0$ u prostoru stanja, gde se klizna promenljiva u δ-domenu definiše kao

$$s_{\delta,k} = c_\delta x_k,\ c_\delta b_\delta = 1. \quad (6)$$

Željene sopstvene vrednosti sistema su definisane spektrom u kontinualnom domenu

$$\lambda = [\lambda_1 \quad \lambda_2 \quad \cdots \quad \lambda_{n-1} \quad 0], \quad (7)$$

pri čemu nulta sopstvena vrednost ukazuje da je dinamika sistema u kliznom režimu redukovanog reda, tj. $n-1$ reda. Nenulte sopstvenene vrednosti se mogu preslikati u δ-domen na osnovu (5) kao $\lambda_{\delta i} = (e^{\lambda_i T} - 1)/T$, $i = 1, \cdots, n-1$, dok nulta sopstvena vrednost ostaje nepromenljiva. Spektar u δ-domenu je sada definisan sa

$$\lambda_\delta = [\lambda_{\delta,1} \quad \lambda_{\delta,2} \quad \cdots \quad \lambda_{\delta,n-1} \quad 0]. \quad (8)$$

Formula za nalaženje vektora klizne površi [22], u ovom slučaju postaje

$$c_\delta = [k_{\delta e} \quad 1] \cdot [A_\delta \quad b_\delta]^\dagger, \quad (9)$$

gde je $k_{\delta e}$ vector pojačanja povratne sprege po stanju koji obezbeđuje spektar (8) u sistemu (4), dok operator † označava pseudo-inverziju matrice.

Na osnovu (6) i (4) sledi da je

$$\delta s_{\delta,k} = \frac{s_{\delta,k+1}-s_{\delta,k}}{T} = c_\delta \delta x_k = c_\delta A_\delta x_k + u_k + d_k. \quad (10)$$

Ekvivalentno upravljanje u δ-domenu se određuje rešavanjem uslova $s_{\delta,k+1} = 0$ po upravljanju u_k, te se korišćenjem prethodne jednačine dobija

$$u_{eq,k} = -c_\delta A_\delta x_k - \frac{s_{\delta,k}}{T} - d_k. \quad (11)$$

Član $s_{\delta,k}/T$ u upravljanju je zadužen za fazu dosezanja, i postaje jednak nuli kada sistem dođe na kliznu površ. Ovom komponentom može da se utiče na fazu dosezanja.

Ostvarljiv deo ekvivalentnog upravljanja (11) je

$$u_k = -c_\delta A_\delta x_k - \frac{s_{\delta,k}}{T} = -(k_{\delta e} + \frac{1}{T} c_\delta) x_k. \quad (12)$$

Zadatak upravljanja je obezbediti brz odziv bez preskoka i značajnu robusnost na poremećaje u sistemu. Takođe treba uzeti u obzir neizbežno postojanje zasićenja u aktuatorima, što uslovljava ograničavanje upravljačkog signala regulatora po amplitudi. Navedeni zahtevi su ostvareni digitalnim regulatorom promenljive strukture sa kliznim režimom [20]. Upravljačka strategija ovog regulatora se sastoji iz dva režima rada. U prvoj fazi, kada je stanje sistema udaljeno od klizne površi, deluje linearno upravljanje sa zadatkom da dovede stanje sistema u blisku okolinu klizne površi koja zavisi od amplitude poremećaja koji deluje. Nakon toga se aktivira nelinearna kompenzacija poremećaja koja ojačava linearnu upravljačku komponentu. Na taj načine se izbegava preskok i pojava integratorskog zamaha usled postojanja nelinearnosti tipa zasićenja.

Zakon upravljanja [20] je opisan sledećim jednačinama:

$$u_k = \begin{cases} U_0 \mathrm{sgn}(u_{\Sigma,k}), & |u_{\Sigma,k}| > U_0 \\ u_{\Sigma,k}, & |u_{\Sigma,k}| \le U_0 \end{cases}, \quad (13a)$$

$$u_{\Sigma,k} = u_{l,k} - p_{2,k} u_{c,k}, \quad (13b)$$

$$u_{l,k} = -c_\delta A_\delta x_k - T^{-1}\left[k_{s1} + (1 - p_{2,k}) k_{s2}\right] s_{\delta,k}, \quad (13c)$$

$$u_{c,k} = u_{c,k-1} + k_{int} T \mathrm{sgn}(s_{\delta,k-1}) \quad (13d)$$

$$p_{1,k} = \begin{cases} 0, |u_{\Sigma,k}| > U_0 \\ 1, |u_{\Sigma,k}| \le U_0 \end{cases}, \quad (13e)$$

$$p_{2,k} = p_{1,k-1}, \quad (13f)$$

$$k_{s1}, k_{s2} > 0, k_{s1} + k_{s2} \le 1. \quad (13g)$$

Može se primetiti da se ukupno upravljanje $u_{\Sigma,k}$ sastoji iz dve komponente: linearne $u_{l,k}$ i nelinearne (kompenzacione) $u_{c,k}$. Kada je stanje sistema daleko od klizne površi, izlaz regulatora u_k je u zasićenju jer linearno upravljanje teži da dovede sistem na kliznu površ u nominalnom slučaju. Izračunato upravljanje $u_{\Sigma,k}$ je velike amplitude koja se onda limitira na U_0, vrednost

koja je prihvatljiva za aktuator. Nakon izlaska regulatora iz zasićenja primenjuje se linearno upravljanje

$$u_{l,k} = -c_\delta A_\delta x_k - T^{-1}(k_{s1} + k_{s2})s_{\delta,k} \quad (14)$$

u trajanju od jedne periode diskretizacije. Ovaj mehanizam je ostvaren pomoćnim promenljivama $p_{1,k}$ $p_{2,k}$. U graničkom slučaju kada su pojačanja $k_{s1} + k_{s2} = 1$, upravljanje (14) postaje tzv. dead-beat upravljanje koje daje $s_{\delta,k+1} = 0$ u slučaju nominalnog sistema $(d_k = 0)$. U realnom sistemu uzima se da je $k_{s1} + k_{s2} \leq 1$ pošto je $d_k \neq 0$ (uključujući i nemodelovanu dinamiku) da bi se podesila širina kvazi-kliznog domena. Ovakvo upravljanje dovodi stanje sistema u neku okolinu klizne površi. U sledećoj periodi diskretizacije redukuje se pojačanje linearnog dela upravljanja i aktivira se nelinearna komponenta, tako da se tada upravljanje definiše realacijama

$$u_k = -c_\delta A_\delta x_k - T^{-1}k_{s1}s_{\delta,k} - u_{c,k}, \quad (15)$$

$$u_{c,k} = u_{c,k-1} + k_{int}T\mathrm{sgn}(s_{\delta,k-1}). \quad (16)$$

Komponenta upravljanja $u_{c,k}$ je izlaz diskretnog integratora sa pojačanjem k_{int} koja teži da kompenzuje dejstvo poremećaja. Dakle, (16) sprovodi nelinearnu estimaciju poremećaja. Na ulaz integratora se dovodi signum funkcija klizne promenljive.

Stabilnost sistema podrazumeva konvergenciju trajektorija sistema ka kliznoj površi u oba režima rada regulatora, u zasićenju i van zasićenja. U [20] su izvedeni uslovi stabilnosti sistema, dati kroz dva tvrđenja. Prvo tvrđenje se odnosi na potrebnu veličinu limita izlaza regulatora.

Tvrđenje 1: Diskretni sistem (4) sa regulatorom (13) koji radi u režimu zasićenja će napustiti ovaj režim za konačan broj perioda uzorkovanja ukoliko važi da je

$$U_0 > |c_\delta A_\delta x_k| + d_0, \forall k \geq 0. \quad (17)$$

Drugo tvrđenje sagledava uslove konvergencije nakon izlaska regulatora iz režima zasićenja.

Tvrđenje 2: Uslovi konvergencije diskretnog sistema (4) sa regulatorom (13), koji radi van režima zasićenja i ima parametre $0 < k_{s1} \leq 1$ i $k_{int} > 0$, će biti ispunjeni unutar oblasti definisane sa

$$|s_{\delta,k}| > \frac{k_{int}T^2}{k_{s1}}. \quad (18)$$

Iz ovog uslova se vidi da za konačno malo T postoji uska oblast oko klizne površi u kojoj ne postoji konvergencija trajektorija ka kliznoj površi i koja utiče na širinu kvazi-klizne oblasti. Može se zaključiti da je prilikom projektovanja sistema poželjno ostvariti što je moguće manje T, jer ne postoji bojazan generisanje prevelikog upravljanja i potencijalne nestabilnosti usled postojanja limitera na izlazu regulatora.

III. Ublažavanje četeringa

Relacije (15) i (16) opisuju rad regulatora (13) u željenom režimu rada van zasićenja. U estimatoru poremećaja (16) figuriše diskontinualna funkcija. Iako diskontinualni signal $\mathrm{sgn}(s_{\delta,k-1})$ prolazi kroz integrator, diskretna realizacija integratora ne može u potpunosti da isfiltrira ovaj signal. Zato ovakav estimator ipak predstavlja izvor četeringa u sistemu.

U ovom radu se ispituje mogućnost dalje redukcije četeringa zamenom diskontinualne signum funkcije u (13d), odnosno (16), nekom kontinualnom aproksimacijom. Kako se signum funkcija može opisati relacijom $\mathrm{sgn}(s_{\delta,k}) = s_{\delta,k}/|s_{\delta,k}|$, ideja je da se primeni u (16) sledeća kontinualna aproksimacija

$$u_{c,k} = u_{c,k-1} + k_{int}T\frac{s_{\delta,k-1}}{\beta + |s_{\delta,k-1}|}, \beta \geq 0. \quad (19)$$

Uticaj parametra β na oblik aproksimacije je prikazan na Sl. 1. Očigledno je da za $\beta = 0$, (19) se svodi na (16), tj. nema aproksimacije.

Nakon uvođenja kontinualne aproksimacije, potrebno je analizirati stabilnost i performanse sistema. Najpre se posmatra rad regulatora (13) sa aproksimacijom (19) u režimu zasićenja. Kako tada aproksimacija (19) nije aktivna i upravljanje je maksimalne amplitude $u_k = U_0\mathrm{sgn}(u_{\Sigma,k})$, uvođenje aproksimacije nema uticaj na ovaj režim, te i dalje važe uslovi (17). Dalje treba analizirati rad sistema van zasićenja upravljačkog signala.

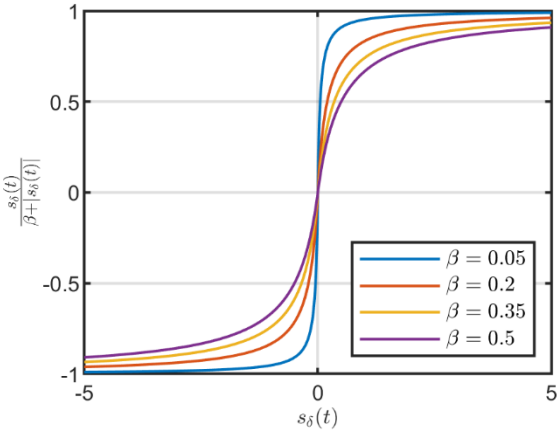

Sl. 1. Izgled kontinualne aproksimacija funkcije $\mathrm{sgn}(s_{\delta,k})$ za različite vrednosti parametra $\beta > 0$.

Nakon izlaska upravljanja iz zasićenja, na osnovu zakona (13) u narednoj periodi diskretizaije deluje upravljanje

$$u_k = -c_\delta A_\delta x_k - T^{-1}(k_{s1} + k_{s2})s_{\delta,k}, \quad (20)$$

pa $\delta s_{\delta,k}$ postaje

$$\delta s_{\delta,k} = -T^{-1}(k_{s1} + k_{s2})s_{\delta,k} + d_k. \quad (21)$$

Pošto je $\delta s_{\delta,k} = T^{-1}(s_{\delta,k+1} - s_{\delta,k})$, iz prethodne jednačine se može naći $s_{\delta,k+1}$ kao

$$s_{\delta,k+1} = (1 - k_{s1} - k_{s2})s_{\delta,k} + Td_k. \quad (22)$$

Važno je primetiti da se u graničnom slučaju $(k_{s1} + k_{s2} = 1)$ dobija $s_{\delta,k+1} = Td_k$, što ukazuje da ovo upravljanje dovodi sistem u $O(T)$ okolinu klizne površi, čije dimenzije zavise i od amplitude poremećaja. Ukoliko nema poremećaja $(d_k = 0)$, dobija se $s_{\delta,k+1} = 0$ te je ovo upravljanje ustvari ekvivalentno upravljanje koje ostvaruje dead-beat odziv.

Već u narednoj periodi diskretizacije, pojačanje regulatora se redukuje $(k_{s2} = 0)$ i aktivira se kompenzaciono upravljanje $u_{c,k}$ (19). Izlaz regulatora se sada formira na osnovu jednačina

$$u_k = -c_\delta A_\delta x_k - T^{-1}k_{s1}s_{\delta,k} - u_{c,k}, \quad (23)$$

$$u_{c,k} = u_{c,k-1} + k_{int}T\frac{s_{\delta,k-1}}{\beta + |s_{\delta,k-1}|}, \quad (24)$$

pa se dinamika klizne promenljive opisuje sa

$$s_{\delta,k+1} = (1 - k_{s1})s_{\delta,k} + T(d_k - u_{c,k}), \quad (25)$$

$$u_{c,k+1} = u_{c,k} + k_{int}T\frac{s_{\delta,k-1}}{\beta + |s_{\delta,k-1}|}. \quad (26)$$

Kompenzaciono upravljanje $u_{c,k}$ ustvari predstavlja estimaciju

poremećaja. Ako se uvede greška estimacije kao $z_k = d_k - u_{c,k}$, dinamika sistema (25), (26) se može izraziti kao

$$s_{\delta,k+1} = (1 - k_{s1})s_{\delta,k} + Tz_k, \quad (27)$$

$$z_{k+1} = -k_{int}T\frac{s_{\delta,k-1}}{\beta+|s_{\delta,k-1}|} + z_k + \Delta_k, \quad (28)$$

gde je $\Delta_k = d_{k+1} - d_k$.

Stabilnost nelinearnog sistema (27), (28) se može analizirati korišćenjem pseudo-linearne forme [21], [23], što u ovom slučaju daje sledeći model

$$\sigma_{k+1} = \Lambda(s_{\delta,k})\sigma_k + p_k, \quad (29)$$

$$\sigma_k = \begin{bmatrix} s_{\delta,k} \\ z_k \end{bmatrix},\ \Lambda(s_{\delta,k}) = \begin{bmatrix} 1-k_{s1} & T \\ \frac{-k_{int}T}{\beta+|s_{\delta,k}|} & 1 \end{bmatrix},\ p_k = \begin{bmatrix} 0 \\ \Delta_k \end{bmatrix}$$

Karakteristična jednačina pseudo-linearnog sistema (29) se nalazi iz uslova $F(z) = \det(zI - \Lambda) = 0$, iz koga se dobija

$$F(z) = a_2z^2 + a_1z + a_0(s_{\delta,k}) = 0, a_2 > 0, \quad (30)$$

$$a_2 = 1, a_1 = k_{s1} - 2, a_0 = 1 - k_{s1} + \frac{k_{int}T^2}{\beta+|s_{\delta,k}|}.$$

Uslovi stabilnosti sistema se mogu odrediti primenom Džurijevog testa stabilnosti, koji se za sistem drugog reda (29) svodi na zahteve $F(1) > 0$, $F(-1) > 0$ i $|a_0| < a_2$. Za karakterističnog polinoma (30), ovi uslovi su sledeće relacije

$$\frac{k_{int}T^2}{\beta+|s_{\delta,k}|} > 0, \quad (31)$$

$$2(2 - k_{s1}) + \frac{k_{int}T^2}{\beta+|s_{\delta,k}|} > 0, \quad (32)$$

$$\left|1 - k_{s1} + \frac{k_{int}T^2}{\beta+|s_{\delta,k}|}\right| < 1. \quad (33)$$

Kako važi da je $k_{int} > 0$, $k_{s1} \leq 1$, $\beta \geq 0$ i $T > 0$, prve dve nejednakosti su uvek ispunjene. Dakle, uslov stabilnosti definiše (33). Pošto je izraz unutar apsolutne vrednosti u (33) uvek pozitivan, apsolutna vrednost se može zanemariti i uslov postaje $k_{int}T^2/(\beta + |s_{\delta,k}|) < k_{s1}$, iz koga se nalazi

$$|s_{\delta,k}| > \frac{k_{int}T^2}{k_{s1}} - \beta. \quad (34)$$

Dakle, sistem (29) je stabilan unutar oblasti definisane relacijom (34), što znači da će u toj oblasti trajektorije sistema biti usmerene ka kliznoj površi $s_\delta = 0$. Važno je istaći da u slučaju konstantnih ili sporopromenljivih poremećaja, za koje se može smatrati da važi $d_k = d_{k-1}$, sistem (29) je autonoman jer je $\Delta_k = 0$. Tada će trajektorije sistema dosegnuti granicu konvergencije $|s_{\delta,k}| = k_{int}T^2/k_{s1} - \beta$. Očigledno je da u neposrednoj okolini klizne površi, datoj sa $|s_{\delta,k}| < k_{int}T^2/k_{s1} - \beta$, uslovi konvergencije nisu zadovoljeni, pa trajektorije napuštaju ovu oblast i tako nastaje kvazi-klizno kretanje.

Iz (34) se vidi da se primenom aproksimacije okarakterisane sa β, pored redukcije četeringa, može povećati oblast konvergencije sistema, tj. smanjiti zona oko klizne površi gde se konvergencija ne garantuje. Interesantno je da se za vrednost $\beta = k_{int}T^2/k_{s1}$ dobija uslov konvergencije

$$|s_{\delta,k}| > 0, \quad (35)$$

koji ukazuje da su u celom prostoru oko klizne površi ispunjeni uslovi konvergencije. Tada se javlja diskretni KR. U slučaju $\beta = 0$, oblast konvergencije (34) se svodi na (18), što ukazuje na valjanost analize.

Ovde treba istaći da izvedeni zaključci važe u slučaju konstantnih i sporopromenljivih poremećaja. Za ostale tipove poremećaja treba očekivati da će njihova amplituda i frekvencija uticati na širinu kvazi-klizne oblasti, koja će svakako biti veća nego teorijski dobijena širina na osnovu oblasti konvergencije (34).

IV. NUMERIČKI PRIMER I SIMULACIONI REZULTATI

Dobijeni teorijski rezultati su provereni digitalnom simulacijom. Za tu svrhu je izabran akademski primer linearnog, nestabilnog i kontrolabilnog objetka upravljanja petog reda, čiji model (1) je definisan matricama

$$A = \begin{bmatrix} 1 & 2 & 3 & -5 & 6 \\ -2 & 6 & -3 & -4 & -7 \\ 2 & -4 & 6 & -10 & 12 \\ -8 & -6 & -4 & 3 & 1 \\ 4 & 12 & -6 & -8 & -14 \end{bmatrix}, b = \begin{bmatrix} 1 \\ -2 \\ 3 \\ -1 \\ 2 \end{bmatrix}.$$

Neka je proizvoljno izabrano početno stanje sistema $x(0) = [10 \quad -5 \quad 0 \quad -10 \quad 5]^{\mathrm{T}}$. Perioda diskretizacije sistema je $T = 0.001$ s.

Zadatak upravljanja je da se sistema iz proizvoljnog početnog stanja dovede u ranotežno stanje (koordinatni početak), organizovanjem KR duž površi sa definisanom dinamikom. Neka je željena dinamika sistema u KR data spektrom sopstvenih vrednosti $\lambda = [-1 \quad -2 \quad -3 \quad -4 \quad 0]$ u kontinualnom domenu. Korišćenjem $\lambda_{\delta,i} = (e^{\lambda_i T} - 1)/T$, $i = 1, \cdots, n-1$, dobija se spektar u δ-domenu

$$\lambda_\delta = [-0.9995 \quad -1.998 \quad -2.9955 \quad -3.992 \quad 0].$$

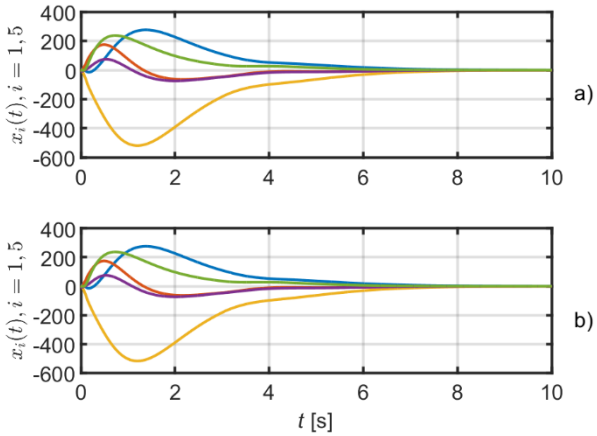

Sl. 2. Koordinate stanja: a) $\beta = 1.1111 \cdot 10^{-4}$; b) $\beta = 0$

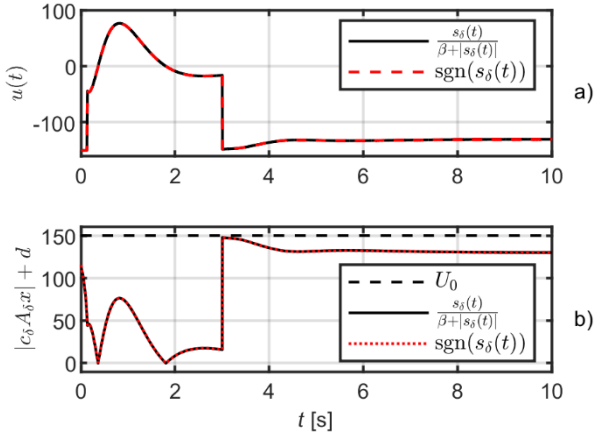

Sl. 3. a) Upravljanja; b) Ispunjenje uslova (17)

Odgovarajuća klizna površ koja obezbeđuje željenu dinamiku

je definisana vektorom

$c_\delta = [0.4437 \quad 0.5794 \quad 0.3072 \quad -0.6614 \quad 0.063]$,

dobijenog iz (9). Parametri regulatora su $k_{s1} = 0.9$, $k_{s2} = 0.1$ i $k_{int} = 100$, dok je ograničenje u sistemu $U_0 = 150$.

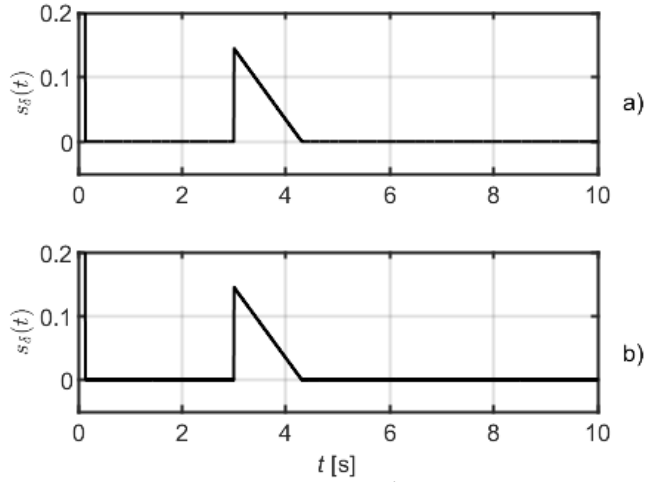

Sl. 4 Klizna promenljiva: a) $\beta = 1.1111 \cdot 10^{-4}$; b) $\beta = 0$

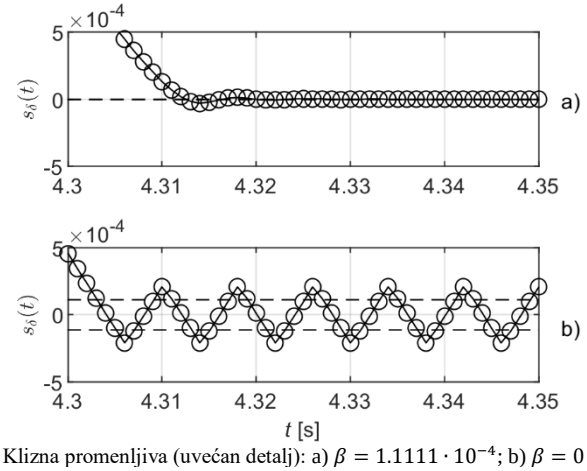

Sl. 5 Klizna promenljiva (uvećan detalj): a) $\beta = 1.1111 \cdot 10^{-4}$; b) $\beta = 0$

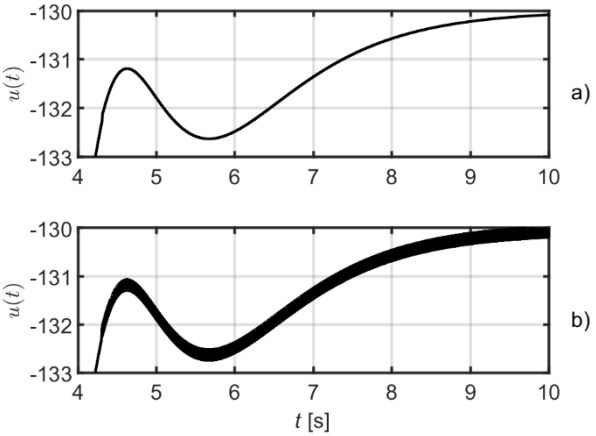

Sl. 6. Upravljanje (uvećan detalj): $\beta = 1.1111 \cdot 10^{-4}$; b) $\beta = 0$

U prvom testu sistem je izložen odskočnom poremećaju $d(t) = 130h(t-3)$, gde je $h(t)$ Hevisajdova funkcija. Posmatrani su slučajevi primene aproksimacije (19) sa karakterističnim vrednošću $\beta = k_{int}T^2/k_{s1} = 1.1111 \cdot 10^{-4}$ i slučaj sa signum funkcijom ($\beta = 0$). Na Sl. 2 i Sl. 3 su prikazane koordinate stanja, upravljanja i ispunjenje uslova izlaska sistema iz zasićenja (17), na kojima oba sistema imaju naizgled iste odzive. Koordinate stanja asimptotski teže koordinatnom početku uprkos dejstvu poremećaja. Izlazi regulatora su inicijalno u zasićenju ali veoma brzo izlaze iz zasićenja, budući da je uslov (17) sve vreme ispunjen. Klizne promenljive, prikazane na Sl. 4, ukazuju da se brzo uspostavlja KR i da dejstvo poremećaja izbacuje sistem iz KR ali da regulatori uspevaju da ponovo uspostave KR.

Međutim, uvećani detalji kliznih promenljivih na Sl. 5, gde su kružićima označene vrednosti klizne promenljive u trenucima odabiranja, ukazuju na različitu prirodu kretanja sistema u neposrednoj okolini klizne površi. Naime, za slučaj $\beta = k_{int}T^2/k_{s1}$ oblast konvergencije (35) obuhvata čitavu okolinu klizne površi, te trajektorija sistema treba da dođe na kliznu površ za dati tip poremećaja. Ovo predviđeno ponašanje sistema je potvrđeno odzivom na Sl. 5a, gde se u sistemu uspostavlja diskretni KR, pa je ostvarena maksimalna tačnost. U slučaju primene signum funkcije u regulatoru ($\beta = 0$), na osnovu (18) se vidi da u naznačenoj okolini klizne površi, oivičenoj isprekidanim linijama na Sl. 5b, ne postoji konvergencija te trajektorije sistema napuštaju ovu oblast. U ovom slučaju uspostavlja se diskretni kvazi-klizni režime, što ukazuje na smanjenu tačnost sistema i pojavu četeringa.

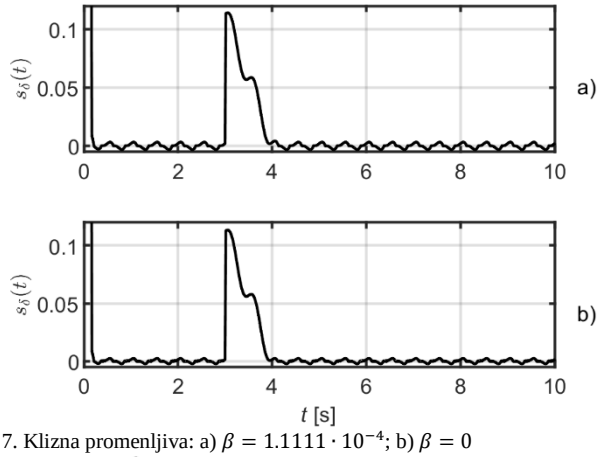

Sl. 7. Klizna promenljiva: a) $\beta = 1.1111 \cdot 10^{-4}$; b) $\beta = 0$

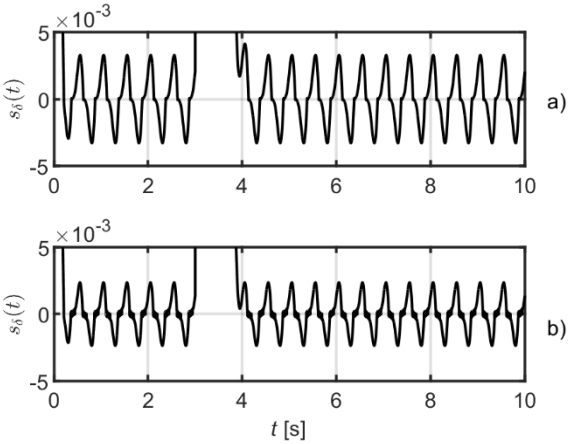

Sl. 8. Klizna promenljiva (uvećan detalj): a) $\beta = 1.1111 \cdot 10^{-4}$; b) $\beta = 0$

Efekti uvođenja kontinualne aproksimacije na redukciju četeringa se vide na Sl. 6, gde su prikazani uvećani detalji upravljačkih signala oba sistema. Očigledno je da je upravljanje u slučaju primene aproksimacije za graničnu vrednost β u potpunosti glatko, dok za $\beta = 0$ upravljanje sadrži

visokofrekvencijsku komponentu po uspostavljanju kvazi-kliznog režima. Ova komponenta, iako je po amplitudi veoma mala, ipak ukazuje na mogućnost pojave četeringa.

U drugom testu se ispituju performanse sistema u prisustvu promenljivih poremećaja. Na sisteme deluje složeni poremećaj koji se sastoji iz konstantnog i sinusoidalnog dela, tj. $d(t) = 10\sin(4\pi t) + 100h(t-3)$. Ostala podešenja u sistemima su identična prethodnom slučaju.

Odzivi kliznih promenljivih su dati na Sl. 7 iz kojih se vidi da sistemi ispoljavaju manju robusnost na promenljive poremećaje u odnosu na sporopromenljive poremećaje. Na osnovu uvećanih delova ovih grafika, prikazanih na Sl. 8, vidi se da u oba slučaja nastaje kvazi-klizni režim. Takođe se vidi da je širina kvaziklizne oblasti u slučaju primene aproksimacije nešto veća u odnosu na slučaj za $\beta = 0$, iako za graničnu vrednost β su uslovi konvergencije ostvareni u celom prostoru. To ukazuje da za ovakav tip poremećaja sistem sa kontinualnom aproksimacijom zbog glatke kompenzacione komponente upravljana gubi izvesni stepen robusnosti, a samim tim i tačnosti.

V. Zaključak

Sprovedenom analizom i simulacionim rezultatima je pokazano da primena predložene kontinualne aproksimacije signum funkcije u digitalnom regulatoru promenljive strukture, pored efekta ublažavanja četeringa, otvara mogućnost proširivanja oblasti konvergencije sistema ka kliznoj površi. U slučaju sporopromenljivih poremećaja data aproksimacija ima blagotvorno dejstvo, jer se redukuje četering i ostvaruje diskretni KR, čime se postiže apsolutna tačnost. U slučaju promenljivih poremećaja, primena aproksimacije koja redukuje četering ipak dovodi do izvesnog smanjenja robusnosti, odnosno tačnosti. U tom slučaju je potrebno je naći kompromis između prihvatljivog nivoa četeringa i zahtevane tačnosti.

Literatura

[1] S. V. Emelyanov, A Method to Obtain Complex Regulation Laws Using Only the Error Signal or Regulated Coordinate and Its First Derivatives, Avtomat. Telemekh. 18 (10), pp. 873-885, 1957

[2] V.I. Utkin, Sliding Modes in Control and Optimization, Springer-Verlag, 1992.

[3] B. Draženović, (1969) The invariance conditions in variable structure systems. Automatica 5, pp. 287–295

[4] Slotine J.J.E. (1984) Sliding controller design for non-linear systems. Int. Jour. Control 40, pp. 421–434.

[5] Bondarev, A.G., Bondarev, S.A., Kostylyeva, N.Y., Utkin, V.I., "Sliding modes in systems with asymptotic observers", Aut. Remote Contr., 46 (1985) no 6, pp. 679-684

[6] Levant A (1993) Sliding order and sliding accuracy in sliding mode control. Int. Jour. Control, 58, pp. 1247–1263.

[7] Utkin V., "Discussion aspects of higher order sliding mode control", *IEEE Trans.* AC, vol. 61, no. 3, pp. 829-833, 2016.

[8] Perez-Ventura U., Fridman L., "When is it reasonable to implement the discontinuous sliding-mode controllers instead of the continuous ones? Frequency domain criteria," *Inter. Jour. of Robust and Nonlinear Control*, vol. 29, pp. 810-828, 2019.

[9] Utkin V., Poznyak A, Orlov Y., Polyakov A., "Conventional and high order sliding mode control," *Jour. of the Franklin Institute*, vol. 357, no. 15, pp. 10244-10261, 2020.

[10] Castillo I., Freidovich L.B., "Describing-function-based analysis to tune parameters of chattering reduction approximations of sliding mode controllers," *Control Engineering Practice*, vol. 95, 104230, 2020.

[11] Milosavljević, Č. (1985): "General Conditions for the Existence of Quasi-sliding Mode on the Switching Hyper-plane in Discrete Variable Structure Systems", *Automatic and Remote Control*, 46, pp. 307-314

[12] Drakunov, S. V., Utkin, V.I. (1989), 'On discrete-time sliding mode', Proc. IFAC Symposium on *Nonlinear Control Systems design*, Capry (Italy), pp. 484-489

[13] Gao, W., Wang, Y. Homaifa A. (1995), "Discrete-time variable structure control systems,*" IEEE Trans. Ind. Electron.*, IE-42, pp. 117-122.

[14] Bartolini G, Ferrara A, Utkin VI (1995) Adaptive sliding mode control in discrete-time systems. Automatica, 31, pp. 769–773.

[15] A. Bartoszewitz, "Discrete-time quasi-sliding mode control strategies," IEEE Trans. Ind. Elect., vol. 45, pp. 633-637, 1998.

[16] Golo G, Milosavljević Č (2000) Robust discrete-time chattering free sliding mode control. Syst. Control Lett. 41, pp. 19–28.

[17] Su W.C., Drakunov S V., Özgüner Ü (2000) An O(T2) boundary layer in sliding mode for sampled-data systems. IEEE Trans. Automat. Contr. 45, pp.4 82–485.

[18] Milosavljević Č, Peruničić-Draženović B, Veselić B, Mitić D (2007) A new design of servomechanisms with digital sliding mode. Electr. Eng. 89, pp. 233–244.

[19] Lješnjanin M, Peruničić B, Milosavljević Č, Veselić B, (2011), Disturbance compensation in digital sliding mode. Int. conf. EUROCON. Lisboa, Portugal (paper 171)

[20] B. Veselić, Č. Milosavljević, B. Peruničić-Draženović, A. Huseinbegović, M. Petronijević, "Discrete-time sliding mode control of linear systems with input saturation," *Int. J. Appl. Math. Comput. Sci*., vol. 30, no. 5, pp. 517-528, 2020.

[21] Koch S, Reichhartinger M, Horn M, Discrete-time equivalents of the super-twisting algorithm, Automatica 107 (2019) 190–199

[22] Draženović B, Milosavljević Č, Veselić B (2013) Comprehensive Approach to Sliding Mode Design and Analysis in Linear Systems. In: Bandyopadhyay B, Janardhanan S, Spurgeon SK (eds) Advances in Sliding Mode Control: Concept, Theory and Implementation. Springer Berlin Heidelberg, Berlin, Heidelberg, pp 1–19

[23] Ghane H, Menhaj M.B, Eigenstructure-based analysis for non-linear autonomous systems, *IMA Journal of Mathematical Control and Information* (2015) 32, 21–40.

Abstract

The paper explores possibility of chattering reduction of a digital sliding mode controller for linear systems with saturated inputs. A nonlinear discontinuous relay function in the control law is substituted by an adequate continuous approximation. Stability of the modified control system is analyzed and the observed system properties are emphasized. The obtained theoretical results have been confirmed by simulation of a numerical example.

Chattering Alleviation of a Digital Sliding Mode Controller for Linear Systems

B. Veselić, Č. Milosavljević, B. Peruničić-Draženović, S. Huseinbegović, M. Petronijević

Autonomno kretanje besposadnog vozila po zadatoj putanji primenom algoritma sa aktivnim potiskivanjem poremećaja

Momir Stanković i Stojadin Manojlović

***Apstrakt*—U radu je predložen algoritam autonomnog kretanja besposadnog vozila po zadatoj putanji primenom koncepta upravljanja sa aktivnim potiskivanjem poremećaja. Nelinearnosti kinematike kretanja i poremećaji linearne i ugaone brzine vozila su formulisani u vidu totalnog poremećaja. Za estimaciju stanja nominalnog modela i totalnog poremećaja, kao dodatne promenljive stanja, projektovan je prošireni opserver stanja. Na bazi estimacija i dostupnih merenja formulisan je upravljački zakon za aktivno potiskivanje totalnog poremećaja u realnom vremenu i upravljanje kretanjem vozila sa definisanom dinamikom praćenja zadate putanje. Simulacionom analizom predloženog algoritma sa tipičnim modelom pogona guseničnog besposadnog vozila je pokazana efikasnost predloženog rešenja u različitim scenarijima praćenja zadate putanje.**

***Ključne reči*—Autonomno kretanje; Besposadno vozilo; Upravljanje sa aktivnim potiskivanjem poremećaja; Prošireni opserver stanja;.**

I. UVOD

Iako su ideje o automatizovanim pokretnim platformama bez ljudske posade (eng. *Unmanned Vehicles - UVs*) postojale još početkom prošlog veka, tek njegovim krajem došlo se do tehnoloških mogućnosti za njihovu realizaciju. Osnovna namena besposadnih platformi je delimična ili potpuna zamena čoveka u napornim, rizičnim, nepristupačnim i sl. civilnim ili vojnim misijama. Uz tehnološki napredak u oblastima senzorskih i aktuatorskih komponenti, obrade signala i algoritama vođenja (navigacije) i upravljanja, zbog potencijalnih mogućnosti ovih specifičnih platformi, poslednjih godina se poklanja sve veća pažnja njihovom razvoju i primeni. Posebnu grupu automatizovanih platformi predstavljaju besposadna vozila (eng. *Unmanned Ground Vehicles - UGVs*) projektovana za kretanje po uređenom ili neuređenom terenu. Razvoj besposadnih vozila u početku je bio zasnovan na automatizaciji kretanja postojećih vozila kojima je upravljao čovek. Međutim, zbog povećanja ekonomičnosti, mobilnosti i manevrabilnosti, danas se besposadna vozila projektuju kao posebna klasa vozila sa točkovima ili gusenicama, sa potpuno automatizovanim funkcijama kretanja i, najčešće, nezavisnim upravljanjem pogonskim točkovima [1].

Sistem za autonomno kretanje besposadnog vozila se, u opštem slučaju, može razdvojiti na tri celine: sistem za analizu terena, sistem za planiranje (proračun) trajektorije i sistem upravljanja kretanjem. Sistem upravljanja kretanjem treba da obezbedi praćenje zadate trajektorije uz minimalna odstupanja. Funkcionalno se može razdvojiti na upravljanje uzdužnim kretanjem, odnosno upravljanje intenzitetom brzine kretanja i na upravljanje ugaonim kretanjem (uglom skretanja) [2]. Algoritam upravljanja treba da obezbedi robusnost i stabilnost kretanja, uzimajući u obzir dinamičko ponašanje i konstruktivna ograničenja samog vozila kao i uticaje poremećaja. Rešenja ovog problema variraju od primene klasičnih do inteligentnih tehnika upravljanja [3].

U ovom radu analiziran je algoritam upravljanja ugaonim kretanjem guseničnog besposadnog vozila za praćenje zadate putanje, primenom koncepta sa aktivnim potiskivanjem poremećaja (eng. *Active Disturbance Rejection Control - ADRC*). Ovaj koncept se pokazao kao veoma robusan, efikasan i praktičan u potiskivanju kako spoljašnjih (ambijentalnih), tako i unutrašnjih (sistemskih) poremećaja [4]. Pri modelovanju sistema, sva odstupanja od nominalnog modela, uključujući greške modelovanja (neodređenost/promene parametara, nemodelovana dinamika) i spoljašnje poremećaje, tretiraju se kao *totalni poremećaj sistema*. Potiskivanjem totalnog poremećaja preko unutrašnje povratne sprege, za kompenzovani (nominalni) sistem, u vidu redne veze integratora, projektuje se kontroler zatvaranjem povratnih sprega po stanjima. Klučna komponenta ADRC kontrolera je prošireni opserver stanja (eng. *Extended State Observer - ESO*), koji se projektuje za nominalni model, a totalni poremećaj se uvodi kao dodatno stanje sistema. Od kvaliteta estimacija ESO-a u najvećoj meri zavisi efikasnost ADRC kontrolera [5].

U radu je projektovan ADRC kontroler na osnovu kinematičkog modela kretanja besposadnog vozila, uz pretpostavke da je intenzitet brzine kretanja konstantan i da se praćenje referentne putanje ostvaruje kontrolisanjem ugaone orijentacije vozila. Pri tome se svi poremećaji koji mogu nastati u toku kretanja vozila usled proklizavanja, neravnog terena ili neadekvatnog odziva pogonskih motora, modeluju kao poremećaji intenziteta brzine vozila i poremećaji ugaone brzine njegove orijentacije. S obzirom da poremećaji intenziteta brzine vozila ne deluju na istom ulazu gde i upravljački signal (eng. *mismatched uncertainty*) model

Momir Stanković – Vojna akademija, Univerzitet odbrane u Beogradu, Generala Pavla Jurišića Šturma 33, 11000 Beograd, Srbija (e-mail: momir_stankovic@yahoo.com).

Stojadin Manojlović – Vojna akademija, Univerzitet odbrane u Beogradu, Generala Pavla Jurišića Šturma 33, 11000 Beograd, Srbija (e-mail: colemanojle@yahoo.com).

sistema je formulisan u pogodnom obliku kako bi se svi poremećaji uključili u totalni poremećaj.

Za estimaciju stanja nominalnog modela i totalnog poremećaja projektovan je linearni ESO. Koristeći estimacije i dostupne merene veličine, formulisan je zakon upravljanja za minimizaciju normalne komponente greške praćenja (eng. *cross-track error*), pri čemu se besposadno vozilo približava zadatoj putanji zahtevanom dinamikom.

II. KINEMATIČKI MODEL KRETANJA VOZILA PO ZADATOJ PUTANJI

Kinematički model autonomnog kretanja vozila u inercijalnom koordinatnom sistemu se može opisati jednačinama:

$$\begin{aligned}\dot{x}(t) &= \big(v_s(t) + v_d(t)\big)\cos\theta_s(t)\\ \dot{y}(t) &= \big(v_s(t) + v_d(t)\big)\sin\theta_s(t)\\ \dot{\theta}_s(t) &= \omega_s(t) + \omega_d(t)\end{aligned} \tag{1}$$

gde su $x(t)$ i $y(t)$ koordinate a $\theta_s(t)$ ugaona orijentacija vozila. Linearna brzina vozila v_s se smatra poznatom uz pretpostavku da je konstantna, a ugaona brzina vozila $\omega_s(t)$ predstavlja upravljačku veličinu, koju treba proračunati tako da vozilo izvrši zahtevani manevar. Uticaj proklizavanja, neravnog terena ili neadekvatnog odziva pogonskih motora na kretanje vozila modelovani su poremećajima linearne $v_d(t)$ i ugaone brzine $\omega_d(t)$. Poremećaji $v_d(t)$ i $\omega_d(t)$ predstavljaju osnovni uzrok odstupanja vozila od zadate putanje pri autonomnom kretanju vozila.

Na Sl. 1 prikazana je zadata putanja kao pravac definisan uglom θ_{ref} u inercijalnom koordinatnom sistemu. U tom slučaju je greška ugaone orijentacije vozila u odnosu na zadatu putanju:

$$\theta_e(t) = \theta_s(t) - \theta_{ref} \tag{2}$$

Poziciono odstupanje vozila definisano je greškom $e_d(t)$ kao normalno rastojanje vozila od zadate putanje.

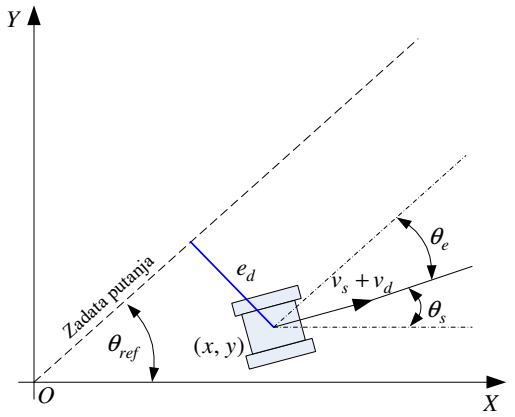

Sl. 1. Zadata putanja kretanja vozila i greške praćenja.

Problem praćenja zadate trajektorije se može definisati kao regulacioni problem minimizacije greške $e_d(t)$ u prisustvu poremećaja $v_d(t)$ i $\omega_d(t)$ primenom odgovarajućeg upravljačkog signala $\omega_s(t)$. Na osnovu Sl. 1 i primenom izvoda na jednačinu (2), dobijaju se izrazi za dinamiku grešaka pozicionog odstupanja i ugaone orijentacije vozila u odnosu na zadatu putanju:

$$\dot{e}_d(t) = \big(v_s + v_d(t)\big)\sin\theta_e(t) \tag{3}$$

$$\dot{\theta}_e(t) = \omega_s(t) + \omega_d(t) \tag{4}$$

Imajući u vidu da je ugaona brzina rotacije vozila $\omega_s(t)$ upravljačka veličina, iz (3) se može uočiti da poremećaj $v_d(t)$ ne deluje na istom ulazu kao i $\omega_s(t)$ (eng. *mismatched uncertainty*), za razliku od poremećaja $\omega_d(t)$ (eng. *matched uncertainty*) [6].

Diferenciranjem (3), i uvrštavanjem (4), dobija se model dinamike greške $e_d(t)$:

$$\begin{aligned}\ddot{e}_d(t) &= \omega_s(t)(v_s + v_d(t))\cos(\theta_e)\\ &+\omega_d(t)(v_s + v_d(t))\cos(\theta_e) + \dot{v}_d(t)\sin(\theta_e)\end{aligned} \tag{5}$$

u kome je uticaj oba spoljašnja poremećaja sveden na zajednički ulaz sa upravljačkim signalom $\omega_s(t)$ (eng. *matched uncertainty*).

Iz (5) se vidi, da je dinamika greške $e_d(t)$, čak i u odsustvu poremećaja ($v_d(t) \equiv \omega_d(t) \equiv 0$), nelinearna. Ako se pretpostavi postojanje početne greške pozicioniranja $e_d(t_0) \neq 0$, željena dinamika minimizacije greške se može definisati kao:

$$\ddot{e}_d^*(t) + k_2\dot{e}_d^*(t) + k_1 e_d^*(t) = 0 \tag{6}$$

gde se pomoću k_1 i k_2 definišu parametri prelaznog procesa. Prema tome, zadatak praćenja zadate putanje predstavlja projektovanje upravljačkog signala $\omega_s(t)$ kojim se obezbeđuje da greška $e_d(t)$ sa zadovoljavajućom tačnošću prati zadatu dinamiku, definisanu sa (6).

III. PROJEKTOVANJE ADRC REGULATORA ZA AUTONOMNO KRETANJE VOZILA

U skladu sa konceptom ADRC-a, izraz (5) se može zapisati u formi:

$$\ddot{e}_d(t) = v_s\cos\big(\theta_e(t)\big)\cdot\omega_s(t) + f(t) \tag{7}$$

gde je:

$$f(t)=\cos(\theta_e)v_d(t)\omega_s(t)+\omega_d(t)(v_s+v_d(t))\cos(\theta_e) +\dot{v}_d(t)\sin(\theta_e)\,, \tag{8}$$

totalni pormećaj, koji obuhvata nelinearnost modela i pretpostavljene spoljašnje poremećaje. Ako se $f(t)$ usvoji kao dodatno stanje sistema, (7) se može predstaviti modelom u prostoru stanja:

$$\dot{\mathbf{x}}(t)=\mathbf{A}\mathbf{x}(t)+\mathbf{B}\omega_s(t)+\mathbf{E}\dot{f}(t) \tag{9}$$

gde je $\mathbf{x}(t)=[e_d(t)\ \dot{e}_d(t)\ f(t)]^T$ vektor stanja, pri čemu matrice u modelu imaju formu:

$$\mathbf{A}=\begin{bmatrix}0&1&0\\0&0&1\\0&0&0\end{bmatrix},\ \mathbf{B}=\begin{bmatrix}0\\v_s\cos(\theta_e(t))\\0\end{bmatrix},\ \mathbf{E}=\begin{bmatrix}0\\0\\1\end{bmatrix} \tag{10}$$

Na osnovu modela (9) linearni prošireni opserver stanja se projektuje na osnovu relacija:

$$\hat{\dot{\mathbf{x}}}(t)=\mathbf{A}\hat{\mathbf{x}}(t)+\mathbf{B}\omega_s(t)+\mathbf{L}(y-\hat{e}_d) \tag{11}$$

gde je $\hat{\mathbf{x}}(t)=[\hat{e}_d(t)\ \hat{\dot{e}}_d(t)\ \hat{f}(t)]^T$ vektor estimiranih stanja, a matrica $\mathbf{L}=[\beta_1\ \beta_2\ \beta_3]^T$ sadrži pojačanja opservera. Koristeći estimacije stanja sistema i totalnog poremećaja, uz učešće merene veličine θ_e, može se formirati upravljački zakon:

$$\omega_s=\begin{cases}-\omega_{s\max}\ ,\ \theta_e\le-\pi/2\\ \dfrac{-k_1\hat{e}_d-k_2\hat{\dot{e}}_d-\hat{f}}{v_s\cos(\theta_e(t))}\ ,\ |\theta_e|<\pi/2\\ \omega_{s\max}\ ,\ \theta_e\ge\pi/2\end{cases} \tag{12}$$

gde je $\omega_{s\max}$ maksimalna ugaona brzina vozila. Uz pretpostavku da su estimacije zadovoljavajuće, tj. $\hat{e}_d(t)\approx e_d(t),\ \hat{\dot{e}}_d(t)\approx\dot{e}_d(t),\ \hat{f}(t)\approx f(t)$, primenom upravljačkog zakona (12) se kompenzuje uticaj totalnog poremećaja, a nelinearna dinamika greške (5) se svodi na zadatu formu (6), gde se dinamika približavanja vozila zadatoj putanji podešava parametrima k_1 i k_2.

Izbor parametara k_1 i k_2 se može izvršiti primenom metode podešavanja polova. Ako se za oba pola sistema sa zatvorenom spregom usvoji da su realni i isti, odnosno $p_{1,2}=-\omega_c$, $(\omega_c>0)$, pojačanja regulatora se mogu odrediti iz jednakosti karakterističnih polinoma:

$$(s+\omega_c)^2=s^2+k_2s+k_1\,, \tag{13}$$

gde je sa ω_c definsan propusni opseg sistema sa regulatorom (12). Zadavanjem propusnog opsega opservera $\omega_o=k\omega_c$, gde je $k>1$, pojačanja opservera se mogu odrediti na sličan način, iz jednakosti karakterističnih polinoma:

$$(s+\omega_o)^3=s^3+\beta_1s^2+\beta_2s+\beta_3. \tag{14}$$

Imajući u vidu mehanizam upravljanja kratnjem besposadnog vozila, treba napomenuti da su linerana brzina v_s i ugaona brzina rotacije vozila ω_s rezultat ugaonih brzina pogonskih točkova. Model kretanja guseničnog vozila sa dve gusenice i dva pogonska točka (za levu i desnu gusenicu) može se predstaviti u obliku:

$$\begin{aligned}v_s&=\frac{r}{2}(w_D+w_L)\\ \omega_s&=\frac{r}{m}(w_D-w_L)\end{aligned} \tag{15}$$

gde su r prečnik pogonskog točka, m normalno rastojanje između gusenica, w_D i w_L ugaone brzine desnog i levog pogonskog točka, respektivno. Ukoliko uzmemo u obzir poremećaje usled proklizavanja gusenica, model (15) se može zapisati u obliku:

$$\begin{aligned}v_s+v_d&=\frac{r}{2}(a_Dw_D+a_Lw_L)\\ \omega_s+\omega_d&=\frac{r}{m}(a_Dw_D-a_Lw_L)\end{aligned} \tag{16}$$

gde se koeficijentima a_D i a_L modeluje klizanje desne i leve gusenice, respektivno. Koeficijenti a_D i a_L su u opsegu $[0,1]$, pri čemu se za vrednosti manje od 1, generišu poremećaji v_d i ω_d. Odgovarajuće brzine pogonskih točkova w_D i w_L se direktno proračunavaju na osnovu zadatih vrednosti v_s i ω_s primenom izraza (15).

IV. SIMULACIONA ANALIZA

Simulaciona verfifikacija predloženog rešenja autonomnog kretanja je realizovana u programskom paketu MATLAB/Simulink na dinamičkom modelu vozila sa parametrima $m=1.4\,\text{m}$ i $r=0.1\,\text{m}$.

U okviru prvog scenarija razmatrano je kretanje vozila po zadatoj trajektoriji, definisanoj uglom $\theta_{ref}=\pi/3\,\text{rad}$. Početni položaj vozila je definisan koordinatama $x(0)=0.3\,\text{m}$, $y(0)=0\,\text{m}$ i uglom $\theta_s(0)=\pi/4\,\text{rad}$. Pretpostavljeno je postojanje proklizavanja obe gusenice, odnosno:

$$\begin{aligned}a_D(t)&=0.85+0.15\sin(2t+\pi/4)\\ a_L(t)&=0.85+0.15\cos(3t)\end{aligned}\ . \tag{17}$$

Pored toga simulirano je postojanje šuma merenja signala $e_d(t)$, koji je uključen od 3 sekunde simulacije. Dobijeni rezultati praćenja zadate trajektorije, za tri ADRC regulatora (12) sa istim propusnim opsegom u zatvorenoj sprezi $\omega_c = 3\,\text{rad/s}$ i različitim vrednostima propusnog opsega opservera ($\omega_o = 4\omega_c$, $\omega_o = 8\omega_c$ i $\omega_o = 16\omega_c$), su prikazani na Sl. 2. Kakakteristike praćenja u odnosu na idelanu putanju definisanu izrazom (6) su dati na Sl. 3, dok su vrednosti zahtevanih upravljačkih signala, odnosno brzina desnog i levog točka prikazane na Sl. 4. Kvalitet estimacija totalnog poremećaja za analizirane vrednosti propusnog opsega opservera je prikazan na Sl. 5.

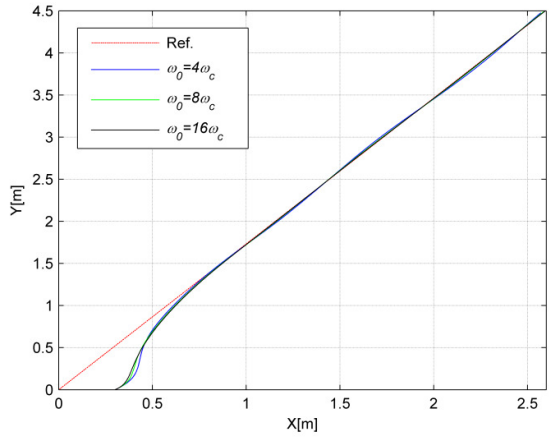

Sl. 2. Karakteristike praćenja zadate putanje za različite vrednosti propusnog opsega opservera

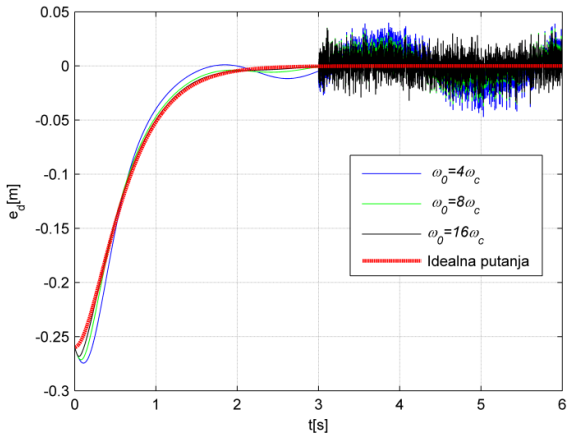

Sl. 3. Uporedne karakteristike praćenja u odnosu na idelanu putanju za različite propusne opsege opservera

Na osnovu rezultata sa Sl. 2 i Sl. 3 vidimo da vozilo, za sve tri vrednosti propusnog opsega opservera, uspešno prati zadatu putanju u uslovima postojanja pormećaja. Kao što je i očekivano, sistem sa najvećim propusnim opsegom opservera ostvaruje putanju najpribližniju idealnoj, što je posledica najmanje greške u estimaciji totalnog poremećaja (Sl. 5). Međutim, sa Sl. 4 se može uočiti da povećanje propusnog opsega opservera dovodi do porasta zahtevanih ugaonih brzina pogonskih točkova, kao i povećanja osetljivosti sistema na merni šum.

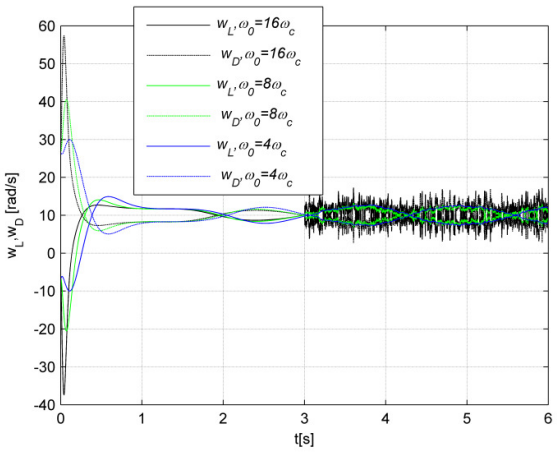

Sl. 4. Signali upravljanja pogonskim točkovima za različite vrednosti propusnog opsega opservera.

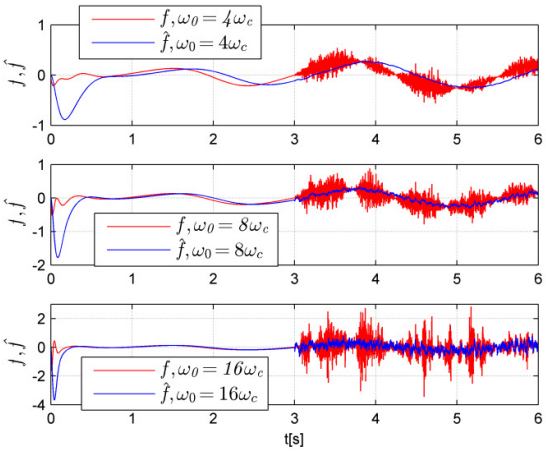

Sl. 5. Estimacije totalnog poremećaja za različite vrednosti propusnog opsega opservera.

U drugom scenariju analizirano je praćenje putanje definisane uglom $\theta_{ref} = \pi/4\,\text{rad}$. Početni položaj vozila je definisan koordinatama $x(0) = 0.3\text{m}$, $y(0) = 1\text{m}$ i $\theta_s(0) = 0\,rad$. Parametri regulatora su podešeni usvajanjem $\omega_c = 3\,rad/s$ i $\omega_o = 8\,\omega_c$, a simulirana su tri slučaja za različite dinamike proklizavanja gusenica. U prvom ($S1$) pretpostavljeno je da nema proklizavanja, odnosno, $a_D = 1, a_L = 1$, dok je u druga dva slučaja proklizavanje modelovano sa:

$$S2: a_D = 0.85, a_L = 0.95;$$
$$S3: a_D(t) = 0.85 + 0.15\sin(2t + \pi/4), a_L(t) = 0.85 + 0.15\cos(3t);$$

Trajektorije vozila, greške praćenja normalne na trajektoriju $e_d(t)$ i estimacije totalnog poremećaja su

prikazane na Sl. 6, Sl. 7 i Sl. 8, respektivno. Na osnovu dobijenih rezultata može se zaključiti da projektovani sistem ostvaruje zadovoljavajuće performanse praćenja u sva tri razmatrana slučaja. Kao što je i očekivano, najbolje performanse se dobijaju kada nema proklizavanja (*S*1) a vrednost totalnog poremećaja nula. U slučaju kada je proklizavanje gusenica konstantno (*S*2), putanja vozila odstupa od idealne u toku prilaska zadatoj trajektoriji, a nakon toga greška praćenja postaje nula, što je rezultat nulte greške estimacije totalnog poremećaja u stacionarnom stanju (Sl. 8). U trećem slučaju (*S*3) se uočava da, usled sinusoidalnog oblika proklizavanja, primenjeni prošireni opserver stanja ne može da estimira totalni poremećaj bez greške u stacionarnom stanju, (vidi Sl. 7), što dovodi do izvesnog odstupanja od zadate putanje.

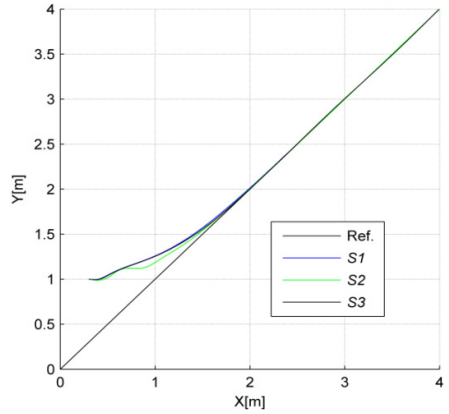

Sl. 6. Karakteristike praćenja zadate putanje za različite dinamike proklizavanja gusenica.

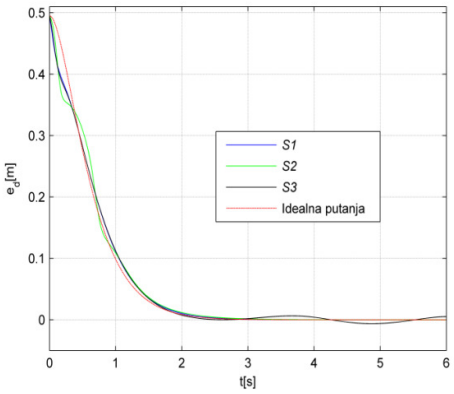

Sl. 7. Uporedne karakteristike praćenja u odnosu na idelanu putanju za različite dinamike proklizavanja gusenica.

V. Zaključak

Autonomno kretanje besposadnog vozila po zadatoj putanji, uz poremećaje linearne i ugaone brzine kretanja, realizovano je primenom kontrolera sa aktivnim potiskivanjem poremećaja. Problem je formulisan u vidu minimizacije najkraćeg (normalnog) rastojanja vozila od zadate putanje. Za estimaciju totalnog poremećaja projektovan je linearni prošireni opserver stanja, pri čemu je totalni poremećaj definisan tako da obuhvati i poremećaje koji ne deluju na istom ulazu kao i upravljački signal. Upravljački signal za aktivno potiskivanje totalnog poremećaja i približavanje vozila zadatoj putanji prema unapred definisanoj dinamici kretanja, je formiran na osnovu estimacija opservera i dostupnih merenja.

Koristeći model kretanja guseničnog vozila sa dve gusenice i dva pogonska točka, pokazano je da se poremećaji linearne i ugaone brzine vozila mogu efikasno estimirati primenom linearnog proširenog opservera stanja, pri čemu se povećanjem propusnog opsega opservera tačnost praćenja poboljšava, ali se povećavaju energetski zahtevi za aktuatore i osetljivost na merni šum. Primenjenim zakonom upravljanja uspešno se elimišu poremećaji tipa početnog stanja i konstantni poremećaji uzrokovani proklizavanjem, dok se uticaj dinamičnijih poremećaja može značajno umanjiti, uz odgovarajuće podešavanje parametara kontrolera.

Ideje za budući rad su, da se pre praktične implementacije na konkretnom besposadnom vozilu, analizira primena ADRC kontrolera za upravljanje intenzitetom brzine i ugaonom pozicijom vozila, sa ciljem autonomnog praćenja složenijih putanja.

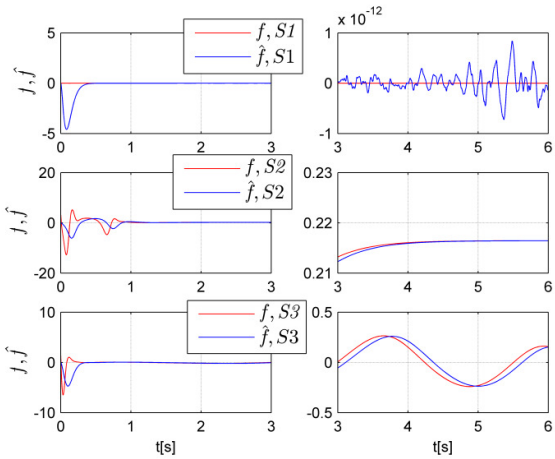

Sl. 8. Estimacije totalnog poremećaja za različite dinamike proklizavanja gusenica (prelazni period - levo, stacionarno stanje - desno).

Zahvalnica

Rad je podržan od strane Ministarstva odbrane Republike Srbije u okviru Projekta VA/TT/1/21-23.

Literatura

[1] Y. Liu, R. Bucknall, "A survey of formation control and motion planning of multiple unmanned vehicles", *Robotica*, vol. *36*, no. 7, pp. 1019-1047, 2018.

[2] J. Shin, D. Kwak, T. Lee, "Robust path control for an autonomous ground vehicle in rough terrain", *Control Engineering Practice*, vol. *98*, 104384, 2020.
[3] J. Ni, J. Hu, C. Xiang, "A review for design and dynamics control of unmanned ground vehicle", *Proceedings of the Institution of Mechanical Engineers, Part D: Journal of Automobile Engineering*, vol. *235*, no. 4, pp. 1084-1100, 2021.
[4] Y. Huang, W. Xue, "Active disturbance rejection control: methodology and theoretical analysis". *ISA transactions*, vol. *53*, no. 4, pp. 963-976, 2014.
[5] J. Han, "From PID to active disturbance rejection control", *IEEE transactions on Industrial Electronics*, vol. 56, no. 3, pp. 900-906, 2009.
[6] C. H. E. N. Sen, X. U. E. Wenchao, L. I. N. Zhiyun, Y. Huang, "On active disturbance rejection control for path following of automated guided vehicle with uncertain velocities", In *2019 American Control Conference (ACC)*, pp. 2446-2451, IEEE, July, 2019.

ABSTRACT

In this paper path following active disturbance rejection controller (ADRC), for unmanned ground vehicle (UGV), is proposed. Model nonlinearities, together with linear and angular velocity uncertainties, are treated as one total disturbance, enhancing both, matched and mismatched disturbances. Linear extended state observer (ESO) for total disturbance and nominal model states estimation is designed. Based on estimations and available measurements, the control signal for path following with predetermined transient behavior, is formulated. Simulation analysis, with tipical tracked unmanned ground vehicle motion configuration, is performed, and results illustrate efficiency of proposed control scheme in diferent path following scenarios.

Autonomous Active Disturbance Rejection Path Following Control of Unmanned Ground Vehicle

Momir Stanković i Stojadin Manojlović

Системи за подршку одлучивању базирани на вештачкој интелигенцији у третману умерене форме билијарног панкреатитиса

Ања Буљевић, Александар Глуховић, Мирна Н. Капетина, Александар Кнежевић, Зоран Д. Јеличић

***Апстракт*—У оквиру овог рада представљено је једно решење система за подршку одлучивању у лечењу умерене форме билијарног панкреатитиса. На основу параметара и показатеља из клиничке праксе, развијен је систем за усмеравање лекара приликом избора методе и поступка лечења овог запаљења панкреаса. Због релативно малог скупа података, услед специфичних медицинских процедура, избор релевантних обележја потврђен је кроз два формализма: корелационом анализом и стаблом одлучивања. На основу одабраних обележја, до финалног решења се долази уз ослонац на теорију потпорних вектора. Предложено решење нашло је своју примену у клиничкој пракси.**

***Кључне речи*: умерена форма билијарног панкреатитиса, корелациона анализа, стабло одлучивања, СВМ.**

I. УВОД

У наставку текста представићемо основне показатеље и параметре који карактеришу умерену форму билијарног панкреатитиса, али и конвенционалне и не тако конвенционалне начине лечења истог. Наиме, полазећи од претпоставке да се ради о мултидисциплинарном проблему са чистом медицинском применом разумевање медицинског дела је од највећег значаја не само за крајње кориснике, већ као и тумачење изабраних обележја и разумевања свих сложених феномена који се могу добити у математичком опису проблема.

Акутни панкреатитис представља ензимско инфламаторно обољење панкреаса, које може захватити како сам орган, тако и околна ткива. Инциденција обољења је око 17/100000 становника. Најчешћи етиолошки чиниоци који се везују за ово стање су билијарна калкулоза (45%) и конзумација алкохолних пића (35%). Умерене форме акутног панкреатитиса, које су и предмет овог истраживања, јављају се у 80% случајева и имају благ клинички ток са стопом морталитета од 1%. Акутни панкреатитис билијарне етиологије узрокован је калкулозом жучне кесе и/или жучних путева. Третман калкулозе билијарног стабла код умерене форме панкреатитиса, по актуелној препоруци Америчког удружења гастроентеролога и ендоскопских хирурга (American Assosiation of Gastroenterology and Endoscopic Surgeons - SAGES), своди се на уклањање жучне кесе лапароскопском холецистектомијом (ЛХ) са интраоперативном холангиографијом (ИОХ), у циљу превенције појаве новог атака болести. Уколико постоји сумња на присуство калкулуса у жучним каналима са повишеним вредностима билирубина, ради се ендоскопска ретроградна холангиопанкреатографија (ЕРЦП) са ендоскопском папилотомијом (ЕПТ), у циљу уклањања калкулуса и детритуса из жучних водова, и обезбеђивања нормалног протока жучи у дванаестопалачно црево. Ова процедура се углавном изводи пре ЛХ, мада се може радити и током ЛХ или након ње, [1].

На студији случајева Војводине, ЛХ је доступна у свим болницама, као и у клиничком центру. Међутим, ЕРЦП процедура могућа је само у Клиничком центру Војводине и то од стране једног лекара. По нашим најбољим сазнањима, укупан број лекара у Србији који изводе ову операцију је 3 или 4. Као кључно питање и задатак намеће се одабир скупа објективних параметара који ће лекара определити да само изведе широко доступну ЛХ или да ипак пацијента пошаље и на додатну процедуру ЕРЦП. Важно је напоменути да су анализирани само објективне параметре јер субјективни параметри (нпр. ултразвучни преглед) не могу да гарантују доследност у резултатима. Други начини прегледа, попут компјутеризоване томографије (ЦТ) и магнентна резнонце, нису широко доступни. При томе, за око 80% пацијената довољна је ЛХ, док свега 20% пацијената захтева и ЕРЦП.

Кључно за анализе у систему за подршку одлу-

А. Буљевић (anjabuljevic@uns.ac.rs)*, А. Глуховић (aleksandar.gluhovic@gmail.com)**, М. Н. Капетина (mirna.kapetina@uns.ac.rs)*, А. Кнежевић (aknezevic021@gmail.com)***, З. Д. Јеличић (jelicic@uns.ac.rs)*
* Универзитет у Новом Саду, Факултет техничких наука, Департман за рачунарство и аутоматику, Трг Доситеја Обрадовића 6, 21000, Нови Сад, Р. Србија
** New Hospital, Алберта Ајнштајна, Нови Сад, Р. Србија
*** Клинички центар Војводине, Хајдук Вељкова 1-9, Нови Сад, Р. Србија

чивању је било да минимизујемо лажно негативне закључке у потреби извођења ЕРЦП што је и заиста у складу са добром клиничком праксом. Због малог скупа података, избор обележја је урађен кроз корелациону анализу и стабло одлучивања што је оправдано са математичког аспекта [2], а такав начин рада се користи и у сличним медицинским истраживањима [3]. Према нашим најбољим сазнањима, овакав приступ подршке одлучивању у лечењу умерене форме акутног панкреатитиса је оригиналан и први пут се презентује у овом раду.

Рад је организован на следећи начин. У поглављу II приказан је одабир дискриминантних обележја. У поглављу III приказано је балансирање података. Формирање система за подршку одлучивању дато је у поглављу IV, док је закључак дат у поглављу V.

Ова студија је одобрена од стране Етичког комитета Медицинског факултета у Новом Саду и Етичке комисије Клиничког центра Војводине.

II. КОРЕЛАЦИОНА АНАЛИЗА И СТАБЛО ОДЛУЧИВАЊА

Први корак за решавање овог реалног проблема била је идентификација дискриминантних обележја (медицинских параметара) који су од круцијалне важности за указивање присуства калкулуса у жучним водовима. За потребе овог пројекта коришћени су медицински подаци пацијената оболелих од акутног панкреатитиса који су прикупљени у Клиничком центру Војводине. Приликом самог пријема пацијената прикупљено је преко 80 параметара. Неки од њих су били дескриптивни подаци о субјективном стању пацијената, затим о историји болести, као и објективни параметри попут налази крви и субјективни као што је ултразвучни преглед. Сви параметри су по правилу распоређени у временским серијама од 12 часова у првих 48 сати по пријему у болницу.

У добијеној бази података налазе се подаци за 100 пацијената лечених од умерене форме билијарног панкреатитиса. У литератури [1] проналазимо да се потенцијални кандидати за ЕРЦП могу узети у разматрање уколико је њихов Глазгов скор мањи од 3. Због ове чињенице, база се смањује на 96 пацијента. Од тих 96 пацијената, код њих 19 је рађен ЕРЦП, док је код 77 пацијената била довољна ЛХ.

Кроз нумеричке поступке издвајања обележја и пратећи начин размишљања лекара издвојили смо 5 објективних параметара: укупни билирубин, директни билирубин, алкална фосфатаза, ЦРП и гамаГТ. Субјективни параметри су показали извесну недоследност и нису могли бити узети у разматрање. Испитивање дискриминантности обележја рађено је на два начина:

1) коришћењем Пирсоновог коефицијента корелације и
2) коришћењем стабла одлучивања.

А. Одабир обележја коришћењем Пирсоновог коефицијента корелације

Поступак идентификације дискриминантних обележја започели смо корелационом анализом. Уколико желимо да испитамо да ли постоји зависност између два (или више) обележја, тада говоримо о утврђивању постојања корелације између тих обележја [4]. Коефицијент корелације је показатељ степена статистичке повезаности обележја и представља меру њихове линеарне зависности. Једна од најчешће коришћених мера повезаности два обележја јесте Пирсонов коефицијент корелације [4]. У табели I су приказани Пирсонови коефицијенти корелације за она обележја која имају највећи тражени коефицијент и они уједно представљају најзначајнија обележја за наш проблем.

Табела I
Пирсонов коефицијент корелација за дискриминантна обиљежја

Назив обележја	$\|\rho\|$
укупни билирубин	0.4051
директни билирубин	0.3837
алкална фосфатаза	0.3703
ЦРП	0.274
гама ГТ	0.2164

Из ове табеле можемо приметити да су чак и најзначајнија обележја по Пирсоновом коефицијенту корелације уствари у слабој корелацији са излазном променљивом. Како бисмо потврдили да су одабрана обележја заиста дискриминантна за наш проблем, урађена је и валидација добијених обележија коришћењем стабла одлучивања.

Б. Одабир обележја коришћењем стабла одлучивања

Други начин одређивања дискриминантних обележја који је имплементиран у овом раду јесте стабло одлучивања. Стабло одлучивања представља графички модел за визуализацију процеса одлучивања када се решавање проблема одлучивања своди на доношење више сукцесивних одлука, [5]. На почетку се бира параметар чија вредност најбоље дели расположиве узорке. Као што је познато, стабло одлучивања се осим за одређивање дискриминантних обележја, може користити и за класификацију података. Због малог броја података, као и слабе корелације улазних параметара са излазом, у овом случају стабло одлучивања је коришћено искључиво за селекцију обележја, док ће се метода вектора носача користити као подршка одлучивању у третману умерене форме билијарног панкреатитиса. Стабло одлучивања, поред селекције, омогућава нам и увид у значајност изабраних обележја, као и сам „пут" селекције. Предност стабла одлучивања у односу на Пирсонов коефицијент корелације јесте аутоматска селекција обележја [6].

За потребе овог рада коришћен је ID3 алгоритам. Квантитативна мера коју ID3 алгоритам користи ка-

ко би одредио најбоља обележја јесте информациона добит [7]. Симулације су вршене са различитим конфигурацијама стабла. Дубина стабла је узимала вредности на интервалу од 3 до 10, док се број листова се налазио у опсегу од 2 до 10. Посматрајући добијена стабла одлучивања примећено је да се као заједнички садржаоци свих стабала издвајају следећа обележја: укупни билирубин, ЦРП, директни билирубин, алкална фосфатаза и гама ГТ. Осим тога, наведена обележја се у већини генерисаних стабала налазе ближе корену стабла, односно на мањим дубинама стабла. Упоређујући резултате које смо добили коришћењем стабла одлучивања и Пирсоновог коефицијента корелације, потврдили смо потпуну подударност између дискриминантних обележја добијених коришћењем ова два поступка.

III. БАЛАНСИРАЊЕ ПОДАТАКА

Следећи проблем који се намеће је небалансираност података. Небалансираност података подразумева ситуацију у којој се број узорака значајно разликује по класама у поступку класификације. Класификатори машинског учења тешко се носе са небалансираним скупом података за обуку, јер су осетљиви на пропорционалност различитих класа, па се као последица јавља тенденција алгоритама да фаворизују класу са највећим уделом испитаника што најчешће резултује „обмањујућом" тачношћу. То је посебно проблематично када је од интереса тачна класификација „ретке" (мањинске) класе, али налазимо висок проценат тачности који је заправо последица исправне класификације већинске класе. Ову чињеницу овде експлицитно наводимо, не само да нагласимо потребу за балансирањем података, већ и да уведемо посебну метрику за оцену квалитета предикције. С обзиром на то да алгоритми машинског учења имају за циљ да смање укупну стопу грешке, неће обраћати посебну пажњу на мањинску класу, и вероватно неће успети да направе тачно предвиђање за ову класу, јер о њој не садржи довољно података.

У бази података разматраног проблема, од укупно 96 пацијената, код само 19 испитаника је рађен ЕРЦП, док код 77 испитаника није рађен ЕРЦП. Као што је наведено у уводном поглављу, приоритет је да се минимизују лажно негативни закључци у потреби извођења ЕРЦП који у овом случају представља мањинску класу. Дакле, неопходно је било урадити балансирање података.

У литератури [8] се може пронаћи неколицина потенцијалних метода за решавање овог проблема, а као најбољи метод се наводи додавање нових података у класе са процентуално мањим бројем узорака. Међутим, у пракси је то веома тешко постићи, па се прибегава неким другим методама. Један од најчешће коришћених је да се из већинске класе избаце узорци како би се број узорака већинске класе изједначио са бројем узорака мањинске класе. При томе, мора се водити рачуна да укупан број узорака мора бити бар 10 пута већи од броја изабраних обележја [9].

Ова препорука за балансирање података је искоришћена у овом раду на следећи начин. На случајан начин се од 77 испитаника код којих није рађен ЕРЦП изабере 40 и тих 40 испитаника улазе у процес обуке СВМ алгоритмом, заједно са 19 испитаника код којих је рађен ЕРЦП. Примећујемо да подаци и даље нису најбоље балансирани, али због ограничења да укупан број узорака мора бити барем 10 пута већи од укупног броја обележја, ово је најбоље што смо могли да добијемо из коришћене базе података.

IV. СВМ МАТЕМАТИЧКИ МОДЕЛ

Након што смо идентификовали параметре од интереса и избалансирали податке, неопходно је било да се на основу издвојених параметара формира систем за подршку одлучивању у третману умерене форме акутног билијарног панкреатитиса. Због заиста малог скупа података, нарочито малог за пацијенте којима је рађен ЕРЦП, определили смо се за математички модел уз ослонац на теорију потпорних вектора (СВМ) [10]. Метода класификације базирана на векторима носачима представља један од модела машинског учења који се веома често користи како за класификациону, тако и за регресиону анализу. СВМ алгоритам је довољно познат алгоритам, па неће бити детаљно извођен у овом раду, а његово детаљно математичко извођење можете пронаћи у литератури [11], [12].

Посебна пажња је била посвећена оптимизацији параметара СВМ алгоритма. Будући да перформансе генерализације СВМ алгоритма у великој мери зависе од параметара C (хиперпараметар који прави компомис између сложености модела и степена до кога се толеришу одступања модела), ε (хиперпараметар који контролише ширину неосетљиве зоне, а његова вредност утиче на број вектора носача) и γ (параметар који одређује облик изабране кернел функције), неопходно је извршити њихову оптимизацију. Према [13], [14], између наведених параметара постоји јака веза, тако да је препорука да се они оптимизују истовремено, а не одвојено. Оптимизација параметара је извршена уз помоћ алгоритма роја честица [15] и као критеријум оптималности је коришћена средња квадратна грешка [16]. Као кернел функције су прослеђиване: радијална, гаусова, линеарна и полиномна кернел функција. Након оптимизација кернел функција и свих њених пратећих параметара, добијено је да се најбољи резултати добију за СВМ алгоритам који има радијалну кернел функцију и добијени су следећи параметри: $C = 10^2$, $\varepsilon = 10^{-3}$ и $\gamma = 10^{-1}$.

Иако је урађено балансирање података, класе и даље нису у потпуности балансиране. Осим тога, СВМ модел је јако осетљив на улазне податке и неретко од скупа улазних података, зависи и тачност класификације СВМ. Како би се добили што објективинији

резултати, спроведен је експеримент описан у наставку. Узорци који се прослеђују СВМ као улазни подаци су прослеђивани на следећи начин:

- од 19 испитаника код којих је рађен ЕРЦП, на случајан начин се бира 80% испитаника (15 испитаника) који се прослеђују СВМ алгоритму за обуку и валидацију, док је на преостала 4 узорка вршено тестирање добијеног модела
- од 77 испитаника код којих није рађен ЕРЦП на случајан начин се изабере 40 испитаника. Од тих 40 испитаника, на случајан начин се бира 80% испитаника (32 испитаника) који се прослеђују СВМ алгортиму за обуку и валидацију, док је на преосталих 8 узорака вршено тестирање добијеног модела.

Као оцена успешности одабраног класификационог модела, уобичајено се користе стандардизоване мере и оцене којима се квантификује рад пројектованог система за класификацију и предикцију. Под оцењивањем, односно процењивањем рада система за предикцију углавном се мисли на одређивање вредности неких од стандардних мера којима се квантификује његов учинак односно перформансе. Мера квалитета представља потенцијал модела да коректно предвиди класу новог податка. Матрица конфузије (engl. *confusion matrix*) представља детаљан и прегледан приказ бројева исправно и погрешно класификкваних узорака на основу којих се могу вршити оцене добијеног модела класификације. Општи облик матрице конфузије за бинарну класификацију је приказан табелом II, где је

- TP (true positive; стварно позитивни) - број узорака који припадају позитивној класи, а додељена им је позитивна класа,
- TN (true negative; стварно негативни) - број узорака који припадају негативној класи, а додељена им је негативна класа,
- FP (false positive; лажно позитивни) - број узорака који припадају негативној класи, а додељена им је позитивна класа,
- FN (false negative; лажно негативни) - број узорака који припадају позитивној класи, а додељена им је негативна класа

Табела II
Општи облик матрице конфузије.

		Предвиђена класа	
		Класа = 0	Класа = 1
Праве класе	Класа = 0	TN	FP
	Класа = 1	FN	TP

Табела III представља један пример матрице конфузије СВМ класификатора за случај када треба да се спроведе ЕРЦП. Примећујемо да је у овом случају од 40 испитаника којима је довољна само ЛХ процедура, наш класификациони модел то погодио за 39 испитаника, док је за само једног испитаника рекао да му је неопхдан и ЕРЦП. Што се тиче 19 испитаника којима је неопходан и ЕРЦП, наш класификациони модел је одговарајућу класу погодио за 17 испитаника, док је за двојицу испитаника погрешно доделио класу.

Табела III
Матрица конфузије за случајеве када је неопходан ЕРЦП.

		Предикција	
		ЛХ	ЛХ и ЕРЦП
Стварни резултати	ЛХ	39	1
	ЛХ и ЕРЦП	2	17

По завршетку креирања класификационог модела, корисно је тестирати његове перформансе на скупу података који му је непознат, при чему је неопходно да тај скуп података садржи информације о класама. Овакав вид тестирања представља непристрасну оцену генерализације. Најчешће се користи K-слојна унакрсна валидација (енг. K-fold cross-validation). K-слојна унакрсна валидација (кросвалидација) је техника евалуације класификационих модела која се изводи тако што се оригинални скуп података дели на k једнаких подскупова. Један подскуп се користи за тестирање, док се сви остали подскупови користе за тренирање. Овај поступак се понавља у k итерација тако да се сваки подскуп користи тачно једном за тестирање. По завршетку свих итерација, издваја се онај модел који је имао најмању грешку класификације, [17].

Већ је напоменуто да је излаз јако осетљив на добијени скуп улазних података, па да би се добили што објективнији резултати поступак описан горе је поновљен у 100 итерација са одабраним СВМ моделом. На овај начин су праћене две тачности модела: тачност над обучавајућим скупом података у процесу кросвалидације и тачност над тестним скупом. Тачност, као једна од најчешће коришћених мера за приказивање успешности класификације, представља однос укупног броја коректних предвиђања и укупног броја предвиђања. Математички, тачност записујемо

$$\text{тачност} = \frac{TP + TN}{TP + TN + FP + FN}.$$

Промена тачности над обучавајућим скупом у процесу кросвалидације за одабрани модел за 100 итерација у зависности од одабраних улазних података дат је на слици 1. Просечна тачност овог модела износи 90.51%.

Промена тачности над тестним скупом за одабрани модел за 100 итерација у зависности од одабраних улазних података дата је на слици 2. Просечна тачност овог модела износи 82.68%.

Поред тачности, морамо обратити пажњу на још неколико показатеља успешности класификације. Прецизност је мера слична тачности, али се односи искључиво на једну посматрану класу. Она представља

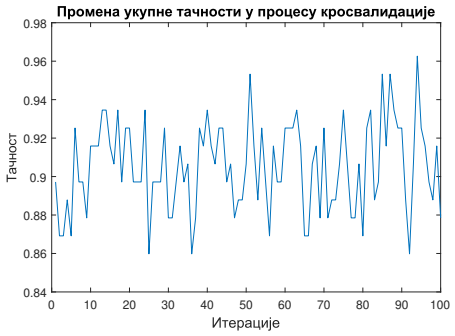

Слика 1. Промена укупне тачности у процесу кросвалидације кроз итерације

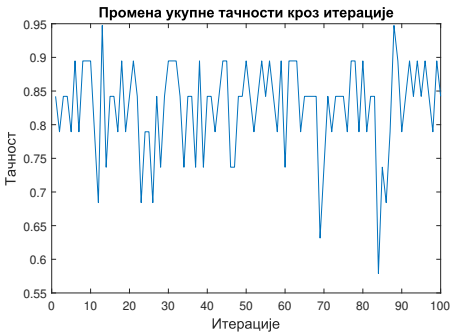

Слика 2. Промена укупне тачности кроз итерације

однос тачних позитивних предвиђања и укупног броја случајева у којима је класификатор предвидио посматрану класу. Осетљивост приказује однос коректно предвиђених вектора атрибута неке класе и укупног броја правих понављања те класе у скупу података. Специфичност је способност теста да коректно идентификује одсуство неког атрибута, а може да се интерпретира и као процена условне вероватноће да атрибут није идентификован, уз услов да га на посматраној позицији заиста нема. Наведене мере математички можемо записати на следећи начин

$$\text{прецизност} = \frac{TP}{TP+FP},$$
$$\text{осетљивост} = \frac{TP}{TP+FN},$$
$$\text{специфичност} = \frac{TN}{FP+TN}.$$

Графици наведених мера прецизности, осетљивости и специфичности су приказани на сликама 3, 4 и 5 респективно. Просечна вредност прецизности износи 73.23%, просечна вриједност осетљивости износи 76.25%, док просечна вредност специфичности износи 64.88%.

Као што је већ речено, нама је од посебне важности тачност погађања за случајеве када је непоходна ЕРЦП процедура, односно битно нам је да одговор класификационог алгоритма за случај када треба да се ради ЕРЦП процедура буде тачан. Због тога је по-

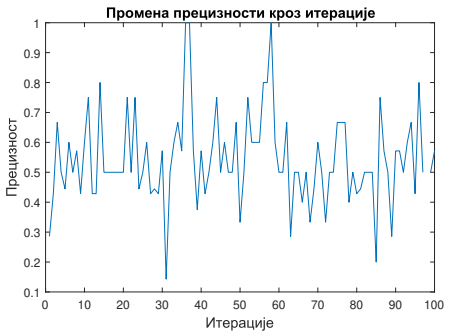

Слика 3. Промена прецизности кроз итерације

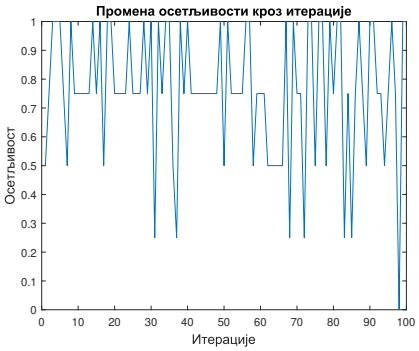

Слика 4. Промена осетљивости кроз итерације

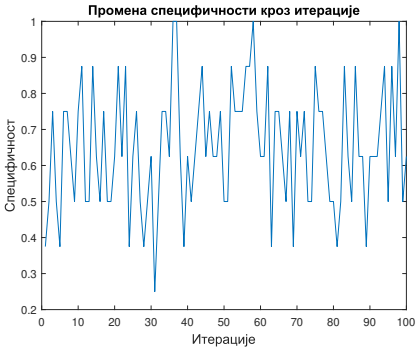

Слика 5. Промена специфичности кроз итерације

себно издвојена и тачност модела само за ову класу и приказана је на слици 6. Просечна вредност тачности за овај случај износи 76.25%.

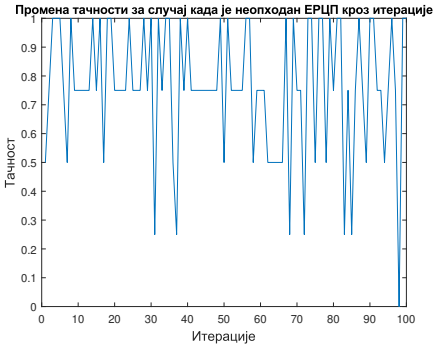

Слика 6. Промена тачности за случај када је неопходан ЕРЦП кроз итерације

Анализирајући вредности за приказане мере, можемо да закључимо да одабрани класификациони СВМ модел даје задовољавајуће резултате. Примећујемо да је укупна тачност модела већа у односу на тачност модела када испитујемо случај када је неопходна и ЕРЦП процедура, али то смо и очекивали пошто та класа представља мањинску класу за овај проблем.

V. ЗАКЉУЧАК

У склопу овог рада пројектован је систем за подршку одлучивању у третману умерене форме билијарног панкреатитиса. Пројектовању система за подршку одлучивању претходила је предобрада података. Приликом самог пријема пацијената прикупљено је преко 80 медицинских параметара, па је било неопходно одабрати најзначајније параметре који би нам указали на присуство калкулозе у жучним водовима. Дискриминантна обележја су одређена коришћењем Пирсоновог коефицијента корелације и као дискриминантна обележја су се издвојили: укупни билирубин, ЦРП, директни билирубин, алкална фосфатаза и гама ГТ. Ваљаност издвојених обележја потврђена је применом стабла одлучивања.

Главни циљ нашег рада је био да минимизујемо лажно негативне закључке у потреби извођења ЕРЦП. За формирање система за подршку одлучивању коришћен је СВМ алгоритам, коме је претходила процедура балансирање података по класама. Оптимизација параматера модела над тестним скупом података је била 82.68%. Пошто нам је од посебне важности била тачна предикција случајева када је неопходан ЕРЦП, издвојена је и просечна тачност модела за овај случај и она износи 76.25%.

Битно је напоменути да лекари у својој клиничкој пракси заиста користе издовјена обележја како би идентификовали присуство калкулузе, а последично следи одлука да ли треба да се ради додатна процедура како би се решио проблем оваквог оболења панкреаса. Оно што се математички не може описати, бар не на малом скупу података, јесте субјективни осећај, знање и искуство искусног лекара из клиничке праксе који приликом ЛХ може да примети да ли у жучним водовима постоји калкулуза и на основу тога да донесе процену да ли је потребан ЕРЦП.

ЗАХВАЛНИЦА

Овај рад је подржан од стране Министарства просвете, науке и технолошког развоја кроз пројекат број 451-03-68/2020-14/200156: „Иновативна научна и уметничка испитивања из домена делатности ФТН-а”

ЛИТЕРАТУРА

[1] А. Глуховић, “Алгоритам примене лапароскопске холецистектомије и ендоскопске ретроградне холангиопанкреатографије са папилотомијом у третману умерене форме билијарног панкреатитиса.” Докторска дисертација. Нови Сад, 2016.

[2] H. Zhou, J. Zhang, Y. Zhou, X. Guo, and Y. Ma, “A feature selection algorithm of decision tree based on feature weight,” *Expert Systems with Applications*, vol. 164, p. 113842, 2021.

[3] Q. Qiu, Y.-j. Nian, Y. Guo, L. Tang, N. Lu, L.-z. Wen, B. Wang, D.-f. Chen, and K.-j. Liu, “Development and validation of three machine-learning models for predicting multiple organ failure in moderately severe and severe acute pancreatitis,” *BMC gastroenterology*, vol. 19, no. 1, pp. 1–9, 2019.

[4] M. A. Hall, “Correlation-based feature selection for discrete and numeric class machine learning,” in *Proceedings of the Seventeenth International Conference on Machine Learning*, ICML ’00, (San Francisco, CA, USA), p. 359–366, Morgan Kaufmann Publishers Inc., 2000.

[5] A. Geron, “Hands-on machine learning with scikit-learn, keras tensorflow.” O’Reilly, 2019.

[6] K. G. (auth.), *Meta-Learning in Decision Tree Induction*. Studies in Computational Intelligence 498, Springer International Publishing, 1 ed., 2014.

[7] L. Breiman, J. H. Friedman, R. A. Olshen, and C. J. Stone, *Classification and Regression Trees*. Monterey, CA: Wadsworth and Brooks, 1984.

[8] G. E. Batista, R. C. Prati, and M. C. Monard, “A study of the behavior of several methods for balancing machine learning training data,” *ACM SIGKDD explorations newsletter*, vol. 6, no. 1, pp. 20–29, 2004.

[9] V. Sugumaran and K. Ramachandran, “Effect of number of features on classification of roller bearing faults using svm and psvm,” *Expert Systems with Applications*, vol. 38, no. 4, pp. 4088–4096, 2011.

[10] C. Cortes and V. Vapnik, “Support-vector networks,” *Machine learning*, vol. 20, no. 3, pp. 273–297, 1995.

[11] B. Schölkopf, A. J. Smola, F. Bach, *et al.*, *Learning with kernels: support vector machines, regularization, optimization, and beyond*. MIT press, 2002.

[12] F. Dedov, *The Python Bible Volume 4: Machine Learning (Neural Networks, Tensorflow, Sklearn, SVM)*. The Python Bible Series, Independently Published, 2019.

[13] V. Cherkassky and Y. Ma, “Practical selection of svm parameters and noise estimation for svm regression,” *Neural networks*, vol. 17, no. 1, pp. 113–126, 2004.

[14] Z. Shaowu, W. Lianghong, Y. Xiaofang, and T. Wen, “Parameters selection of svm for function approximation based on differential evolution,” in *International Conference on Intelligent Systems and Knowledge Engineering 2007*, pp. 529–535, Atlantis Press, 2007.

[15] Ž. Kanović, M. R. Rapaić, and Z. D. Jeličić, “Generalized particle swarm optimization algorithm-theoretical and empirical analysis with application in fault detection,” *Applied Mathematics and Computation*, vol. 217, no. 24, pp. 10175–10186, 2011.

[16] Y. Ren and G. Bai, “Determination of optimal svm parameters by using ga/pso,” *Journal of computers*, vol. 5, no. 8, pp. 1160–1168, 2010.

[17] C.-W. Hsu, C.-C. Chang, C.-J. Lin, *et al.*, “A practical guide to support vector classification,” 2003.

Abstract

This paper presents one solution for the decision support system in the treatment of moderate form of biliary pancreatitis. Based on parameters and indications from clinical practices, the system for directing doctors in selecting methods and procedures for treating this pancreas ailment has been developed. Due to specific medical procedures, the data set is relatively small, so the choice of relevant features was confirmed through two formalisms: the correlation analysis and the decision tree. Based on the selected features, the final solution is reached by the theory of supporting vectors. The proposed solution has found its application in clinical practice.

Decision support system based on artificial intelligence in the treatment of moderate form of biliary pancreatitis

Anja Buljević, Aleksandar Gluhović, Mirna N. Kapetina, Aleksandar Knežević, Zoran D. Jeličić

Predikcija ishoda protetičke rehabilitacije nakon amputacije donjih ekstremiteta uz oslonac na algoritme veštačke inteligencije

Jovana Arsenović, Aleksandar Knežević, Mirna N. Kapetina i Zoran D. Jeličić

***Apstrakt*—Protetička rehabilitacija trenutno predstavlja najbolji tretman za pacijente sa amputacijom donjih ekstremiteta. Međutim, fabrikacija proteze i prateća protetička rehabilitacija predstavljaju veoma dug i skup proces koji nekada ne dovodi do poboljšanja mobilnosti i kvaliteta života pacijenata. Zbog toga je neophodno predvideti ishod rehabilitacionog tretmana. Glavni zadatak ovog rada bio je da se napravi alat, uz oslonac na algoritme veštačke inteligencije, koji bi se mogao primeniti u ranim fazama, kako bi se napravila što bolja predikcija ishoda rehabilitacije pacijenata sa amputacijom donjih ekstemiteta, odnosno kako bi se predvideo K-nivo (engl. *Medicare Functional Classification Level, K-level*), ishod testa dvominutnog hoda (engl. *two minute walk test*) i testa ustani i kreni (engl. *timed up and go test*). Evaluacija modela vršena je nad realnim podacima pacijenata Klinike za rehabilitaciju, Kliničkog centra Vojvodine. Dobijeni rezultati pokazuju značajno poboljšanje, u pogledu performansi klasifikatora, u odnosu na prethodne metode i potvđuju izbor nekih od najznačajnijih parametara prilikom identifikacije pacijenata.**

***Ključne reči*—Predikcija, veštačka inteligencija, metoda vektora nosača - SVM, stabla odluke, amputacija, rehabilitacija.**

I. Uvod

Amputacija donjih ekstremiteta predstavlja hirurški postupak koji se primenjuje radi odstranjivanja ishemičnog, inficiranog, nekrotičnog tkiva ili lokalnog tumora, kada nije moguća resekcija [1]. U svetu se godišnje izvrši preko milion amputacija noge, procena je Svetske zdravstvene organizacije i Međunarodne dijabetološke federacije, dok se prema podacima Kliničkog centra Vojvodine, u toj ustanovi godišnje izvrši više od 100 amputacija donjih ekstremiteta iznad nivoa skočnog zgloba [1]. Kretanje predstavlja osnovnu potrebu čoveka, a hod je primarni način kretanja ljudi, tako da je glavni cilj rehabilitacionog procesa ponovno uspostavljanje ove funkcije. Poboljšanje sveobuhvatnog stanja i kvaliteta života osoba sa amputacijom donjih ekstremiteta omogućava protetička rehabilitacija.

Proteze mogu omogućiti funkionalni hod i nadomestiti fizički nedostatak i trenutno predstavljaju najbolje rešenje za osobe sa amputacijom donjih ekstremiteta [2]. Nažalost, nisu sve osobe sa amputacijom dobri kandidati za protetičku rehabilitaciju, a ovaj skup i dug proces nekad ne dovodi do poboljšanja mobilnosti i kvaliteta života u meri u kojoj se očekivalo. Stoga postoji potreba da se predvidi ishod potencionalnog rehabilitacionog tretmana.

Cilj ovog istraživanja bio je da se napravi alat, uz oslonac na algoritme veštačke inteligencije, koji bi se mogao što ranije primeniti, kako bi se napravila što bolja predikcija ishoda rehabilitacije pacijenata sa amputacijom, odnosno kako bi se predvideo K-nivo i ishodi testa dvominutnog hoda i testa ustani i kreni. Da bi predikcija bila što uspešnija potrebno je identifikovati parametre za predikciju, odnosno one faktore koji utiču na osposobljenost za hod uz pomoć proteze. Prilikom identifikovanja pacijenata, odnosno tokom donošenja odluke da li je pacijent dobar kandidat za propisivanje proteze i započinjanje protetičke rehabilitacije, lekari se fokusiraju na određenje parametre (engl. *feature*, u daljem tekstu obeležje, atribut, faktor, varijabla ili parametar). Oni moraju biti strogo definisani, što jednostavniji za procenu, da ih ne bude previse, a ni premalo, tako da doprinose najboljoj tačnosti klasifikatora i ne predstaljaju problem lekarima za određivanje. Svi autori koji su pisali na ovu temu, složili su se da postoji više faktora koji utiču na uspešnost predikcije hoda uz pomoć proteze, ali koji su dominantni i dalje je predmet istraživanja.

U radu [3] za konstruisanje predikcionog modela baziranog na vektorima nosačima (engl. *support vector machine*, u daljem tekstu SVM) korišćeno je 11 varijabli: starost, pol, uzrok i nivo amputacije, period od amputacije do protetičke rehabilitacije, funkcionalni komorbidetni indeks, pisustvo šećerne bolesti, prisustvo partnera, ograničena ekstenzija kuka ili kolena rezidualnog ekstremiteta i mobilnost pri prijemu. Za izbor najboljih obeležja u radu [3] korišćen je genetski algoritam, koji je izdvojio starost, funkcionalni komorbidetni indeks, nivo amputacije i mobilnost pri prijemu kao dominantne faktore. Kriterijum optimalnosti bila je tačnost klasifikacije nad test skupom. Preciznost modela bila je u intervalu od 72,5% do 82,5%. Kao dominantna obeležja za klasifikaciju u radu [4] izabran je test šestominutnog hoda (engl. *6-minute walk test*) i test stojanja na jednoj nozi (engl. *one-leg standing test*). Na osnovu ovih parametara K-nivo su predviđali sa osetljivošću blizu 90%. Ono što su u ovom radu istakli jeste da je klasifikacija rađena samo za pacijente sa transtibijalnom amputacijom. U radu [5] kao nezavisni

Jovana Arsenović (email: arsenovic.jovana@uns.ac.rs), Mirna N. Kapetina (email: mirna.kapetina@uns.ac.rs), Zoran D. Jeličić (email: jelicic@uns.ac.rs) - Univerzitet u Novom Sadu, Fakultet tehničkih nauka, Katedra za automatsko upravljanje, Trg Dositeja Obradovića 6, 21000 Novi Sad, Srbija.

Aleksandar Knežević (email: aleksandar.knezevic@mf.uns.ac.rs) – Univerzitet u Novom Sadu, Medicinski fakultet, Katedra za fizikalnu medicinu i rehabilitaciju, Hajduk Veljkova 3, 21137 Novi Sad, Srbija.

prediktivni faktori predloženi su pol pacijenta, starost, dužina trajanja rehabilitacije i dužina čekanja na početak primarne protetičke rehabilitacije, dok su u radu [6] izdvojena sledeća obeležja: pređenja razdaljina i trajanje hoda, nivo amputacije, pol i vremenski interval od amputacije do protetičke rehabilitacije. Trenutno, ne postoje tačno definisane kliničke preporuke za određivanje kandidata za protetičku rehabilitaciju, kao ni jasnih faktora koji bi potencijalno mogli predvideti ishod rehabilitacije. U radovima [7, 8] izvršen je sistematičan pregled literature napisan na ovu temu od 2007. godine do 2015. Faktori koji su označeni kao potencijalni prediktori su starost, nivo amputacije, funkcionalni status pri prijemu, kao i komorbiditeti. Međutim, u radu [9], koji se takođe bavio pregledom literature na ovu temu, jedino je uočena snažna veza između parametra balans i sposobnosti hoda uz pomoć proteze.

Poglavlje 2 sadrži opis dostupnog skupa podataka, kao i mehanizme za rešavanje problema nedostajućih podataka i balansiranje skupa podataka. U poglavlju 3 dat je opis predloženih metoda i izbora obeležja za klasifikaciju. Ostvareni rezultati i diskusija predstavljeni su u poglavlju 4. Naposletku, u zaključku, u sklopu poglavlja 5, dat je rezime i naznačeni su pravci daljeg isteživanja.

II. Eksperimentalni podaci

U radu je analiziran uticaj različitih atributa na predikciju ishoda rehabilitacionog tretmana pacijenata sa amputacijom donjih ekstremiteta. Podaci koji su korišćeni u istraživanju, prikupljani su u Kliničkom centru Vojvodine u period između 2010. i 2012. godine. Bazu podataka činila su 104 pacijenta, različitog pola i starosti (62,1 ± 10,9 godina) koja su bila podvrgnuta eksperimentu. Kriterijum za uključivanje pacijenata u istraživanje bila je jednostrana amputacija donjih ekstremiteta iznad nivoa skočnog zgloba pacijenata koji su prvi put snadbeveni protezom. Svi ispitanici dali su pismeni informativni pristanak za učešće u ovoj studiji. Istraživanje je dobilo saglasnost za sprovođenje od strane Etičke komisije Medicinskog fakulteta u Novom Sadu i Kliničkog centra Vojvodine.

A. Balansiranost skupa podataka

Kao što je već napomenuto, 104 pacijenta je učestvovalo u istraživanju, a njihova klasna raspodela za kategoriju K-nivo je prikazana na slici 1. Sa grafika se može očitati da je međuklasna razlika u broju ispitanika veoma velika.

Klasifikatori mašinskog učenja ne mogu se nositi sa nebalnsiranim setom podatka, odnosno ovi algoritmi imaju tedenciju da favorizuju klasu sa najvećim udelom ispitanika [10]. Ovakva neuravnoteženost može posebno da bude problematična kada nas zanima tačna klasifikacija manjinskih klasa, klasa sa najmanjim brojem ispitanika, kao što su u našem slučaju klase označene kao 0 i 4.

K-nivo predstavlja međunarodno priznatu skalu koja se koristi za predstavljanje ishoda rehabilitacionog tretmana pacijenata sa amputacijom donjih ekstremiteta. Donja granica K-nivoa, označena klasom 0, predstavlja nemogućnost samostalnog hoda uz pomoć proteze, dok je maksimalni ishod

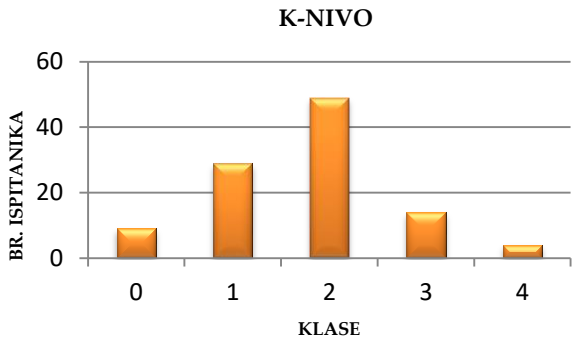

Sl. 1. Raspodela ispitanika prema klasama za kategoriju K-nivo.

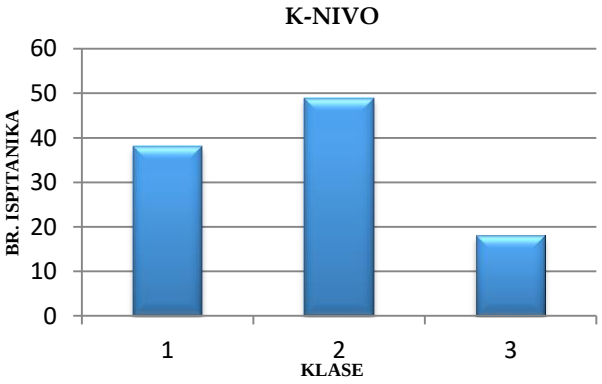

Sl. 2. Modifikovane klase kategoriju K-nivo.

rehabilitacionog tretmana označen klasom 4. Sa slike 1 se očitava velika međuklasna razlika u broju ispitanika.

Da bi se smanjila neuravnoteženost broja ispitanika po klasama, izvršena je modifikacija klasa (slika 2), po uzoru na [3, 4]. Novi nivo 1 označavao bi nemogućnost samostalnog hoda uz pomoć proteze ili strogo ograničen hod na veoma kratkim relacijama (hod u kućnim uslovima), praktično, sama proteza ne bi značajno poboljšala mobilnost pacijenta, niti njegov kvalitet života. Posle modifikacije, ovoj klasi pripadalo je 38 ispitanika. Nivoom 2 predstavljao bi se ishod rehabilitacije pacijenata koji su imali mogućnost hoda na relacijama koje bi bile i izvan kuće ali uz značajna ograničenja, dok pacijenti nivoa 3 bi bili osposobljeni za hod na dugim relacijama, uz minimalna ili čak bez ograničenja. Nakon modifikacije, ovim grupama pripadalo je 49, odnosno 17 ispitanika, respektivno.

Na osnovu rezultata testa dvominutnog hoda i testa ustani i kreni, formirane su nove kategorije, koje bi potencijalno predstavljale ishode rehabilitacionog tretmana. Ukoliko bi za vreme testa dvominutnog hoda ispitanik prešao manje od 26 metara, klasifikovan bi bio u klasu TMWT1. U slučaju da bi ispitanik prešao između 25 metara i 55 metara, pripadao bi klasi TMWT2, a ukoliko bi prešao više od 55 metara za vreme dvominutnog testa pripadao bi klasi TMWT3. Što je veći indeks klase, odnosno što je ispitanik prešao više metara za vreme testa, ishod rehabilitacionog tretmana je bolji.

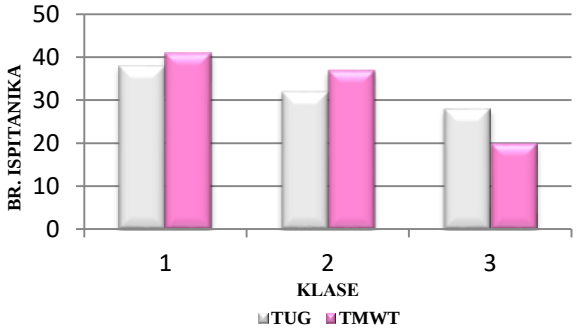

Sl. 3. Raspodela ispitanika za test ustani i kreni - TUG (belo) i test dvominutnog hoda - TMWT (roze).

Test ustani i kreni 28 ispitanika završilo je za manje od 30 sekundi i svrstano je u klasu TUG3, 32 ispitanika klasifikovano je u TUG2, odnosno bilo im je neophodno između 30 i 60 sekundi za test, dok je njima 38 bilo potrebno više od 60 sekundi da bi završili test. Ovi podaci grafički su predstavljeni na slici 3.

Modifikacijom klasa smanjena je razlika broja ispitanika među klasama ali je i dalje postojala razlika koja bi potencijalno mogla uzrokovati favorizaciju većinske klase. Dodatno, ta razlika je smanjenja ponavljanjem uzoraka manjinske klase na slučajan način.

B. Rešavanje problema nedostajućih podataka

Istraživanje, koje je realizovano u Kliničkom centru Vojvodine, sprovedeno je kao prospektivna serija slučaja, što za posledicu ima mali broj nedostajućih podataka u bazi. Od 19 parametara kojima su predstavljeni pacijenti, kod samo 3 parametra se javljaju nedostajući podaci (slika 4).

Jedan od najpopularnijih načina rešavanja problematike nedostajućih podataka jeste zamena nedostajućih podataka uzoračkom srednjom vrednošću ili modom [11]. Iako se ovom metodom umanjuje varijabilnost podatak (varijansa) i procene kovarijanse i korelacije u podacima (jer se ignoriše odnos između varijabli), zbog malog broja nedostajućih podataka smatrano je da ove promene nemaju statistički uticaj na konačni rezultat.

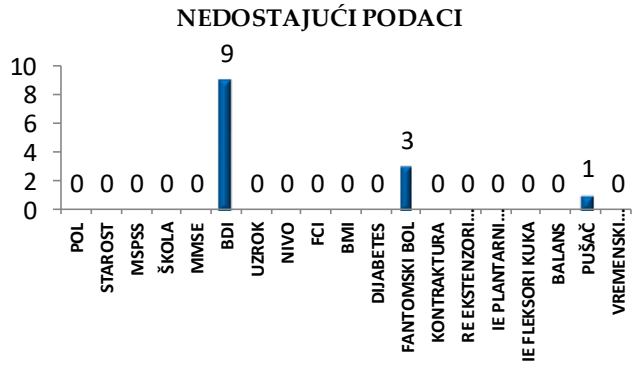

Sl. 4. Raspodela nedostajućih podataka prema parametrima. Nedostajući podaci se javljaju kod obeležja Bekova skala depresivnosti, fantomski bol i obeležja pušač.

III. IZBOR OBELEŽJA I METODE ZA KLASIFIKACIJU

Izbor adekvatnih obeležja ima ključan uticaj kako na kvalitet, tako i na efikasnost klasifikacije. Odabir (selekcija) obeležja podrazumeva biranje bitnijih (diskriminatornih) obeležja iz celog skupa podataka [11]. Na slici 5 prikazane su Gausove krive za obeležja balans, nivo amputacije i fantomski bol. Sa slike zaključujemo da obeležje fantomski bol nije diskriminatorno. Srednja vrednost obeležja svake klase, prikazane na apcisi, imaju slične vrendosti. Takođe, i verovatnoće ovog obeležja po klasama su veoma slične, pa je na osnovu ovog obeležja gotovo nemoguće klasno razdvojiti ispitanike. Međutim, obeležja balans i nivo amputacije moguće je okarakterisati kao diskriminatorna. Za potvrdu izbora obeležja i određivanje njihove značajnosti, korišćena je i tehnika stable odluke.

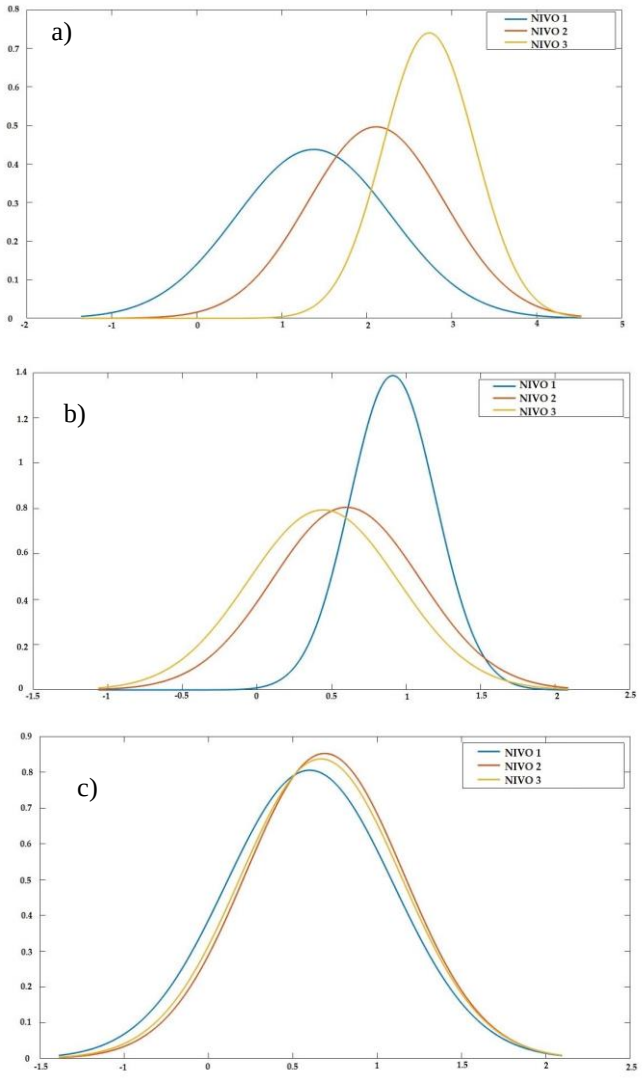

Sl. 5. Gausove krive za obeležje balans (a), nivo amputacije (b) i fantomski bol (c). Na osnovu ovih grafika možemo da zaključimo da su obeležja balans i nivo amputacije diskriminatorna, dok obeležje fantomski bol nije.

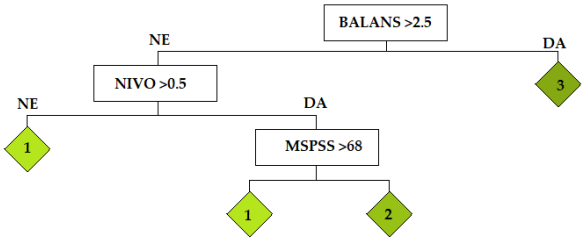

Sl. 6. Stablo odluke kako pokazatelj zančajnosti obeležja balans. Sa grafika je jasno uočljivo da veoma lako možeo izdvojiti klasu 3, odnosno pacijente sa potencijalnim visokim ishodom rehabilitacije.

A. *Stabla odluke*

Zbog svoje sistemske strukture, metoda stabla odluke je jednostvna i razumljiva za ljude. Izdvajanjem puta od odgovoarajuće klase, odnosno lista, pa sve do korena stabla, dobija se odgovor zašto je donesena neka odluka, pri čemu se iz svakog čvora čita razlog trenutnog izbora. Takođe, svako stablo odluke se jednoznačno može definisati preko skupa pravila "ako-onda" (engl. *if-then*), koja su osnovni gradivni blokovi baza znanja ekspertskih i drugih sistema zasnovanih na znanju [12].

Stabla odluke izvršavaju klasifikaciju u dve ili više klasa, na osnovu vrednosti obeležja kojima opisujemo uzorke, propuštajući ih niz stablo od korena ka listovima. Na početku klasifikacije bira se obeležje čija vrednost najbolje deli raspoložive uzorke. Algoritam ID3, koji je razvijen za učenje stable odluke i koji je korišćen u ovom radu, obeležja deli na osnovu statističke veličine koja se naziva informacioni blok i koja se definiše preko entropije (entropija je 0 ako svi uzorci pripadaju istoj klasi a 1 ako klase imaju isti broj uzoraka) [12]. Analizom baze podataka, algoritam je procenio da je najbitnije obeležje balans. Sa slike 6 može se videti da se pomoću obeležja balans lako mogu izdvojiti pacijenti čiji bi ishod rehabilitacionog tretmana bio maksimalan (što je ujedno i potvrda za za Gausovu krivu sa slike 5).

Na slici 7 prikazano je stablo odluke sa izdvojenim parametrima za kategoriju K-nivo. Obeležja koja je stablo označilo kao diskriminatorna su: balans, nivo amputacije, starost, indeks telesne mase (engl. *body mass index* - BMI), mišićna snaga ekstenzora kuka rezidualnog ekstremiteta (*RE E kuka* na grafiku), Bekova skala depresivnosti (engl. *Beck depression inventory* - BDI), starost pacijenta pri prijemu, multidimenzionalna skala ostvarene socijalne podrške (engl. *multidimensional scale of perceived social support test* - MSPSS), kao i parametre mišićne snage ekstenzora kuka (*IE E kuka* na grafiku) i plantarnog fleksora (*IE F plan* na grafiku) intaknog ekstremiteta.

B. *Metoda vektora nosača*

Odabrana obeležja prosleđuju se algoritmima baziranim na vektorima nosačima. Primarna verzija SVM algoritma na ulazu uzima skup podataka i zatim određuje kojoj od dve moguće klase svaki uzorak pripada, odnosno traži se funkcija $f(\boldsymbol{x})$ koja je u funkciji hiper-ravni H, koja predstavlja razdvajajuću marginu za dva stanja sistema u prostoru obeležja [11], H: $\boldsymbol{w}^T\boldsymbol{x} + b = 0$, kao i dve hiper-ravni (koje se nazivaju vektori nosači) H_1: $\boldsymbol{w}^T\boldsymbol{x} + b = 1$ i H_2: $\boldsymbol{w}^T\boldsymbol{x} + b = -1$, uz uslov da ne postoje tačke između H_1 i H_2 i da je razmak između margina maksimalan. Šematski, to je predstavljeno na slici 8.

Iako je SVM algoritam primarno razvijen za binarnu klasifikaciju, on se može koristiti i za problem višeklasne klasifikacije. Standardan algoritam za rešavanje ovakvog problema je rastavljanje problema od M klasa na seriju problema od po dve klase, i konstrukcijom više binarnih klasifikatora [11]. Jedan od pristupa je metod „jedan protiv jedan", koji formira za svaki par klasa po jedan klasifikator [12]. Ti klasifikatori su osposobljeni za razlikovanje uzoraka jedne klase od uzoraka druge klase. Klasifikacija nepoznatog uzorka se vrši prema maksimalnom broju „glasova", gde svaki klasifikator „glasa", za jednu klasu.

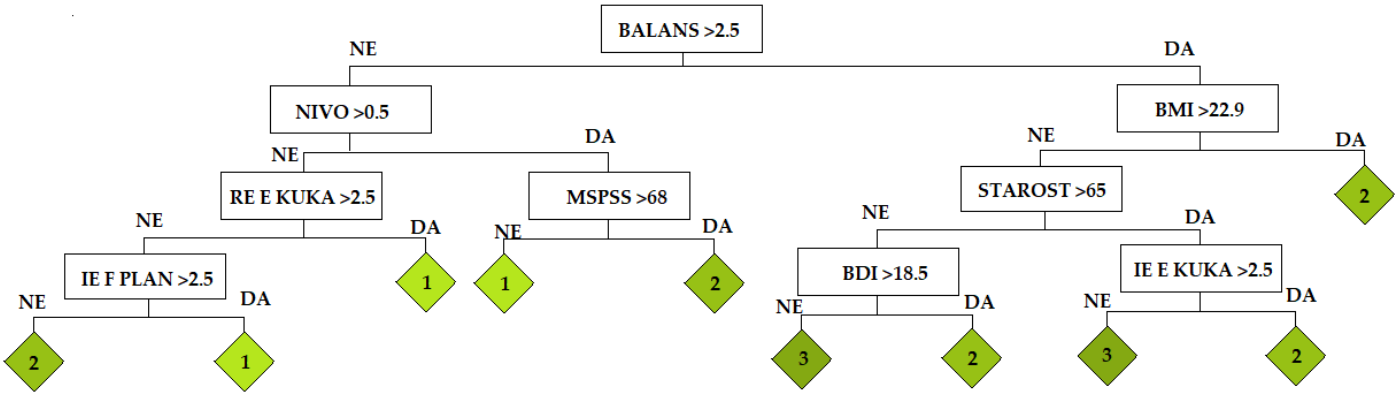

Sl. 7. Stablo odluke za ketegoriju K-nivo.

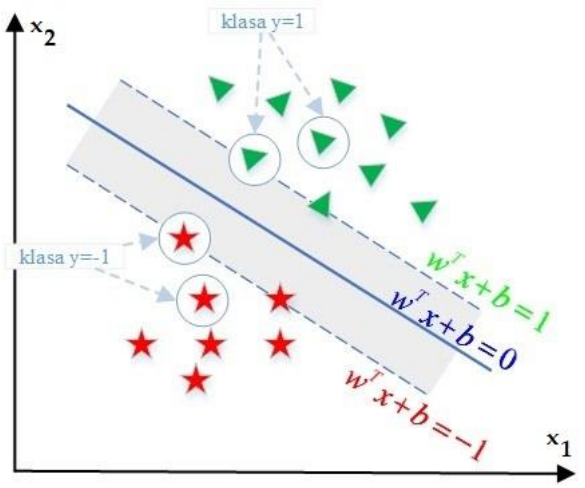

Sl. 8. Hiper-ravan *H* i njene margine u ravni parametara x_1 i x_2. Zelenim trouglovima predstavljeni su uzorci koji pripadaju klasi y=1, dok su zvezdicama predstavljeni uzorci klase y=-1.

IV. REZULTATI I DISKUSIJA

Za generisanje i simulaciju rada SVM predikcionog modela i stabla odluke korišćen je programski paket *Matlab*. Pripremljeni podaci prosleđeni su algoritmu stabla odluke, koji radi po principu ID3 algoritma. Obeležja izabrana na ovaj način prosleđena su SVM algoritmu. Za rešavanje ovog problema izabran je linearni kernel. Rezultati su dobijeni evaluacijom obučenih modela nad odgovarajućim test skupovima, dobijenih krosvalidacijonom metodom sa 10 particija. U svakoj iteraciji koristilo se 9 različitih particija za obuku, odnosno 9 podskupova skupa svih uzoraka, dok se preostali skup koristio za testiranje.

Tabela I predstavlja matricu konfuzije SVM klasifikatora za K-nivo, nakon rešavanja problema nedostajućih podataka i balansiranja klasa. Iz tabele se može iščitati da algoritam u veoma visokom procesu tačno klasifikuje. Tačnost SVM klasifikatora, odnosno procenat korektnih predviđanja od ukupnog broja predviđanja, iznosila je 89.3%. Tačnost klasifikacije ostalih kategorija prikazana je na slici 9. Najveća tačnost postignuta je prilikom predviđanja kategorije K-nivo (89,3%), dok najlošije performanse se javljaju kod klasifikacije kategorija testa ustani i kreni (81,88%). Pored tačnosti, i ostale mere za evaluaciju klasifikatora za kategoriju K-nivo su veoma visoke. Osetljivost klasifikacije, odnosno procenat korektno predviđenih od ukupnog broja pravih ponavljanja te klase za K-nivo iznosi 83,95%, specifičnost (sposobnost testa da identifikuje odsustvo neke klsse) 91,97%, dok je preciznost (odnos tačnih predviđanja i ukupnog broja predviđanja) iznosila 83,7%.

V. ZAKLJUČAK

Uzimajući u obzir stalno povećanje broja pacijenata sa amputacijom donjih ekstremiteta, kao i cenu i trajanje rehabilitacionog tretmana, predikcija ishoda rehabilitacionog tretmana predstavlja jedno od veoma aktuelnih pitanja savremene rehabilitacione medicine. Brojni radovi napisani na

TABELA I
MATRICA KONFUZIJE ZA KATEGORIJU K-NIVO

		Predviđene klase		
		1	2	3
Prave klase	1	**50**	4	0
	2	7	**38**	9
	3	0	6	**48**

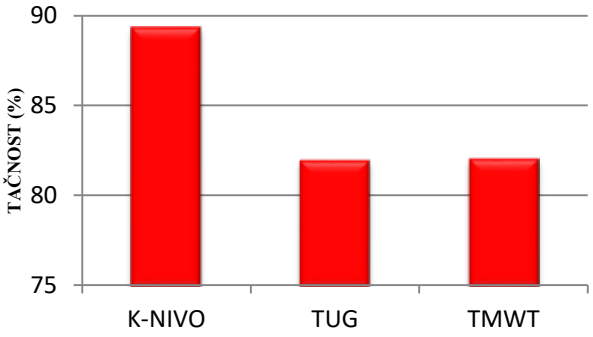

Sl. 9. Tačnost klasifikacije za različite kategorije.

ovu temu, čiji je jedan mali deo korišćen kao smernice i inspiracija ovom radu, svedoče o značaju ove tematike.

Glavni cilj razvijanja sistema za predikciju uspešnosti rehabilitacionog tretmana treba da bude identifikacija tačno onih obeležja koja će doprineti uspešnoj predikciji, to jest pronalasku onih parametara koji će omogućiti korektnu identifikaciju pacijenata sa amputacijom pogodnih za propisivanje proteze i uključivanje u odgovarajući rehabilitacioni tretman. Obradom podataka i selekcijom obeležja metodom stable odluke, postignute su veoma visoke performance SVM klasifikatora. Obeležje koje je označeno kao balans izdvojeno je kao jedan od najznačajnijih prilikom identifikacije pacijenata pogodnih za propisivanje proteze. Maksimalna efikasnost postignuta je prilikom predikcije K-nivoa i iznosila je 89.30%.

Ovakav sistem veštačke inteligencije, zbog svojih visokih performansi, moguće je primeniti i u kliničkoj praksi. Dalji rad u budućnosti trebalo bi da se skoncentriše na testiranju algoritma nad proširenom bazom podataka, odnosno predviđanje nad originalnom petostepenom skalom.

ZAHVALNICA

Ovaj rad podržan je od strane Ministarstva prosvete, nauke i tehnološkog razvoja kroz projekat broj 451-03-68/2020-14/200156: "Inovativna naučna i umetnička ispitivanja iz domena delatnosti FTN-a".

LITERATURA

[1] A. Knežević, "Faktori koji utiču na nivo osposobljenosti za hod uz pomoć proteze nakon amputacije donjih ekstremiteta,"Doktorska disertaciija, Katedra za fizikalnu medicine i rehabilitaciju, Medicinski fakultet, Univerzitet u Novom Sadu, Srbija, 2014.

[2] K. K. Chui, M. M. Jorge, S. C. Yeng, M. M. Lusardi, *Orthotics and Prosthetics in Rehabilitation, fourth edition,* St. Louis, Missouri, Elsevier, 2021.

[3] A. Knežević, M. Petković, A. Mikov, M. Jeremić Knežević, Č. Demeši Drljan, K. Bošković, S. Tomašević Todorović, Z. Jeličić, "Factors that predict walking ability with a prosthesis in lower limb amputees," -Srpski arhiv za celokupno lekastvo, 507-513, Sept-Okt 2016.

[4] N. Majdič, G. Vidmar, H.Burger, "Establishing K-levels and prescribing transtibial prostheses usig six-minute walk test and one-leg standing test on prosthesis: a retrospective audit," International Journal of Rehabilitation Research, 266-271, Sep 2020.

[5] B. Majstorović, M. Pešta, "Factors predicting rehabilitation outcome in patiens after unilateral transtibial amputation due to peripheral vascular disaese," Military Medical and Pharmaceutical Journal of Serbia, 357-362, Maj 2020.

[6] T. Pohjolainen, H. Alaranta, "Predictive factors of functional ability after lower limb amputation, " Annales chirurgiae et gynaecologice, 36-9, 1991.

[7] K. Sansam,V. Neumann, R. O'Connor, B. Bhakta, "Predicting walking ability following lower limb amputation: a systematic review of the literature," Journal of Rehabilitation Medicine, 593-603, Jul 2009.

[8] J. T. Kahle, M. J. Highsmith, H. Schaepper, A. Johannesson, M. S. Orendurff, K. Kaufman, "Predicting walking ability following lower limb amputation: an updated systematic literature review," Technology and Innovation, 125-137, Sep 2016.

[9] J. Van Velzen, C. van Bennekom, L. van der Woude, H. Houdijk, "Physical capacity and walking ability after lower limb amputation: a systematic review," Journal of Clinical Rehabilitation, 999-1016, Nov 2016.

[10] C. Micheloni, A. Rani, S. Kumar, G. L. Foresti, "A balanced neural tree for pattern classification," Elsevier: Neural Networks, 81-90, Mar 2012.

[11] V. Crnojević, "Prepoznavanje oblika za inženjere," Novi Sad, Srbija, Fakultet tehničkih nauka u Novom Sadu, edicija: Tehničke nauke, 2014.

[12] M. Milosavljević, "Veštačka iinteligencija," Beograd, Srbija, Univerzitet Singidunum, 2019.

ABSTRACT

Prosthetic rehabilitation is currently the best treatment for patients with lower limb amputation. However, prosthesis fabrication and accompanying prosthetic rehabilitation are very long and expensive process that sometimes does not lead to improved mobility and quality of life of patients. Therefore, it is necessary to predict the result of rehabilitation treatment. The main task of this work was to make a tool, based on artificial intelligence algorithms, which could be applied as early as possible, to make the best possible prediction of the result of rehabilitation of patients with amputation of the lower extremities, or to predict the K-level (Medicare Functional Classification Level), Walking Ability Level, Two-Minute Walk Test and Timed Up and Go Test. Evaluation of the model performed on data from the Rehabilitation Clinic, Clinical Center of Vojvodina. The obtained results show a significant improvement, in terms of classifier performance, compared to previous methods and confirm the choice of some of the most important parameters in patient identification.

Predicting results of prosthetic rehabilitation in lower limb amputees by using artificial intelligence algorithms

Jovana Arsenović, Aleksandar Knežević, Mirna N. Kapetina and Zoran D. Jeličić

Multipurpose remote monitoring system based on microservice architecture

Luka Bjelica, Miloš Panić, Marko Pejić

***Abstract*—This paper presents a cloud-native, multi-purpose, and reusable system for collecting, processing and storing data, with the aim of monitoring an arbitrary physical system. The proposed system can be divided into three main parts: a private network containing a set of microservices that perform complete data processing, applications that implement the low-level logic for collecting data from remote sensors, and a web client which enables interaction between the user and the rest of the system. The final product of this paper is a system based on the microservice architecture named *isobar.ot*, that allows monitoring of the chosen set of values of an arbitrary physical system, through a simple and functional user interface. Using the system presented in this paper, the user is able to control the entire course of remote monitoring: from the selection and specification of the collected data scheme, through the definition of alarm values, to displaying changes of values and alarms in real-time.**

Keywords: distributed systems, microservice architecture, remote monitoring systems, cloud-native systems, Internet of Things

I. Introduction

Monitoring the various parameters of arbitrary physical systems is a crucial part of every industrial facility. Supervisory Control and Data Acquisition (SCADA) systems are ubiquitous in almost all industries: from the food industry to the power industry, which results in a need for continuous improvements of the existing, and development of new solutions [1].

This paper concerns the development of the modern solution for remote monitoring systems that can be used for monitoring an arbitrary physical system. It is based on a microservice architecture with cutting-edge tools and technologies. Motivation for choosing this topic came from a necessity for a system that can work with large amounts of data and is flexible in a relation to a supervised physical system, which makes it usable as a part of Internet of Things (IoT) systems [2].

One of the biggest challenges when designing such a system is the scalability, i.e., the ability of the system to work with a large number of sensors and serve a large number of clients without a drop in performance. Furthermore, such a system requires a simple and functional user interface in order to provide an operator with an efficient way to monitor changes in the collected data, have insight into the alarming events in real-time, as well as defining new locations, alarm types, schemes of the data that is collected, etc. For the above-mentioned goals to be fulfilled, the proposed system is designed according to the principles of microservice architecture.

After the Introduction, basic principles, advantages and disadvantages of the microservice architecture and the architecture of the proposed solution are explained in Section II. Technical details about the implementation, along with the tools and technologies that were used are introduced in Section III. Results and user interface are shown in Section IV and the concluding remarks along with future plans are given in the final Section V.

L. Bjelica (bjelicaluka@uns.ac.rs), M. Panić (panic.sw19.2018@uns.ac.rs), M. Pejić (markopejic@uns.ac.rs), University of Novi Sad, Faculty of Technical Sciences, Department of Computing and Control Engineering, Trg Dositeja Obradovića 6, 21000 Novi Sad, Serbia.

II. Architecture

Two mandatory requirements that the proposed system must meet are working with a large amount of data and serving a large number of clients. The architecture of the proposed system is designed so that the mentioned requirements are satisfied for the arbitrary amount of data and number of clients.

Microservice Architecture

Microservice architecture implies the development of applications in the form of small, isolated, and independent services that communicate with each other via clearly defined protocols. Such a method for developing systems came about due to the aim of overcoming flaws and problems that come with monolith architecture.

The traditional approach to developing software implies the use of monolithic architecture. One of the flaws of monolithic architecture is that it poorly copes with overload [3]. One approach to handling overload is to vertically scale the existing machine on which the application runs. That is expensive and not efficient enough to solve the problem completely. The other approach is to use horizontal scaling and create multiple instances of the application. This approach leads to inefficient use of hardware resources because there is no possibility to scale only those parts of the system that require it [3]. In addition, the degree of reusability of individual components is reduced because they are tightly coupled with the system they were initially developed for.

The main advantage of the microservice architecture-based systems is that the individual microservices can be scaled independently. That way, better utilization of hardware resources is achieved so that only the parts of the system that are affected by overload get scaled. Additional advantages that the microservice architecture brings are independent

development of individual components as well as the high degree of their reusability [3].

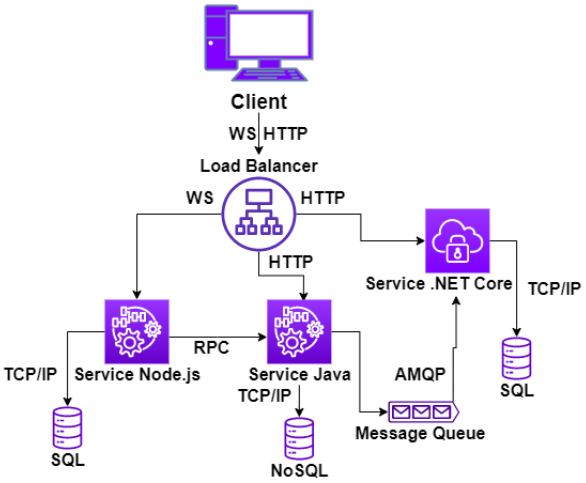

Fig. 1. Microservice Architecture Scheme

Fig. 1 presents the example of the microservice architecture scheme. It can be noticed that system based on the microservice architecture is suitable for scaling individual parts that require it because each part represents an independent application. There is also the possibility of using different technologies for implementing individual services, as well as the use of different communication mechanisms and protocols depending on the need.

System development follows the *divide and conquer* principle, which divides a large and complex system into smaller units, which are easier to develop. It is important to mention that dividing the system into smaller entities does not solve the complexity problem, but rather it delegates it to a level above, that is, to connect the system's components and their orchestration.

Previously stated benefits surpass hardware limitations of a single machine on which the system is running and thus make the microservice architecture an adequate solution for implementing remote monitoring systems.

System Architecture

The proposed system represents a set of components, each being an independent application with a unique role. The system is made out of services that are responsible for: authentication, user groups and user profiles, schemes of data that is collected from arbitrary physical sensors, validation, persistence and aggregation of the collected data, detecting alarms, generating reports from the aggregated data, and displaying the user interface.

The architecture of the proposed system is presented in Fig. 2. The system runs on the cloud and is completely independent of the physical system from which it receives the data.

The responsibility for collecting data from physical sensors and sending it to the system is encapsulated within the Local Processing Unit (LPU). LPU acts as an intermediary

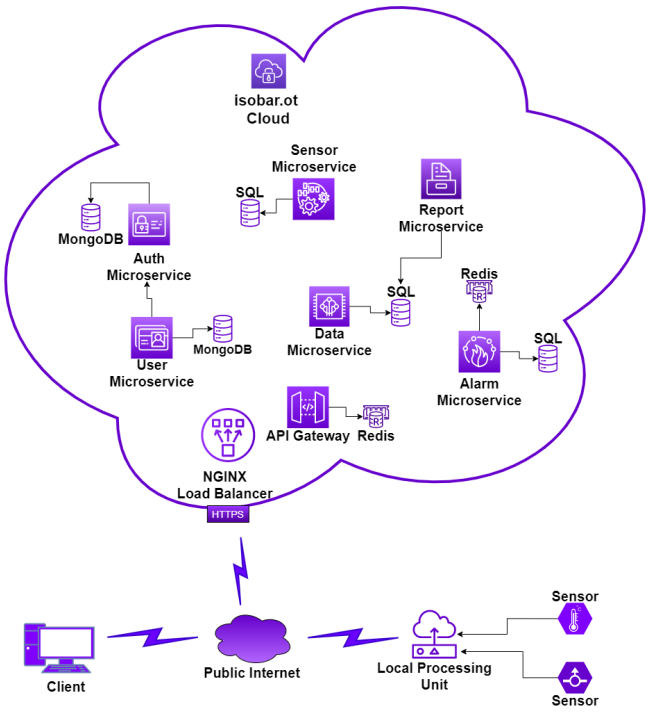

Fig. 2. System Architecture Scheme

between physical sensors which collect raw data, and the part of the system which is launched on a cloud.

The services are a part of the private, isolated network and it's not possible to address them directly from the public internet. The ingress service, acting both as a reverse proxy and load balancer [4], is the only way to access services from the outside. All inter-service communication is done in a synchronous manner with one exception. The only asynchronous communication is data ingress where the API Gateway service sends the data to the Data and Alarm services separately and is not interested in the content of the response.

A brief description of individual services that make up the system follows:

1) Authentication Service: The role of the authentication service is to provide a safe way to persist user credentials. This service implements the logic for generating access tokens that are used by other services for restricting unauthorized access to individual resources. It's worth pointing out that the authorization is highly dependent on the context it's used in and implies that details of role-based access control (RBAC) used for restricting access to individual resources need to be defined in the service that owns the resources. Otherwise, every service that implements RBAC would be tightly coupled to the service that implements authorization logic. The problem with that approach is that the authorization service may represent a bottleneck of the system. Tight coupling of services is not a problem if they are running inside the same process. Knowing that the presented system is distributed, this approach presents a big problem because it increases the degree of inter-service

communication and causes the known problem "chatting" [5]. The problem mentioned above is the reason why the authorization is not implemented within the authentication service.

2) User Service: The service responsible for working with user profiles and user groups is a very important component of the system because it enables isolating data at the level of user groups. This service is responsible for protecting user's personal information and controlling which user group does the user belong to. Considering that most of the resources on the system are tied to a specific user group, user has access limited only to those resources tied to the group it belongs to.

3) Sensor Abstractions Service: A key component of the proposed system is a service that provides a way for arbitrary sensors that collect data on a supervised physical system. The role of this service is to persist information about the schemes of data that is being collected, as well as information about the concrete sensors that send that data. The entities used by this service are sensor abstractions, i.e., schemes of data that is being collected, and the information about the concrete physical sensors along with their locations. The idea behind defining data schemes is the possibility of validation of incoming data on the service, as well as the possibility of using the same data scheme for multiple different sensors. The scheme represents a set of individual tags (physical values of interest), each containing a name and a primitive data type. Apart from the name and the simple type, for every tag in the data type, aggregation methods are listed, based on which, aggregation service knows how to process raw data.

4) Data Validation Service: Received data first goes through a validation process, which is carried out based on the previously defined data type. This service is also responsible for verifying the validity of the public API token, using which the LPU unit proves authenticity. Apart from validation, this component presents a suitable place for dispatching events about received data in real-time. Events are dispatched through previously defined bidirectional communication protocol with the aim of achieving *publisher-subscriber* mechanism [6].

5) Data Persistence and Aggregation Service: The component which contains markedly the most complex logic and which requires the most hardware resources is data persistence and aggregation service. Before it gets aggregated, the raw data are persisted inside a temporary data store that is being cleared after a fixed period of time. The reason why raw data aren't stored permanently is that the amount of data is immensely large and that storing it isn't efficient. The more efficient solution is doing periodical data aggregation, such that users are able to define a time period after which the aggregation is performed. Additionally, users are able to define the methods by which data aggregation is performed, which later allows them to follow trends and generate reports of interest. By that, the system gets better performances, not only in terms of memory usage but also in decreasing the time needed for generating certain reports.

6) Report Service: The purpose of the persisted data lies in the ability to generate certain reports from them, with the aim of monitoring trends and presenting behavior of arbitrary values that are collected. This service implements the logic for generating reports on the aggregated data that is permanently persisted in the system. The report takes into account the specific frequency at which the data was aggregated as well as the time interval within which the data was collected. It also provides the ability to define and store report types that contain all the information needed to generate a particular report, except for the time interval.

7) Alarm Service: Detecting critical values, that is, data values which deviate from predefined boundaries can be very significant for physical systems which the proposed system is monitoring. The responsibility of this component is the detection of critical values and dispatching events about them, in real-time. Critical values are detected by rules previously defined in alarm types. Alarm type contains priority, a threshold value, and the information about whether the threshold presents an upper or lower limit of the normal state. A property from the data type can have a set of predefined alarm types tied to it. During alarm detection, every alarm type that is tied to a certain property is taken into consideration. When the critical value is detected, an event is dispatched through a predefined, real-time communication protocol. After the alarm event is dispatched, the client has the option of caching that alarm for a certain time period and thus preventing the system from dispatching more of the same events tied to the alarm of a certain priority, type, and limit value.

8) User Interface Service: This service provides elements needed for the graphical presentation of real-time data and generated reports. In addition to that, it contains elements that can be used to create certain resources, set certain rules, and take care of users and user groups.

III. Implementation

The microservice architecture allows the usage of numerous technologies for implementing individual components so that the most suitable technology for the requirements specific to that component is used. Fig. 3 shows an overview of all technologies used for implementing certain parts of the system.

Implementation of Individual Components

The authentication service implementation was realized using the .NET Core [7], while the MongoDB [8] database was used for the persistence of user accounts. Each user account consists of a unique name, password, and role. In case of the data leak, *hashing and salting* [9] of passwords is applied with the aim of preventing their misuse.

For the purpose of implementation of the service for working with user groups and profiles, .NET Core was used. User groups and profiles are in a one-to-many relationship, i.e., a profile belongs to exactly one group, while a group can contain several user profiles. The user group contains a name, surname, and e-mail address. To ensure that the

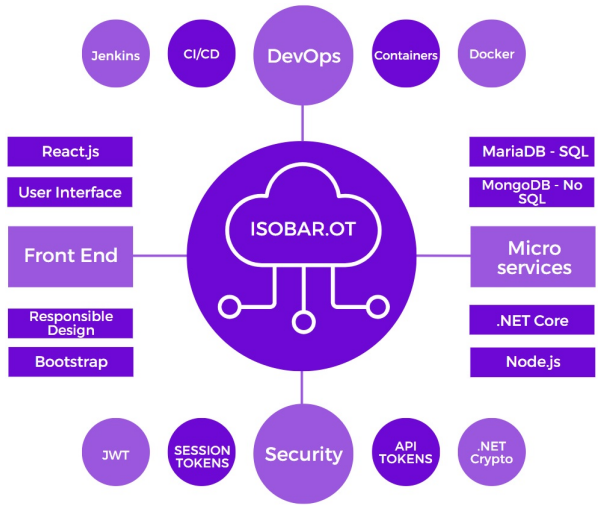

Fig. 3. Overview Of The Used Technologies

connection between user groups and accounts is modeled properly, MariaDB [10] relational database was used.

Another of the services implemented using .NET Core is a service for defining abstractions of physical sensors, i.e., schemes of data that come from remote sensors. Entities relevant to this microservice are sensor schemes, physical sensors, and locations. Since these entities are interrelated, a relational database MariaDB was used for data persistence. Primitive data types which are supported are real numbers, boolean values, enumerations, and text. Each sensor has its own public API token, which is a randomly created string of letters and digits that can be altered. Altering the public API token of a sensor is a significant function since it provides a mechanism of protection from receiving false data from a party that has obtained the token in an unauthorized way.

The implementation of the data validation logic is separated into the data validation service implemented in the Node.js [11] environment. This service uses Redis [12] cache as temporary storage for a public API key as well as the data scheme of the authenticated sensor. This decreases communication with the service in charge of validating public API tokens and evades creating the system's bottleneck. Sending data in real-time is done by using a WebSocket, using the socket.io library [13].

Data persistence and aggregation service is implemented using .NET Core and MariaDB database. One of the main reasons for choosing MariaDB as a relational database is the native support for built-in mechanisms that can be used for storing and manipulating data in dynamic JSON [14] format. The collected data is stored in a temporary table whose content is deleted after an all-day cycle of aggregations. The system supports several different aggregation time periods, of which the smallest is five minutes, and several different methods for aggregating real numbers including minimum, maximum, sum and mean. The aggregated data is stored in separate tables in the database, each corresponding to a single resolution.

.NET Core was used for the implementation of the report service. This service reads data from the database in which the persistence and data aggregation service has stored the processed data. Report generation was realized with the help of mechanisms for manipulating data in JSON format that are supported by the MariaDB database.

Implementation of alarm service is done inside the Node.js environment, while the MariaDB database was used for storing information about the alarm schemes and concrete critical values themselves. Sending data in real-time is done using WebSocket, which makes users promptly informed about every critical value of the monitored system. This service also uses Redis cache for storing critical values to avoid notifying the client unnecessarily. Another role of Redis is to synchronize socket.io events between multiple instances of the application.

The user interface was implemented using React.js [15] and Bootstrap [16] libraries.

Automation of Development Processes

Developing a system that is based on a microservice architecture increases the maintenance complexity because the source code of the system is made up of multiple smaller and often independently maintained code bases. Continuous Integration (CI) represents a necessary part of the development process of systems composed of many components with independently maintained code bases. That includes validation and testing of individual functionalities, as well as the rebuilding of components affected by changes. Continuous Deployment (CD) is the process of automatic reflection of changes to the final system which is used in production. In systems that are subject to frequent changes, the CD represents a necessity and can be very important in both the development and deployment phases of the system. In the development process, an instance of the staging application is created in order to provide access to the application to everyone that is involved. That significantly increases the degree of error detection in the development phase and reduces the chances of a bug in production.

Developing the system comprised of components that are implemented in different technologies, complicates the requirements for the environment in which individual components can be started. The concept of containers is introduced with the aim of providing a virtual environment at the operating system level, which can be predefined, packaged, and quickly launched. Such an environment has a high degree of portability and can be run on any platform on which a container engine can be run. The proposed system uses Docker [17] for the containerization of individual components. Docker provides an API for defining, packaging, transferring, and running virtual environments in form of containers. It also supports the creation of isolated private networks within which containers can intercommunicate and reference eachother using the local DNS server [18].

High availability and fault tolerance deserve special attention for distributed systems that are running in a production environment. A highly available system tends to minimize service downtime while a fault-tolerant one ensures that no

data is lost during minor or major failures. The goal is to have both a highly available and fault-tolerant system that ensures high service uptime without data loss. The fact that the proposed system can be deployed on a multi-node cluster and that the data replication on multiple nodes is supported ensures that the aforementioned goals are met in a production environment. By distributing traffic across multiple nodes, the uptime of the individual services, resilience to data loss, and the request processing capacity are increased.

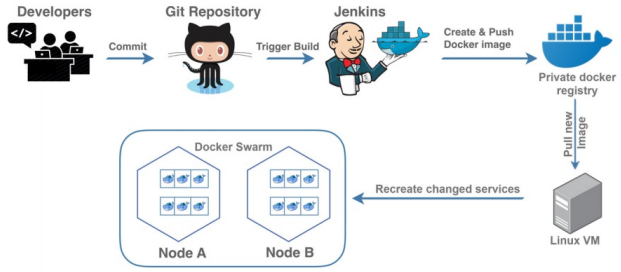

Fig. 4. Automatic Development Process Scheme

Fig. 4 illustrates the scheme of the automated CI/CD pipeline used by the proposed system in a development environment. Once the changes are made, they are synchronized with the remote codebase located on GitHub. The application that implements the CI/CD pipeline, i.e. Jenkins [19] gets notified, via the WebHook submission mechanism, about the changes that have been made on a certain branch. When an event containing information about the changes reaches Jenkins, a predefined pipeline is started. The pipeline runs the process of validating changes and rebuilding Docker Images if the changes prove to be valid. Additionally, the affected parts of the system get synchronized with newly integrated changes by a command that gets executed using SSH (Secure Shell) on the machine on which the system is running.

The proposed system can be instantiated using the *docker-compose* tool, for the needs of the development environment or using the *kubectl* tool for production environments. The role of the aforementioned tools is to take care of pulling, configuring, starting, and shutting down previously defined services, creating private networks within which the services communicate and scaling certain services depending on the needs of the system.

IV. Results

The final product of this paper is a functional remote monitoring system, based on microservice architecture and modern technologies, called *isobar.ot*. The system described in this paper supports the processing and persistence of arbitrary data sets, as well as tracking of trends in the collected data, i.e., periodical changes in the data values and the detection of critical values in real-time. In addition, the system allows the generation of reports from the persisted data for a certain period of time, which allows the user to analyze the behavior of the physical system that is monitored.

The most valuable aspects of the proposed system are the fact that it can be reused for many different physical systems, and also its scalability which is ensured by the microservice architecture. The system solves one of the basic problems that come with the IoT systems, which is giving semantics to the raw data collected from the physical sensors so that storing and processing of data is realized in a uniform way, independent of the nature of data.

Besides various simulations, such as collecting data on weather conditions, that were used to test the system's reusability, there are two successful use-cases of the proposed system. Both of them are Road Traffic Monitoring Systems (RTMS) that are deployed in India and Croatia. The first receives data from two different sensor types: laser and radar. The laser sensor sends detailed information about the passed vehicles such as speed, class, and it's dimensions. The radar detects vehicle's speed and relative position and send them in real-time.The second use-case receives data from a camera that detects which class of vehicle has passed. The previously mentioned use-cases prove that the proposed solution can be used to monitor arbitrary physical systems. In both cases, the system ensures high availability and fault tolerance, i.e. it is deployed on a multi-node cluster and uses data replication in order to prevent data loss.

User Interface

Fig. 5 shows the appearance of the user interface, which monitors critical values in real-time. The hide option gives users an opportunity to declare that they are aware of a particular alarm, to take all necessary steps, and not want the system to notify them more about the alarm so that they can pay attention to other alarms.

PROPERTY	TYPE	CRITICAL VALUE	PRIORITY	LOCATION	SENSOR	
sinus	Above	79.1056663295	Low	Zrenjanin	Sinus Simulation	Hide
sinus	Above	86.9963516663	Medium	Zrenjanin	Sinus Simulation	Hide
sinus	Above	95.2598516295	High	Zrenjanin	Sinus Simulation	Hide
tanh	Below	-50.1444326271	High	Ćurug	Tanh Simulation	Hide
cosinus	Below	-5.88190451025	Medium	Novi Sad	Cosinus Simulation	Hide

Fig. 5. Alarms Monitoring in Real-Time

The *Dashboard* section (Fig. 6) presents the appearance of the user interface through which data arrived from sensors is tracked. Selecting the sensors is done from the drop-down menu, where all the sensors belonging to the corresponding user groups are listed. It is possible to choose more than one sensor and to display data in real-time graphically and in a table.

For the purpose of testing the proposed system, simulation sensors are implemented, which represent individual applications independent of the rest of the system. Their role is to simulate the operation of LPU units by sending random values or values of certain mathematical functions, instead of collecting data from physical sensors. Some of the functions supported by simulation sensors are sine, cosine, sigmoid, ReLU (Rectified Linear Unit), and the like.

Fig. 6. Live Data Display

V. Conclusion

This paper presents a cloud-native, multi-purpose remote monitoring system, based on microservice architecture. The implemented system is named *isobar.ot* and consists of three main parts: local processing units (LPU) used for implementing low-level logic for collecting data from physical sensors and sending it to the cloud, an isolated private network with a set of microservices that perform the entire processing and persisting data on the cloud, a client web application that allows users to interact with the rest of the system.

The biggest advantage of the proposed system lies in its ability to monitor arbitrary physical systems, and the ability to work with a large number of sensors and serve a large number of clients. These advantages are achieved by relying on microservice architecture and modern technologies.

Despite the fact that inter-service communication is brought to a minimum, there are cases where a better solution for communication would be to use asynchronous protocols, such as AMQP [20]. Another disadvantage of the proposed system is that some services use data that are not owned by them, i.e., they have to turn to services that have that data. This reduces the failure resistance of interdependent parts of the system. A potential solution to this problem is to use caching more frequently or replicate the data used by multiple services while maintaining asynchronous consistency.

In addition to overcoming the previously mentioned shortcomings of the proposed system, the plan for further development is the implementation of a data export service in the form of a file of a certain format, such as PDF, CSV, JSON, and the like. Also, the plan is to implement support for receiving data in several different protocols, and not only in HTTP. Another possibility for further development of the proposed system is the implementation of a uniform control component. The task of this component is to provide a mechanism for managing the monitored physical system, at a high level. That way, the proposed system would be extended to a fully functional supervisory and control system, which is certainly in the plan for future development.

References

[1] A. Goel and R. Mishra, "Remote data acquisition using wireless - scada system," *International Journal of Engineering*, vol. 3, 03 2009.
[2] L. Atzori, A. Iera, and G. Morabito, "The internet of things: A survey," *Computer Networks*, vol. 54, no. 15, pp. 2787–2805, 2010.
[3] O. Al-Debagy and P. Martinek, "A comparative review of microservices and monolithic architectures," in *2018 IEEE 18th International Symposium on Computational Intelligence and Informatics (CINTI)*, pp. 149–154, 2018.
[4] "Nginx documentation." https://docs.nginx.com/nginx/admin-guide/load-balancer/http-load-balancer/, 2021.
[5] J. Ghofrani and D. Lübke, "Challenges of microservices architecture: A survey on the state of the practice," 05 2018.
[6] C. R. Ozansoy, A. Zayegh, and A. Kalam, "The real-time publisher/subscriber communication model for distributed substation systems," *IEEE Transactions on Power Delivery*, vol. 22, no. 3, pp. 1411–1423, 2007.
[7] ".net core documentation." https://docs.microsoft.com/en-us/dotnet/, 2021.
[8] "Mongodb documentation." https://docs.mongodb.com/, 2021.
[9] "Adding salt to hashing: A better way to store passwords." https://auth0.com/blog/adding-salt-to-hashing-a-better-way-to-store-passwords/, 2021.
[10] "Mariadb documentation." https://mariadb.com/kb/en/documentation/, 2021.
[11] "Node.js documentation." https://nodejs.org/en/docs/, 2021.
[12] "Redis documentation." https://redis.io/documentation, 2021.
[13] "Socket.io documentation." https://socket.io/docs/v3/index.html, 2021.
[14] "Json documentation." https://www.json.org/json-en.html, 2021.
[15] "React documentation." https://reactjs.org/, 2021.
[16] "Bootstrap documentation." https://getbootstrap.com/docs/5.0/getting-started/introduction/, 2021.
[17] "Docker documentation." https://docs.docker.com/, 2021.
[18] D. Jaramillo, D. V. Nguyen, and R. Smart, "Leveraging microservices architecture by using docker technology," in *SoutheastCon 2016*, pp. 1–5, 2016.
[19] "Jenkins documentation." https://www.jenkins.io/doc/, 2021.
[20] "Amqp documentation." https://www.amqp.org/, 2021.

Integrated Particle Filter for Multi Target Tracking

Zvonko Radosavljević, Dejan Ivković and Branko Kovacević

***Abstract*— Target tracking in heavy cluttered environment requires methodology for false track discrimination and data association. Recently, we present a new particle filter (PF) approach which recursively calculates the probability of target existence for the false track discrimination. Our approach treats possible detections of targets followed by other tracks as additional clutter measurements. It starts by approximating the a priori probabilities of measurement origin. The posterior data association probabilities are calculated to discriminate clutter measurements when updating trajectory probability density function. A new complete recursive track initiation, confirmation and deleting algorithm based on PF and Integrated Track Splitting (ITS) and named Integrated Particle Filter (IPF) is presented. Through the extended simulations showed the effectiveness of this approach in a five targets scenario.**

***Index Terms*—Target tracking, data association, particle filter, Integrated Track Splitting.**

I. Introduction

Each sensor measurements may either be a spurious (clutter) or a target measurement. The target existence and trajectory are not a priori known [1]. The tracks are initialized using measurements, thus both true tracks and false tracks simultaneously exist. The false track discrimination (FTD) is a procedure to terminate a majority of false tracks and confirm majority of true tracks [2],[3]. A track quality measure needs to be calculated for successful FTD. The multiple hypothesis tracker (MHT) [4][5] is one of the first widely used algorithm for target tracking in clutter. The measurement-oriented MHT, often known as the Reid algorithm [1], forms new tracks and measurement allocation hypotheses centered around global origin of measurements. The MHT uses statistical methods (track score) to discriminate between false and true tracks. The probability of target existence obtained by utilizing Markov chain propagation models and Bayes update is used as the track quality measure in Integrated Probabilistic Data Association (IPDA) of [6] and Integrated Track Splitting (ITS) [7],[8].

The application of the Sequential Monte Carlo estimation framework to real multi-target tracking problems is plagued by many difficulties. Among other things, realistic models for the target dynamics and measurement processes are often nonlinear and non-Gaussian, so that no closed-form analytic expression can be obtained for the tracking recurs.

When tracking a single object closed-form expressions are generally not available for nonlinear or non-Gaussian models, and approximate methods are required. The extended KF liberalizes models with weak nonlinearities around the current state estimate, so that the KF recursions can still be applied. However, the performance of the EKF degrades rapidly as the nonlinearities become more severe. To alleviate this problem the unscented KF (UKF) [9], [10] maintains the second-order statistics of the target distribution by recursively propagating a set of carefully selected sigma points [11]. This method requires no linearization, and generally yields more robust estimates.

When tracking with Particle Filter [12],[13] an analog to the predicted measurements covariance is not directly available and could only be constructed as an approximation to the current particle cloud. A common alternative is to use a form of soft gating based upon a Student'st likelihood, combine the same function and probabilistic data association approaches to develop a new method for tracking in clutter using a particle filter. This is done by deriving an expected likelihood from known measurements and clutter statistics.

In this paper, we propose the integrated particle filter (IPF) solution for the target tracking in clutter. Each track trajectory pdf is represented by a disjoint set of particles, and the probability of target existence is integrated into the track state, similar to [14], [15], [16]. The FTD may use the probability of target existence as the track quality measure. The standard IPF is a single-target tracker, and we also include multi target approach [17] for target tracking. They all share common recursion elements, being distinguished by the data association calculus. In addition to the recursive calculation of the probability of target existence and non-uniform clutter, we also include the state dependent probability of target detection, and maneuvering (multi-model) target trajectories [18].

Rest of the paper is organized as follows. The models and the particle filter background are presented in Section 2. The common IPF framework is detailed in Section 3, and the implementations of IPF is presented in Section 4. This approach is indicated by simulations in Section 5, followed by the concluding remarks in Section 6.

II. Problem Statements

The dynamic target trajectory state models at the time k are given by the:

$$x_k = Fx_{k-1} + v_k \tag{1}$$

where F is the propagation matrix, v_k is a zero mean and

Branko Kovacević is with the School of Electrical Engineering, University of Belgrade, 73 Bulevar kralja Aleksandra, 11020 Belgrade, Serbia (e-mail: kovacevic_b@etf.rs).

Zvonko Radosavljević and Dejan Ivkovic are with the Military Technical Institute of of Belgrade, Ratka Resanovica 1, 11000 Belgrade, Serbia (e-mail: zvonko.radosavljevic@gmail.com and divkovic555@gmail.com).

white Gaussian sequence with covariance *R*. At each scan the sensor returns a random number of random target and clutter measurements. The measurement of existing and detectable target is taken with a probability of detection P_D. At time *k*, one sensor delivers a set of measurements $z_k = \{z_{k,j}\}_{j=1}^{M_k}$ track out of which a set of measurements are selected for track update. Converted target measurement *y* is given by [19] :

$$y_k = Hx_k + w_k \tag{2}$$

where *H* is measurements matrix and the measurements noise w_k is zero mean and white Gaussian sequence. A measurements of target is present in each scan with a probability of detection P_D . Clutter measurements follow the Poisson distribution characterized at location by clutter measurements density $\rho_k(y)$ [19].

Particle filtering samples at the continuous posterior density function of interest into a set of weighted particles. If the weights are chosen appropriately, then these weighted set of particles represent the posterior density in a way that the posterior density function can be made arbitrarily close to the equivalent set of weighted particles. The target trajectory state *pdf* at scan *k* is defined by set of particles $\{x_k, w_k\}$, parameterized by set of *N* particles $\{w_l^i, x_k^i\}_{i=1}^N$ where should be satisfied $\sum_{i=1}^{N} w_l^i = 1$. Using sequential importance sampling [xx], particle filters can approximate the posterior density function, regardless of the time interval k of the trajectory model [20].

III. INTEGRATED PARTICLE FILTER

The track state consists of the target existence event, and the trajectory state, and for each track we recursively calculate the probability of target existence, and the trajectory state probability density function (pdf). The trajectory state pdf are only defined conditioned on target existence. Depending on the calculated probability of target existence we may conclude that the target exists and confirm the track. Each confirmed track stays confirmed until termination. Alternatively, if the calculated probability of target existence dips below certain level we conclude that the target does not exist and terminate the track [21].

Key topics of new IPF algorithms are:

- new particles arise by re-sampling;
- heavy particles are multiply,
- weak particles are extinguished
- measurements are used to correct the weight of the particles and the probabilities of target existence.

At begin, lets define key parameters. The number of particles from $(k-1)^{th}$ scan, $N_{k-1} = N$ does not change from scan to scan. Lets represent particle $\{x_{k-1}^i, w_{k-1}^i\}$, $i = 1,..., N_{k-1}$ from $(k-1)^{th}$ scan , mean and weight. Number of measurements arriving from k^{th} scan are M_k, and $N_p = N$ is number of particles after re-sampling step. Probability of target detection, as the function of target trajectory state is $p_D(x_k) = P_D$. Also we have equation [22]:

$$\tilde{P}_D = \sum_i w_{k-1}^i p_D(x_k^i) = P_D \sum_i w_{k-1}^i = P_D \tag{3}$$

Proposed IPF algorithm is perform by the following steps:

- prediction step,
- measurements likelihood calculating
- update step and
- re-sampling step.

A. *Prediction step:*

At begin, we calculate probability of target existence, by the:

$$\psi_{k|k-1} = \Delta_{11} \cdot \psi_{k-1|k-1} \tag{4}$$

The mean of particle is given by the:

$$x_k^i = f(x_{k-1}^i, v_k^i) = Fx_{k-1}^i + v_k^i \tag{5}$$

where particle propagation noise is $v_k^i \approx N(0, Q)$ and measurements sets is given by $Z_k = \{z_k^1,..., z_k^{M_k}\}$

B. *Measurements likelihoods*

After KF prediction, we estimate measurements by the:

$$\hat{y}_k^i = Hx_k^i \tag{6}$$

In order to compute statistical distance:

$$d^2{}_{ij} = (z_{k,j} - \hat{y}_k^i)^T (R_k)^{-1} (z_{k,j} - \hat{y}_k^i), \quad j = 1,..., M_k \tag{7}$$

Probability density function is given by the:

$$p_{k,j}^i = \frac{1}{\sqrt{\det(2\pi R_k)}} \exp[-0.5 \cdot d^2{}_{ij}] \tag{8}$$

where likelihoods of measurements is:

$$p_{k,j} = \sum_i w_{k-1}^i \cdot p_{k,j}^i \tag{9}$$

Now, we can calculate measurements likelihood ratio, by the equation:

$$\Lambda_k = 1 - P_D + P_D \sum_j \frac{p_{k,j}}{\rho_{k,j}} \tag{10}$$

Beta's coefficients we can update by the:

$$\beta_{k,j} = \frac{1}{\Lambda_k} \begin{cases} 1 - P_D, & j = 0 \\ P_D \dfrac{p_{k,j}}{\rho_{k,j}}, & j > 0 \end{cases} \tag{11}$$

C. Update step:

In update step, we first calculate weight of particles, in purpose of trajectory state update, by the [23]:

$$w_k^i = w_{k-1}^i \cdot (\beta_{k,0} + \sum_{j=1}^{M_k} \beta_{k,j} \frac{p_{k,j}^i}{p_{k,j}}) \quad (12)$$

At the end of update step, we calculate target existence probability of track, by the equation:

$$\psi_{k|k} = \frac{\Lambda_k \psi_{k|k-1}}{1-(1-\Lambda_k)\psi_{k|k-1}} \quad (13)$$

D. Resampling step:

Resampling step calculates mean and weight of particles, by the foloowing [24]:

$$\{x_k^i, w_k^i\} \Rightarrow \left\{ x_k^I, w_k^I = \frac{S_w}{N_p} = \frac{1}{N} \right\}, I = 1,2,...,N \quad (14)$$

where

$$S_w = \sum_{i=1}^{N_{k-1}} w_k^i = 1 \quad (15)$$

$$u_1 = U\left[0, \frac{1}{N}\right] \quad (16)$$

$$u_l = u_1^l + (l-1)\frac{1}{N}, i_c = i_{c-1} + w_k^i, i = 1,...,N \quad (17)$$

where S_w is sum of weights, $U[.]$ means uniform distribution, u_l is interval of weights.

E. *Output Calculation*

Finally, we can calculate the output state estimate and covariance (for output purpose only):

$$\hat{x}_{k|k} = \sum_{l=1}^{Np} w_k^l x_k^l \quad (18)$$

$$P_k = \left(\sum_{l=1}^{Np} w_k^l \cdot x_k^l \cdot x_k^{l\,T} \right) - \hat{x}_k \cdot \hat{x}_k^{\,T} \quad (19)$$

IV. IMPLEMENTATION OF IPF

In this section, a brief instruction of IPF sofware implemenattion, we describe. Track initiation and termination is an part for establishing the records of the new targets and terminating the unwanted records of the inexistent targets when they leave the surveillance region. But in the heavy cluttered environment, there exists due to the unknown state of the target and the sequence of measurements which originate from the target. Here, we present a track management procedure.

Track initiation is composed of two parts:

- produce temporal tracks and
- confirm the temporal tracks.

Track termination is of two meanings:

- reject the temporal tracks;
- terminate the confirmed tracks when the detected targets leave the surveillance region.

A. Software implementation of IPF

One cycle of the recursive IPF algorithms software implementation consists of the following procedure:

for scan = 1 : number of scans
--Read Measurements
-Target Tracking with IPF
-Initializing of Measurements Selection
-Measurements selection (measurement likelihood for all particles)
-Taking into account clutter density
-Update Tracks of IPF
-Single Target Track Data Association
-Update Weights
-Resampling
-Estimate IPF
-Tracks Initializing
-Update Old Samples
-Update Status
-Update Age
-Eliminate Wide
-Merge Close Tracks
-Eliminate Tracks -Out of Bound
-Update Tracks (Confirmation and Deleting)
-Prediction of IPF
-Determine Target Track
-Target Statistics of Scans (True, False, Confirmed,…)
-Reduce Tracks
End

V. SIMULATIONS

For the purpose of research, a simulation scenario with five targets motion scenario (Fig.1). Targets are initially positioned at the edges of a circle with the center at (500,500) and a radius of 450. Each target moves with a uniform speed towards the center of the circle, which they should reach in 20 scans, after which they carry on with uniform motion for further 20 scans. A random (noise) component is added to the speed vector of each target, with covariance (2*R/400).

A random component is added to the speed vector of each target, thus at scan 20 the variance of the distance between each target and the centre of the circle will be double the sensor measurement error noise covariance matrix. In the two targets scenario, the targets initial separation is 20^o, instead of fifteen targets scenario with the targets initial separation 10^o. The following definitions of true and false tracks are used. Each initiated track is false with respect to all existing targets. A false track becomes a true track with respect to a target when the state estimate is sufficiently close to the true target state.

Each simulation experiment consists of a number of simulation runs. In each simulation run, targets will repeat their trajectories. The measurements are generated independently. Each algorithm uses the same set of measurements. False tracks may be initiated using target measurements, either in a conjunction with a clutter

measurement, or by using measurements from different targets in different scans.

Thus, the average number of initialized false tracks per scan will depend on the number of targets present. The average number of initialized false tracks per scan was 8, and 120 for the two and fifteen targets experiments, respectively. A confirmed false track in one scan is 300 and 200 for the two and fifteen targets cases, respectively. The performance measures used to compare the algorithms confirmed true tracks, root mean square error positions and target retention statistics. Results are presented by a number of confirmed true tracks and Root Mean Square Error Position.

The target retention statistics was obtained by noting the identity of the confirmed true track following each of the targets at scan 14. These identities are checked again at scan 38, and the following statistics is accumulated for each experiment:

nCases: total number of cases of a target being followed by a confirmed track at scan 14;

nOK: percentage of tracks still following the original target at scan 38;

nSwitched: percentage of tracks that end up following a different target at scan 38;

nLost: percentage of tracks not following any target at scan 38,

nMerged: percentage of tracks lost due to merging between tracks counted in nCases between scans 14 and 38

For the target retention statistics, each algorithm identifies the confirmed true track for a specific interval that includes intersection of trajectories. The targets intersect at scan 24 and many joint events occur around that time. In the experiment, the identities of the confirmed true tracks are obtained at scan 17 for performance comparison.

Parameters were used: probability of target detection is pD=0.8, number of Monte Carlo runs is 100, duration of one recursion 40, measurements noise matrix -R=[25 0; 0 25], maximum of target speed -25 [m/s], variance of acceleration q =0.75, number of particles -1000, maximum number of components -40, starting cross statistics in 14 scan, ending cross ststistics scan 38.

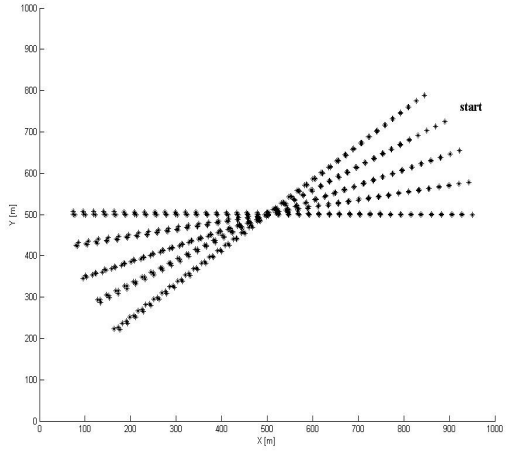

Fig. 2. Simulation scenario (Five targets)

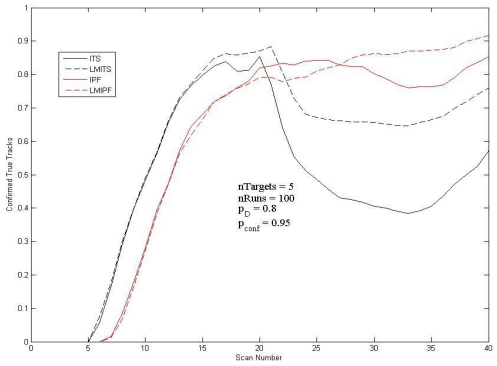

Fig. 2. confirmed true tracks diagram over time (five target)

The sampling period of radar sensor is T=1s. Duration of the scenario is 40 scans. The system input is modeled as follows: vector state $\mathbf{x}(k) = [x\ \dot{x}\ y\ \dot{y}]^T$ where the Cartesian coordinates of the target position are, and are the appropriate velocities. Transition matrix and process noise matrix are given by:

$$F = \begin{bmatrix} 1 & T & 0 & 0 \\ 0 & 1 & 0 & 0 \\ 0 & 0 & 1 & T \\ 0 & 0 & 0 & 1 \end{bmatrix} \tag{20}$$

$$Q_k = q \begin{bmatrix} T^3/3 & T^2/2 & 0 & 0 \\ T^2/2 & T & 0 & 0 \\ 0 & 0 & T^3/3 & T^2/2 \\ 0 & 0 & T^2/2 & T \end{bmatrix} \tag{21}$$

respectively. Measurements matrix and measurements noise matrix is given by:

$$H = \begin{bmatrix} 1 & 0 & 0 & 0 \\ 0 & 0 & 1 & 0 \end{bmatrix}, \quad R_k = \begin{bmatrix} \sigma_x^2 & 0 \\ 0 & \sigma_y^2 \end{bmatrix} \tag{22}$$

respectively.

All simulations were done in a software package MATLAB, with CPU Intel Core i7, 2.93 GHz. Results of simulation are governed by the number of confirmed true tracks (Fig, 2) and target retention table. We compare standard ITS and proposed IPF algorithms.

Target retention table

	ITS	**IPF**
nCases[n]	**91**	**80**
nOK[%]	31.86	42.5
nSwit[%]	15.38	18.75
nLost[%]	52.76	38.75
merged	26	14
CPU [s]	1.65	1.81

The results confirm the justification of the proposed IPF approach compared to standard ITS algorithm. IPF has a smaller percentage of losses and switched targets and higher percentage of full tracking targets with approximately the same CPU consumption.

VI. CONCLUSION

The multiple target tracking algorithm, known IPF, is proposed and was tested in a special scenarios with five crossing targets. It uses the well-known features of ITS algorithms that account the probability of target existence of objective forms, trace and ease of use offered by the Particle Filter. A Simulation results with two-dimensional scenario showed that the proposed algorithm ends up with good performance and small computational load. Proposed algorithm, which has been presented for tracking multi, have the ability to estimate the number of targets. Tracking the trajectories of the target over time, operate with missed detections and give the trajectories of the targets.

REFERENCES

[1] D. Reid, 'An algorithm for tracking multiple targets', IEEE Trans. AC, vol. AC-24, no. 6, pp. 843–854, 1979.

[2] Blackman, S.:'Multiple-target tracking with radar applications' (Artech House, 1986)

[3] Kurien, T.:'Issues in the design of practical multitarget tracking algorithms', IEEE Trans. Autom. Control, 1979, 24, (6), pp. 843–854

[4] Challa, S., Evans, R., Morelande, M., Mušicki, D.: 'Fundamentals of object tracking' (Cambridge University Press, 2011)

[5] Musïcki, D., Evans, R., Stankovic´, S.: 'Integrated probabilistic data association (IPDA)', IEEE Trans. Autom. Control, 1994, 39, (6), pp. 1237–1241

[6] Mušicki, D., La Scala, B.: 'Multi-target tracking in clutter without measurement assignment', IEEE Trans. Aerosp. Electron. Syst., 2008, 44, (3), pp. 877–896.

[7] Bar-Shalom, Y., Tse, E.: 'Tracking in a cluttered environment with probabilistic data association', Automatica, 1975, 11, pp. 451–460

[8] Mušicki, D., Evans, R.: 'Multiscan multitarget tracking in clutter with integrated track splitting filter', IEEE Trans. Aerosp. Electron. Syst., 2009, 45, (4), pp. 1432–1447

[9] Z. Radosavljević, T.L. Song, B.Kovacevic, Linear Multi-Target IPF Algorithm for Automatic Tracking, Scientific Technical Review, 2016,Vol.66,No.1,pp.3-10, Belgrade 2016.

[10] Bar-Shalom, Y., Li, X.R., Kirubarajan, T.: 'Estimation with application to tracking and navigation' (John Wiley and Sons, 2001)

[11] Julier, S.J., Uhlmann, J.K.: 'Unscented filtering and nonlinear estimation', Proc. IEEE, 2004, 92, (3), pp. 401–422

[12] Alspach, D.L., Sorenson, H.W.: 'Nonlinear Bayesian estimation using Gaussian sum approximation', IEEE Trans. Autom. Control, 1972, 17, (4), pp. 439–448

[13] Ristic, B., Arulampalam, S., Gordon, N.: 'Beyond the Kalman filter' (Artech House, 2004)

[14] Hue, C., Le Cadre, J., Pérez, P.: 'Sequential Monte Carlo methods for multiple target tracking and data fusion', IEEE Trans. Signal Process., 2002, 50, (2), pp. 309–325

[15] Marrs, A., Maskell, S., Bar-Shalom, Y.: 'Expected likelihood for tracking in clutter with particle filters'. SPIE: Signal and Data Processing of Small Targets, April 2002, vol. 4728, pp. 230–239

[16] Vermaak, J., Godsill, S.J., Pérez, P.: 'Monte Carlo filtering for multi-target tracking and data association', IEEE Trans. Aerosp. Electron. Syst., 2005, 41, (1), pp. 309–332

[17] Song, T.L., Mušicki, D.: 'Adaptive clutter measurement density estimation for improved target tracking', IEEE Trans. Aerosp. Electron. Syst., 2011, 47, (2), pp. 1457–1466

[18] Gordon, N.J., Salmond, D.J., Smith, A.F.M.: 'Novel approach to nonlinear/ non-Gaussian Bayesian state estimation'. IEE Proc., Radar, Sonar and Navigation, 1993, vol. 140, no. 2, pp. 107–113

[19] Song, T.L., Mušicki, D., Kim, D.S.: 'Target tracking with target state dependent detection', IEEE Trans. Signal Process., 2011, 59, (3), pp. 1063–1074.

[20] Song T.L., Mušicki D., Kim D.S., and Radosavljević Z.: 'Gaussian mixtures in multi-target tracking: a look at Gaussian Mixture Probability Hypothesis Density and Integrated Track Splitting', IET Proceedings: Radar, Sonar and Navigation, vol. 6, 2012, no. 5, pp. 359-364..

[21] Radosavljević Z., Mušicki D.: Limits of target tracking in heavy clutter, ASIA-Pacific International Conference of Synthetic Aperture Radar APSAR 2011, Seoul, Korea, 2011.

[22] Z .Radosavljevic, D. Ivkovic, 'An Approach of Track Management System in Software Defined Radar', Scientific Technical Review, 2018, Vol.68,No.1, pp.73-80, Belgrade 2018, UDK 681:5.017:623:746.3

[23] Z. Radosavljević, ,IPDA Filters in the Sense of Gaussian Mixture PHD Algorithm, Scientific Technical Review, 2016,Vol.66,No.3, pp.34-40, Belgrade 2016, UDK : 681:5.017:623:746.3, COSATI:17-09, 12-01.

[24] Radosavljević, Z., Musïcki, D., Kovačević, B., Kim, W.C., Song, T.L.: 'Integrated particle filter for target tracking'. 13th Int. Conf. on Electronics, Information and Communication, ICEIC 2014, Kota Kinabalu, Malaysia, January 2014.

Hough transform in visual product quality control

Aleksandra Marjanović, Sanja Vujnović and Željko Đurović

***Abstract*— Product quality inspection is one of the indispensable steps in the production process, and there are more and more factories that are trying to automate that procedure by using computer vision algorithms. Additional efforts are made to keep these algorithms simple and fast when time is of the essence. This paper relies on Hough transform as a standard tool in image processing and discusses its possibilities in a time-constrained scenario. Being that the considered product is ball-shaped, the extension of Hough transform for circle detection is used to detect product in appropriate cells on the conveyor belt. The problem setup may seem easy, but unpredictable parameters of the industrial surroundings make it challenging. The detection algorithm is tested on a real-life image database collected at one chemical factory in Serbia.**

***Index Terms*—Visual product quality control, Defect detection, Hough transform, Circle detection.**

I. Introduction

With the development of modern technology, the efficiency and reliability of industrial plants is increasing, whether it is in terms of improving the hardware of existing systems or in terms of applying intelligent control laws that can monitor and regulate a large number of signals simultaneously. The automation of the production process is especially important in places that do not represent an ideal working environment for humans, such as plants in the electric power and chemical industries.

In the last decades advanced algorithms have found their place not only for increasing the quality of the production process, but also because of high expectations from customers, fierce competition, and stricter requirements of regulatory bodies and in quality control of the final product [1]. One of the basic forms of quality control is visual inspection of products and in many factories it is carried out in an old-fashioned way, by a human inspector. This, however, can be a very demanding job that requires a person to be in constant focus during a shift of about 8 hours, looking at the same product thousands of times. Research shows that in this process the error rate is high and goes over 25%. It is only natural that automated solutions for visual inspection of product quality, which rely on the methods of computer vision and artificial intelligence, are becoming more and more common [2], [3]. Apart from lowering the errors in the quality control process, there is another great advantage of implementing these kinds of solutions by the manufacturer. Mainly, the redirection of people from a repetitive non-creative job, which in some industries can be unpleasant for people's physical health, to jobs that are of greater importance, and which could not be done without people [4]. According to Markets Insider estimates, the machine vision sector will have earnings of about $ 12.29 billion from the start of their use until 2023, with an annual growth rate of about 7.61%.

The requirements placed on such a quality control system are very often contradictory. On the one hand, they must be fast enough for the production system to run smoothly, and on the other hand, more advanced algorithms that would increase the accuracy of such systems are also numerically more complex and require more time to execute. This paper discusses a segment of the visual inspection system in a modern chemical production plant that operates with a large capacity of several hundred products per minute. This leaves room for about a hundred of milliseconds for product processing, which should include image recording, image processing and decision making, as well as taking appropriate action. The job of engineers, therefore, is to design the simplest possible decision system with the highest possible success rate. Of course, it should be emphasized that the mechanical part of the system should be fast and reliable, but at the same time simple and cheap enough to be cost-effective for serial production.

The problem tackled in this paper refers to quality control in the production process of scented sanitary balls. Prior to the automation of this process, the inspection was performed by a person by monitoring for several hours the batches of balls that are at the output of the shaping subsystem. Apart from the fact that this kind of work is tiring for the sense of sight, it is also tiring for the sense of smell due to strong vapors in the plant. Due to all these facts, the company's management came up with the idea of automating this segment of production. This paper describes the first step in the product quality assessment procedure, which refers to the detection of products within the intended slot. In real industrial conditions this can be quite challenging, as will be explained later. The algorithm must be simple and fast enough at the same time, so that in combination with the algorithm for checking the regularity of the ball and communication between individual components it is suitable for real time application.

Marjanović is with the School of Electrical Engineering, University of Belgrade, 73 Bulevar kralja Aleksandra, 11020 Belgrade, Serbia (e-mail: amarjanovic@etf.bg.ac.rs).

Sanja Vujnović is with the School of Electrical Engineering, University of Belgrade, 73 Bulevar kralja Aleksandra, 11020 Belgrade, Serbia (e-mail: svujnovic@etf.bg.ac.rs).

Željko Đurović is with the School of Electrical Engineering, University of Belgrade, 73 Bulevar kralja Aleksandra, 11020 Belgrade, Serbia (e-mail: zdjurovic@etf.bg.ac.rs).

Following Introduction, Section II provides a review of Hough transform and its application in line and circle detection. Section III describes in detail the setup of product visual inspection process, focusing on the challenges during product detection phase and the possibilities of overcoming them using Hough transform. Finally, Section IV shows main results concerning the influence of image down sampling on detection accuracy, as a tool for reduction of computational efforts.

II. HOUGH TRANSFORM

Hough transform in its original form is a tool that enables fast and efficient detection of straight lines in digital images [5]. Namely, if we want to find among the n points in the plane those that belong to one line, the number of operations that should be done by the brute-force method is proportional to n^3, which is unusable in the context of real time execution. On the other hand, Hough transform starts from the idea that one point (x_i, y_i) located on the line

$$y = ax + b \tag{1}$$

maps to the line in (a, b) space

$$b = -x_i a + y_i. \tag{2}$$

Similarly, any other point on the line (1) will map into the line in (a, b) space, which intersects the line (2) in the point determined by parameters a and b in Eq. (1). In other words, the problem of searching for line parameters is reduced to searching the space (a, b) with the aim of finding the point where the largest number of lines intersect [6]. A limiting circumstance in this consideration is the fact that the vertical line has an infinite slope. This problem is overcome starting from the idea that every point on the line in (x, y) space can be represented by a sinusoid in the parametric space (ρ, θ)

$$x \cos\theta + y \sin\theta = \rho, \tag{3}$$

which is shown in Fig. 1.

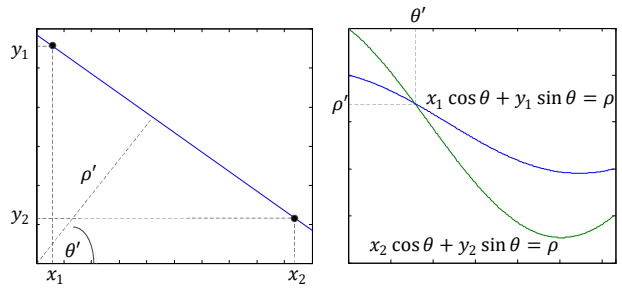

Fig. 1. The concept of Hough transform.

Similarly, the cross section of these sinusoids contains the correct parameters ρ and θ. In this way, the previous search is reduced to a search by angle $\theta \in [-\pi/2, \pi/2]$ and $\rho \in (-\infty, \infty)$. The implementation of this algorithm first involves the quantization of space (ρ, θ) into so-called accumulator cells. Then, each point (x_k, y_k) is observed and the corresponding quantized value ρ is calculated for each quantized value of the parameter θ and the final search for the cell in which the most sinusoids were found. Over time, the extensions of this procedure to the problem of finding second-order curves and arbitrary shapes have been considered [7], [8]. Thus, for the detection of a circular contour, three parameters should be determined, the coordinates of the center of the circle and the radius:

$$(x - x_0)^2 + (y - y_0)^2 = R^2. \tag{4}$$

Similarly as before, a different representation of the circle over the radius and polar angle can be considered:

$$\begin{aligned} x &= x_0 + R\cos\theta \\ y &= y_0 + R\sin\theta, \end{aligned} \tag{5}$$

where $\theta \in [0, 2\pi)$. In this case, the accumulator is three-dimensional, and the procedure for incrementing the cell values is based on the previously described procedure. Namely, each pair of points is a potential center (x_0, y_0), and the radius range is the potential radius. Bearing in mind that the search is now done in three-dimensional space, computational time of single curve detection is high. Over time, improvements to this algorithm have been proposed, such as the use of genetic algorithms [9] and harmony search [10], which shorten computational time and allow sufficiently precise circuit parameters to be found. Also, there are extensions of this algorithm to the detection of arbitrary curved lines.

III. PRODUCT DETECTION ALGORITHM

To better understand the idea of applying Hough transform in the process of visual quality inspection, let us describe the setting of the problem in a little more detail. The balls arrive one by one for individual inspection, sorted on the appropriate conveyor belt, separated by barriers (Fig. 2). The part of the system related to the visualization of the product consists of three cameras separated in space, two on the side and one from above, which have the task to look from different angles at the cell in which the product should be located. After that, in case there is a product in the cell, a quality control algorithm is applied, which should assess whether the ball is defective or not. If there is no defect, the ball should be passed to the next step of the production process. If, however, the ball is defected the pneumatic blower should be signaled to throw the ball off the production line, after which it is sent for recycling, i.e., the beginning of the mixture making step. Processing images from two side cameras can be done in the same way, because the image obtained from them is similar. Namely, it shows a ball leaning on the barrier that is immediately behind the ball when the direction of movement of the conveyor belt is observed, and in one case the ball is leaning on the left and in the other on the right barrier.

Additionally, behind the ball (as seen from the camera), there is a partition that provides an appropriate, contrasting background color depending on the color of the ball. On the other hand, the third camera is placed above the ball, and the picture from it shows the ball leaning on the barrier, but also a part of the base, that is. the conveyor belt on which the ball lies. Precisely because of this difference, processing images from the third camera is somewhat more complicated than the first two. Namely, after a few minutes, and then a few hours of using the system, the belt becomes dirty, sometimes with the color of the balls that previously passed over it, which is shown in Fig. 3 (one and the same belt is often used to process different colors of balls, depending on the requirements). In order for the belt to be cleaned, the machine must be stopped for a few minutes. However, if the cleaning is not carried out in a timely and adequate manner, this can complicate the algorithm for processing images from the third camera.

The step of checking whether there is a ball between the two barriers is the first step in the algorithm, and it should be the fastest one, so that there is enough time to perform a more time-consuming step, which refers to checking the quality of the ball. By analyzing the image from the first two cameras, this is very easy to check, because the background behind the ball is not dirty. However, if the same algorithm is applied to images from the third camera, many false alarms appear, which further leads to a misconception about the number of defective balls, because empty slots are classified as irregular balls in the next step. An additional problem in the analysis of the image from the third camera is the fact that during operation the voltage on the light is variable, so the brightness of the ball changes with it, and it is difficult to automatically adjust the camera exposure, because it is almost impossible to find a reference point that will not be influenced by the color of the ball. These and similar problems are precisely the consequence of working in industrial conditions, which can be very unpredictable.

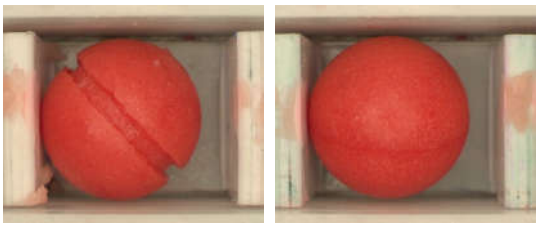

Fig. 2. Examples of full cells.

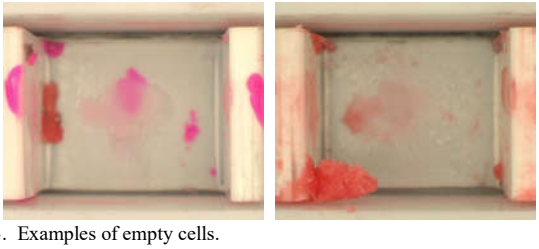

Fig. 3. Examples of empty cells.

This is exactly the problem we will try to solve by applying Hough transform. Because the picture of an empty cell often consists of stains at the bottom of conveyor belt, as well as smaller masses which should not be counted as the ball and will certainly be eliminated from further production process due to smaller dimensions, Hough transform is proposed to find circular contours in an image whose radius is in a predefined range, and in accordance with what the expected radius of the ball is. The algorithm consists of several steps:

- In the first step, depending on the color, it is necessary to find the appropriate color space, i.e. the appropriate representation, in which it will be easier to notice the difference between the ball and the background. In some cases, it will be some of the RGB components, other times HSV space will be more useful, etc.
- In the next step, using the Canny edge detector, the previously selected gray image is translated into a black and white image, by carefully selecting the thresholds of the said detector. The thresholds are chosen so that the edges of the ball are detected as clearly as possible, although in real conditions this implies the detection of background noise.
- Finally, the Hough transformation is applied to check whether among the detected points in the black and white image there are those that belong to the same circular contour of the appropriate size, which indicate the presence of a ball in the image. Due to the nature of the algorithm, it will certainly find a circle, and based on the parameters of the circle and the number of detected points, a decision is made whether the ball exists in the image or not.

Additionally, as mentioned earlier, this procedure involves searching in 3D space, which requires computing resources. Bearing in mind that the ball has some expected size, i.e. the radius, as well as the limited space in which the center of the sphere can appear, the first step in enhancing the speed of the algorithm refers to the appropriate narrowing of the search space for all three parameters. The second step refers to the examination of the extent to which it is possible to work with a resampled image of lower resolution, i.e. the extent to which the decimation procedure affects the finding of the circular contour and its parameters. The results of this consideration are presented in the next chapter.

IV. RESULTS

Testing of the proposed algorithm was done on a database consisting of 3000 images with empty cells and 3000 images with the product (2800 regular products and 200 defects). All images have the same 600x500 resolution. Let us first observe the performance of circular contour detection in different images. Fig. 4 and Fig. 5 clearly show that the extended detection algorithm gives a good result, in terms of successful contour detection. The images on the left show the original images of the balls, and on the right is the result of the application of Canny edge detector, together with a drawn contour whose parameters correspond to a circle that fits the largest number of points. Fig. 6 shows the results in the case

of images without products. What can be noticed at first glance is that the algorithm again managed to find a circular contour, although it is not obvious in the original image. But that is still the expected result, because the algorithm finds the circle on which the largest number of points from the BW image is located. The essential difference between these two cases is in the number of points which the detected circle fits.

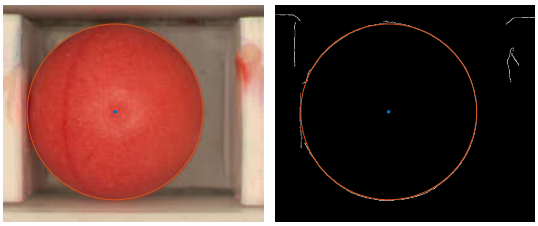

Fig. 4. Examples of circle detection on a regular product.

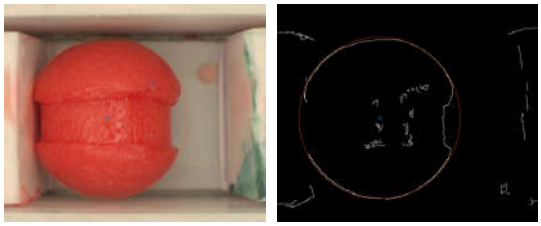

Fig. 5. Examples of circle detection on a defect.

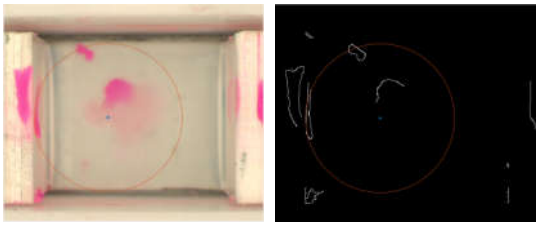

Fig. 6. Examples of circle detection on an empty cell.

Table 1 shows first- and second-order statistics for the number of detected points per circle N, as well as the execution time of the algorithm T on the Intel(R) Core(TM) i7-9700KF CPU at 3.60 GHz configuration It can be observed that the number of detected points is significantly higher in the case when the ball exists than when the cell is empty. A more detailed analysis showed that there is a clear gap between these two cases, which means that the detection problem can be successfully solved by setting an appropriate threshold. In addition, another interesting fact is that in the case off a defect, the number of detected points is slightly smaller than in the case of regular products. This result is justified bearing in mind that the defect of the product is often reflected in its irregular contour, which deviates from the circular contour in a few segments. However, for most products, this deviation is not significantly pronounced, which is why these two cases are not linearly separable considering this parameter space. Execution time analysis in different cases also gives the expected results. Namely, in the case of a defective ball, the output from the Canny edge detector is slightly higher than in the case of a regular one. Therefore, the number of points that need to be processed during the formation of the accumulator matrix is higher. On the other hand, one could expect that in the case of empty cells, the number of points returned by the Canny edge detector is not large. However, depending on the lighting and the degree of conveyor belt contamination, the number of points may be approximately the same as in the case of regular balls. Therefore, the execution time of the algorithm in that case is somewhat less, but not significant. Even though 30ms does not sound like a long time, it is not affordable when there is around 150ms available for the overall product inspection process.

TABLE I
AVERAGE DETECTION PARAMETERS PER DIFFERENT TYPES OF IMAGES

	N_{mean}	N_{std}	T_{mean}	T_{std}
Regular product	312.6	76.3	29.5ms	2.1ms
Defect	265.9	65.9	32.1ms	3.3ms
Empty cell	41.5	13.17	26.8ms	4.2ms

The last result led us to the idea of decimation, i.e. downsampling. Several cases depending on the degree of decimation were considered. Table 2 presents the results that show the degradation of detection parameters depending on the degree of decimation. In addition to the two parameters discussed earlier, this analysis also observed the extent to which the position of the center and the radius of the detected circle change with decimation in comparison to the case of no decimation. What can be noticed from the last two columns is that the relative changes in the position of the center and the radius are very small. What is perhaps a slightly more indicative information is that the maximum absolute deviation in the center position in the case of an empty cell is between 80 and 90 pixels, and in the case of a full cell between 18 and 22 pixels depending on the parameter k. Similarly, during decimation, there is a maximum absolute change in the radius of 12-18 pixels for full cells, and 26-28 pixels for empty cells. In other words, the difference obviously exists, but it is negligible when compared to the radius. Another important parameter is the mean execution time of the algorithm. The results show that this parameter is smaller for higher k, and that it decreases by about 30% for higher decimation.

TABLE II
AVERAGE DETECTION PARAMETERS FOR DIFFERENT DEGREE OF DECIMATION

		N_{mean}	T_{mean}	$\Delta x/R$	$\Delta R/R$
$k=2$	Full	156.9	24.1ms	4.4e-3	0.7e-3
	Empty	22.9	21.8ms	25.3e-3	9.0e-3
$k=3$	Full	103.9	21.4ms	3.3e-3	1.5e-3
	Empty	14.6	20.2ms	26.4e-4	11.5e-3
$k=4$	Full	79.7	20.2ms	6.5e-3	2.2e-3
	Empty	11.9	19.3ms	36.4e-3	16.3e-3
$k=5$	Full	62.9	19.7ms	5.1e-3	4.6e-3
	Empty	9.3	18.9ms	35.9e-3	19.3e-3

Based on previous considerations, the introduction of decimation is justified. Let us analyze how this procedure affects the number of points N as a crucial parameter for decision making. The mean value of the number of points on the detected circle decreases with a higher degree of decimation, which is expected. Again, when looking at the mean value in these two cases, it would seem that there is a large enough gap between the classes, however it turns out that they are closer to each other with higher decimation, primarily due to irregular products. Therefore, although the previous arguments are in favor of a higher degree of decimation, one must still be cautious and a compromise must be made. In this sense, it is shown that for $k = 4$ it is still possible to set a threshold on the number of detected points for classification purposes, and yet significantly speed up the execution of the algorithm.

V. Conclusion

The paper discusses the possibilities of applying Hough transform in detection of a ball-shaped product in the appropriate cell on the conveyor belt during the product quality control, based on the digital image. Firstly, it was shown that images without a product can be classified quite easily from the case when the cell is full by setting a decision threshold. The possibilities of the BW image decimation procedure for the purpose of accelerating the detection algorithm, are further discussed. This step was evaluated by the execution time and individual parameters of object detection in relation to the case when no decimation exists. It has been shown that the execution time is significantly reduced to about 20 ms, which is about 30% shorter than in the original case. In terms of the parameters of the detected circle, the algorithm is not too sensitive, while the unfavorable influence of the degree of decimation is reflected in the reduction of the gap between the two classes in terms of the number of detected points on the circle. As a compromise solution, the decimation parameter $k = 4$ is proposed, for which the proposed algorithm does not make any mistakes during the decision-making process on the available database.

Acknowledgment

This research was supported by the Ministry of Education, Science and Technological Development of the Republic of Serbia.

References

[1] T. Johnson, S. Fletcher, W. Baker, R. Charles, "How and why we need to capture tacit knowledge in manufacturing: Case studies of visual inspection," *Applied ergonomics*, vol. 74, pp. 1-9, 2019.

[2] A. Djavadifar, J. Graham-Knight, M. Körber, P. Lasserre, H. Najjaran, "Automated visual detection of geometrical defects in composite manufacturing processes using deep convolutional neural networks," *Journal of Intelligent Manufacturing*, pp. 1-19, 2021.

[3] T. Wang, Y. Chen, M. Qiao, M, H. Snoussi, "A fast and robust convolutional neural network-based defect detection model in product quality control," *The International Journal of Advanced Manufacturing Technology*, vol. 94, no.9, pp. 3465-3471, 2018.

[4] D, Brückner, "Innovating quality control mechanisms in aseptic drug manufacturing by means of isothermal microcalorimetry and tunable diode laser absorption spectroscopy," *Diss. University_of_Basel*, 2017.

[5] P. Hough, "Method and Means for Recognizing Complex Patterns," U.S. Patent *3 069 654*, 1962.

[6] R. Duda, P. Hart, "Use of the Hough Transformation to Detect Lines and Curves in Pictures," *Communication of the ACM*, vol. 15, no 1, pp. 11–15, 1972.

[7] D. Ballard, "Generalizing the Hough transform to detect arbitrary shapes," *Pattern Recognition*, vol. 13, no. 2, pp.111-122, 1981.

[8] H. Yuen, J. Princen, J. Illingworth, and J. Kittler, "Comparative study of Hough Transform methods for circle finding," *Image and Vision Computing*, vol. 8, no. 1, pp. 71–77, 1990.

[9] V. Ayala-Ramirez, C. Garcia-Capulin, A. Perez-Garcia, R. Sanchez-Yanez, "Circle detection on images using genetic algorithms," *Pattern Recognition Letters*, vol. 27, no. 6, pp. 652–657, 2006.

[10] E. Cuevas, N. Ortega-Sanchez, D. Zaldivar, M. Perez-Cisneros, "Circle detection by harmony search optimization," *Journal of Intelligent and Robotic Systems: Theory and Applications*, vol. 66, no. 3, pp. 359–376, 2012.

Some new results on stability of incommensurate fractional systems and their $\mathscr{L}_p$-norms

Rachid MALTI
Université de Bordeaux – IMS UMR 5218 CNRS, France
Email: firstname.lastname@ims-bordeaux.fr

***Abstract*—Stability of fractional systems is yet an open problem especially when dealing with incommensurate differentiation orders. The objective of the invited talk is twofold. First of all, a new method [1] for determining stability regions, in the parametric space, of fractional incommensurate systems is presented. It is based on interval arithmetics and allows, beyond the stability property, to specify the regions in the parametric space that have the same number of unstable poles. Hence, all transfer functions which parameters belong to the same stability region have the same stability property.**

Contrary to rational systems, the stability property of fractional systems does not guarantee the existence (or the boundedness) of the $\mathscr{L}_p$-norms, $1 \leq p \leq \infty$, of their impulse response. Hence, the second objective of the talk is to examine the existence conditions of these $\mathscr{L}_p$-norms [2]. The established results are used to choose a performance index for evaluating stable feedback control system performances.

I. Introduction

Fractional systems has been attracting a lot of interest during the last two decades in different fields of engineering and science, since the seminal work by Oldham and Spanier [3], [4] for modeling diffusive phenomena.

Fractional systems can be described in transfer function form:

$$F(s) = \frac{\sum_{i=0}^{M} b_i s^{\beta_i}}{1 + \sum_{j=1}^{N} a_j s^{\alpha_j}} \tag{1}$$

where the exponents of s can be ordered $0 < \alpha_1 < \alpha_2 < \ldots < \alpha_N$, $0 \leq \beta_0 < \beta_1 \ldots < \beta_M$ and $(a_i, b_j) \in \mathbb{R}^2, \forall i = 0, 1, \ldots, M, \forall j = 1, 2, \ldots, N$. The multivalued function $s \mapsto s^\nu$ becomes holomorphic in the complement of its branch cut line of the complex plane, chosen to be along the negative real axis, $\mathbb{R}_{\leq 0}$, including the branching points 0 and ∞. Hence, $F(s)$ is a meromorphic function in the complement of $\mathbb{R}_{\leq 0}$ of the complex plane: $\mathbb{C} \setminus \mathbb{R}_{\leq 0}$.

The $\mathscr{L}_p$-norm of $f(t)$, the impulse response of $F(s)$, is defined as[1]

$$\begin{cases} \|f\|_p = \sqrt[p]{\int_0^{+\infty} |f(t)|^p \, dt} & \text{for } 1 \leq p < \infty \\ \|f\|_\infty = \sup\limits_{t \in \mathbb{R}_{\geq 0}} |f(t)| \end{cases} \tag{2}$$

[1]Note that $f(t)$ is a continuous-time function and hence the supremum is used instead of the essential supremum in the definition of $\|f\|_\infty$.

A function $f(t)$ is said to belong to the Lebesgue space $\mathscr{L}_p(\mathbb{R}_{\geq 0})$ with $p \in [1, \infty]$, or $\mathscr{L}_p$ in short, if its p-norm is finite: $\|f\|_p < \infty$.

The system $F(s)$ is $\mathscr{L}_p$-stable, $1 \leq p \leq \infty$, if and only if:

$$\sup_{u \in \mathscr{L}_p, u \neq 0} \frac{\|f \star u\|_p}{\|u\|_p} < \infty \tag{3}$$

where $\star$ stands for the convolution product and $u(t)$ the system input. Condition (3) is satisfied, $\forall p \in [1, \infty]$, when

$$f \in \mathscr{L}_1(\mathbb{R}_{\geq 0}) \tag{4}$$

In such a case:

$$\|f \star u\|_p < \|f\|_1 \|u\|_p \tag{5}$$

The bounded-input-bounded-output (BIBO) stability is defined as the $\mathscr{L}_\infty$-stability.

Due to its simplicity, the most used criterion for testing stability of fractional systems is Matignon's theorem [5, theorem 2.21]. It allows deciding whether a system is stable by locating its s^ν-poles. It generalizes the classical Routh-Hurwitz criterion for rational systems. It is extended to take into account variations of $\nu \in (0, \infty)$ in [6].

Theorem 1. *A commensurate transfer function, of order ν, $F(s) = \frac{T(s^\nu)}{R(s^\nu)}$, where T and R are coprime polynomials, is BIBO-stable if and only if*

$$0 < \nu < 2 \tag{6}$$

and for every $s \in \mathbb{C}$ such that $R(s) = 0$

$$|\arg(s)| > \nu \frac{\pi}{2} \tag{7}$$

However, Matignon's theorem applies only for stability checking of commensurate fractional systems. When the system is incommensurate, some other criteria, mainly based on Cauchy's principal theorem [7] or its derivatives such as the Nyquist theorem [8] are used. However, these methods are quite difficult to implement in practice.

Since (4) is only a necessary condition, the system might be $\mathscr{L}_p$-stable and yet have an impulse response, f, with an infinite $\mathscr{L}_p$-norm $\forall p \in [1, \infty]$. This feature is not common in the classical rational systems: when a rational system is $\mathscr{L}_p$-stable then its $\mathscr{L}_p$-norms are finite.

II. Stability of uncommensurate fractional systems

This section of the paper contains results of a joint work with Milan R. Rapai'c and Vukan Turkulov, which is currently submitted at the ICFDA'2021 conference [1].

Bonnet and Partington [9] proved that $F(s)$ is BIBO-stable if and only if it is analytic in the right-half complex plane $\{\mathscr{Re}(s) \geq 0\}$. In such a case

$$F(s) \in \mathscr{H}_\infty(\mathbb{C}_+) \tag{8}$$

where $\mathscr{H}_\infty(\mathbb{C}_+)$ is the Hardy space of analytic functions on the open right-half plane $\mathbb{C}_+$.

On the other hand, it can be proven from Rouché's theorem that all system poles vary continuously with its parameters anywhere in the complex-plane except the branch-cut, $\mathbb{R}_{\leq 0}$. Moreover, when transfer function differentiation orders vary, new poles can appear or vanish only on the branch-cut. Hence, the basic idea is to consider that if a fractional system is stable for a given parametric point then it remains stable unless its poles cross the imaginary axis. Further, assuming that there is no possible simplification between poles and zeros of $F(s)$ in (1), the stability of $F(s)$ depends only on the position of the zeros of the characteristic function:

$$\bar{f}(s, \boldsymbol{\alpha}) = 1 + \sum_{j=1}^{N} a_j s^{\alpha_j} \tag{9}$$

A. Problem formulation

According to the previous remarks, the following problems can be formulated in the parametric space:

(P1) Finding stability and instability regions. In this case, the objective is to check whether, for positive $\boldsymbol{\alpha} \in \mathbb{R}^n_{\geq 0}$, $\bar{f}(\rho e^{j\theta}, \boldsymbol{\alpha})$ has zeros in the right half complex plane including the imaginary axis. However, due to the symmetry of complex conjugate zeros, the searching domain can be restreint to the first quadrant of the complex s-plane: $(\rho, \theta) \in \mathbb{R}_{\geq 0} \times \left[0, \frac{\pi}{2}\right]$.

(P2) Finding the Stability Crossing Sets (SCS) between stability and the instability regions. In this case, the searching domain in the complex plane is restraint to $(\rho, \theta) \in \mathbb{R}_{\geq 0} \times \{\frac{\pi}{2}\}$. Hence, only values of $\boldsymbol{\alpha} \in \mathbb{R}^n_{\geq 0}$, for which the poles are crossing the imaginary axis towards the instability region are searched for.

Hence, the problems (P1) and (P2) can be formulated as finding the set of all feasible parameters

$$\boldsymbol{\theta} = (\rho, \theta, \boldsymbol{\alpha})^T \in \Omega = \left(\mathbb{R}_{\geq 0} \times \Theta \times \in \mathbb{R}^n_{\geq 0}\right), \tag{10}$$

where $\Theta = \left[0, \frac{\pi}{2}\right]$ for (P1) and $\Theta = \left\{\frac{\pi}{2}\right\}$ for (P2), satisfying

$$\begin{cases} \mathscr{Re}\{\bar{f}(\rho e^{j\theta}, \boldsymbol{\alpha})\} = 0 \\ \quad \text{and} \\ \mathscr{Im}\{\bar{f}(\rho e^{j\theta}, \boldsymbol{\alpha})\} = 0 \end{cases} \tag{11}$$

If $\exists \boldsymbol{\theta} = (\rho, \theta, \boldsymbol{\alpha})^T \in \Omega$ such that $\bar{f}(\rho e^{j\theta}, \boldsymbol{\alpha}) = 0$, then, for the problem (P1), the characteristic function has zeros in the closed right half complex plane and, for the problem (P2), on the imaginary axis, which allows determining the SCS.

Both of these problems can be formulated as a Constraint Satisfaction Problem $\mathcal{CSP}$[2]

$$\mathcal{CSP}: \begin{cases} \mathscr{Re}\{\bar{f}(\rho e^{j\theta}, \boldsymbol{\alpha})\} = 0 \\ \mathscr{Im}\{\bar{f}(\rho e^{j\theta}, \boldsymbol{\alpha})\} = 0 \\ 0 < \rho < \mathcal{R}, \quad \theta \in \Theta, \\ \alpha \in \mathbb{R}^n_{\geq 0} \end{cases} \tag{12}$$

where $\mathcal{R}$ is ∞ in theory and is finite in practice for evident implementation reasons. The solution set $\mathbb{S}$ for the problem (12) is rewritten as:

$$\mathbb{S} = \{\boldsymbol{\theta} \in \Omega \mid \mathscr{Re}\{\bar{f}(\rho e^{j\theta}, \boldsymbol{\alpha})\} \subset [0] \text{ and } \mathscr{Im}\{\bar{f}(\rho e^{j\theta}, \boldsymbol{\alpha})\} \subset [0]\}. \tag{13}$$

The characterization of the whole set $\mathbb{S}$ can be formulated as a set inversion problem:

$$\mathbb{S} = f^{-1}([0]) \cap \Omega, \tag{14}$$

and solved by guaranteed methods using interval arithmetics, introduced in the next subsection.

B. Introduction to interval arithmetics

Interval analysis was initially introduced by Moore [10]. An interval $[x] = [\underline{x}, \overline{x}]$ is a closed, bounded, and connected set of real numbers. The set of all intervals is denoted by $\mathbb{IR}$. Real operations are extended to intervals as follows. Given $[x] \in \mathbb{IR}$ and $[y] \in \mathbb{IR}$:

$$[x] + [y] = [\underline{x} + \underline{y}, \overline{x} + \overline{y}], \tag{15}$$

$$[x] - [y] = [\underline{x} - \overline{y}, \overline{x} - \underline{y}], \tag{16}$$

$$[x] \times [y] = [\min(\underline{x}\underline{y}, \underline{x}\overline{y}, \overline{x}\underline{y}, \overline{x}\overline{y}), \max(\underline{x}\underline{y}, \underline{x}\overline{y}, \overline{x}\underline{y}, \overline{x}\overline{y})] \tag{17}$$

$$[x]/[y] = \begin{cases} [x] \times \left[\frac{1}{\overline{y}}, \frac{1}{\underline{y}}\right], & \text{if } 0 \notin [y] \\ (-\infty, \infty), & \text{if } 0 \in [y]. \end{cases} \tag{18}$$

Interval arithmetics do not define an algebra because $(\mathbb{IR}, +)$ is not a group. Indeed, elements of $\mathbb{IR}$ do not have an inverse. Take for instance $A = [-1, 1] \in \mathbb{IR}$, then $A + (-A) = [-2, 2]$ is not equal to the degenerated interval $[0] = [0, 0] = \{0\}$. Either, $(\mathbb{IR}, +, *)$ is not a ring etc. Additionally, arithmetic operations on intervals introduce often pessimism because the result of each operation must be included in an interval.

[2]Usually a $\mathcal{CSP}$ is formulated using inequalities

$$\mathcal{CSP}: \begin{cases} \underline{x} \leq \mathscr{Re}\{\bar{f}(\rho e^{j\theta}, \boldsymbol{\alpha})\} \leq \overline{x} \\ \underline{y} \leq \mathscr{Im}\{\bar{f}(\rho e^{j\theta}, \boldsymbol{\alpha})\} \leq \overline{y} \\ 0 < \rho < \mathcal{R}, \quad \theta \in \Theta, \\ \alpha \in \mathbb{R}^n_{\geq 0}, \end{cases}$$

where $\underline{x}, \overline{x}, \underline{y}, \overline{y}$ can also be set to small enough values $-\epsilon, \epsilon, -\epsilon, \epsilon$; as in the fourth initialization of the example in section II-E5.

C. Solving the $\mathcal{CSP}$

1) Contractors: The $\mathcal{CSP}$ (12) is solved by a contractor $\mathcal{C}$, which is an operator which permits to reduce the domain $[\boldsymbol{\theta}]$ without any bisection. Hence, contracting the box $[\boldsymbol{\theta}]$ means replacing it by a smaller box $[\boldsymbol{\theta}]^*$ such that the solution set $\mathbb{S}$ remains unchanged, i.e. $\mathbb{S} \subset [\boldsymbol{\theta}]^* \subset [\boldsymbol{\theta}]$ [11]. There exists different types of contractors depending on whether the system to be solved is linear or not.

In our study, a non linear type contractor named *forward-backward contractor* is used to reduce the initial searching space. The basic idea when implementing this contractor is to decompose a principal constraint into primitive constraints. Each primitive constraint involves elementary operators and functions such as $\{+, -, \times, /, \exp, \log, \ldots\}$. The next example illustrates how a given constraint is used to contract a domain.

2) Example: Consider the constraint:

$$\begin{cases} f(\mathbf{x}) = x_3 - x_2 x_1 = 0, \\ x_1 \in [2, 10],\ x_2 \in [1, 10],\ x_3 \in [1, 5], \end{cases} \tag{19}$$

which can be rewritten as:

$$x_3 = x_2 x_1.$$

The forward interval constraint propagation removes all inconsistent values from $[x_3]$ as follows:

$$[x_3] = ([x_1] \times [x_2]) \cap [x_3] = [2, 5].$$

Then, the backward interval constraint propagation removes all inconsistent values from x_1 and x_2 as follows:

$$[x_1] = ([x_3]/[x_2]) \cap [x_1] = [2, 5],$$
$$[x_2] = ([x_3]/[x_1]) \cap [x_2] = [1, 5/2].$$

After a forward and a backward propagation, the contracted box is $[\mathbf{x}] = \big([2, 5], [1, 5/2], [2, 5]\big)^T$ which contains the solution of the $\mathcal{CSP}$.

In some cases the contractor cannot reduce enough the parameters domain. In such cases, bisection of the variable vector $\boldsymbol{\theta}$ is necessary. The algorithm SIVIA [12], which is described in the following section is based on the association of contractors and splitting.

D. Set Inversion Via Interval Analysis (SIVIA)

This algorithm, proposed by Jaulin and Walter in [12], allows to obtain an inner $\underline{\mathbb{S}}$ and an outer $\overline{\mathbb{S}}$ enclosures of the solution set $\mathbb{S}$ (if it exists), such that:

$$\underline{\mathbb{S}} \subseteq \mathbb{S} \subseteq \overline{\mathbb{S}}. \tag{20}$$

SIVIA is a recursive algorithm based on partitioning of the parameter set into three regions: feasible, undeterminate and unfeasible. SIVIA uses an inclusion test $[t] : \mathbb{IR} \to \mathbb{N}$ which is a function allowing to prove if an interval $[\boldsymbol{\theta}]$ is feasible in which case it is added to the set $\underline{\mathbb{S}}$. Any undetermined region is bisected and tested again, unless its size $w([\boldsymbol{\theta}])$ is less than a precision parameter η tuned by the user and which ensures that the algorithm terminates after a finite number of iterations. The outer approximation is then computed as $\overline{\mathbb{S}} = \underline{\mathbb{S}} \cup \Delta\mathbb{S}$ where $\Delta\mathbb{S}$ is the union of all remaining undetermined boxes. Hence, the SIVIA algorithm is presented in algorithm 1.

Algorithm SIVIA (in: $[t], [\boldsymbol{\theta}], \eta$; out: $\underline{\mathbb{S}}, \overline{\mathbb{S}}$)

1) Option: Call contractor on $\boldsymbol{\theta}$.
2) If $[t]([\boldsymbol{\theta}]) = [0]$, return;
3) If $[t]([\boldsymbol{\theta}]) = [1]$, then $\underline{\mathbb{S}} := \underline{\mathbb{S}} \cup [\boldsymbol{\theta}]; \overline{\mathbb{S}} := \overline{\mathbb{S}} \cup [\boldsymbol{\theta}]$, return;
4) If $w([\boldsymbol{\theta}]) \leq \eta, \overline{\mathbb{S}} := \overline{\mathbb{S}} \cup [\boldsymbol{\theta}]$;
   Else bisect $[\boldsymbol{\theta}]$ into $[\boldsymbol{\theta}_1]$ and $[\boldsymbol{\theta}_2]$;
5) SIVIA (in: $[t], [\boldsymbol{\theta}_1], \eta$; out: $\underline{\mathbb{S}}, \overline{\mathbb{S}}$);
6) SIVIA (in: $[t], [\boldsymbol{\theta}_2], \eta$; out: $\underline{\mathbb{S}}, \overline{\mathbb{S}}$).

Algorithm 1: The algorithm

The option in line 1 allows either to call the contractor or not at each execution of the SIVIA algorithm which complexity is known to be exponential!

E. Example

Consider the following transfer function having two differentiation orders.

$$F(s, \boldsymbol{\alpha}) = \frac{1}{s^{\alpha_2} + 2s^{\alpha_1} + 1}, \tag{21}$$

where $\boldsymbol{\alpha} = (\alpha_1, \alpha_2) \in \mathcal{A}_1 \times \mathcal{A}_2 \subset \mathbb{R}^2_{\geq 0}$, $\mathcal{A}_1$ and $\mathcal{A}_2$ define the searching domains. It can be analyzed by checking the position of the zeros of the characteristic function

$$f(s, \boldsymbol{\alpha}) = s^{\alpha_2} + 2s^{\alpha_1} + 1 \tag{22}$$

$$\bar{f}(\rho e^{j\theta}, \boldsymbol{\alpha}) = \rho^{\alpha_2} \cos(\theta\alpha_2) + 2\rho^{\alpha_1} \cos(\theta\alpha_1) + 1 + \mathrm{j}\,(\rho^{\alpha_2} \sin(\theta\alpha_2) + 2\rho^{\alpha_1} \sin(\theta\alpha_1)) \tag{23}$$

1) Implementing the forward-backward contractor on the system under study: A first contractor could be implemented, after the real part of $\bar{f}$:

$$\mathscr{R}e\{\bar{f}(\rho e^{j\theta}, \boldsymbol{\alpha})\} = 0 \Leftrightarrow \rho^{\alpha_2} \cos(\theta\alpha_2) + 1 = -2\rho^{\alpha_1} \cos(\theta\alpha_1) \tag{24}$$

A second one could also be implemented, after the imaginary part of $\bar{f}$:

$$\mathscr{I}m\{\bar{f}(\rho e^{j\theta}, \boldsymbol{\alpha})\} = 0 \Leftrightarrow \rho^{\alpha_2} \sin(\theta\alpha_2) = -2\rho^{\alpha_1} \sin(\theta\alpha_1) \tag{25}$$

However, handling sin and cos functions in each contractor is not an easy task because asin and acos functions return angles in their principal determination, i.e. between 0 and π for the acos, and between $-\frac{\pi}{2}$ and $\frac{\pi}{2}$ for the asin. In that case, care must be taken to set back the angles to the correct determination. Another alternative, is to combine (24) and (25) to obtain another contractor with less sin and cos functions. Such a contractor, named *combined contractor*, is obtained by squaring both equations and summing them up

$$\rho^{2\alpha_2} + 2\rho^{\alpha_2} \cos(\theta\alpha_2) + 1 = 4\rho^{2\alpha_1}. \tag{26}$$

```
function [x]=Comb_Contractor_Red(x)
 global nb_siv;
 xx = x;
 rho = x(1); theta = x(2);
 alpha1 = x(3); alpha2 = x(4);
%Forward
 x1 = rho^(2*alpha2);
 x2 = 2*rho^alpha2;
 x3 = theta*alpha2;
 x4 = cos(x3);
 x5 = x2*x4;
 x6 = x1 + x5 + 1;
 x7 = 4*rho^(2*alpha1);
%Backward
 x7    = intersect(x6, x7);
 alpha1= intersect(alpha1,1/2*log(x7/4)/log(rho));
 rho   = intersect(rho, (x7/4)^(1/(2*alpha1)));
 x6    = intersect(x6, x7);
 x5    = intersect(x5, x6 - x1 - 1);
 x2    = intersect(x2, x5/x4);
 alpha2= intersect(alpha2, log(x2/2)/log(rho));
 rho   = intersect(rho, (x2/2)^(1/alpha2));
 x1    = intersect(x1, x6 - x5 - 1);
 rho   = intersect(rho, x1^(1/(2*alpha2)));
 alpha2= intersect(alpha2, log(x1)/(2*log(rho)));

 x = [rho, theta, alpha1, alpha2];
 if any(isnan(x))
     x=xx;
 end
end
```

Fig. 1. The implementation of the combined contractor (26) using the IntLab toolbox [13] under Matlab.

A single cos function remains in (26) instead of two in the previous two contractors, which is easier to handle. This contractor is implemented in Fig.1, using the IntLab toolbox [13] under Matlab.

The algorithm is applied to the characteristic function (22), using four different initializations. In the first three, the problem (P2) is considered and in the fourth, the problem (P1) is treated.

2) First initialization: The initial searching box and tolerance are respectively set to:

$$\boldsymbol{\theta} = (\rho, \theta, \alpha_1, \alpha_2)^T \in [0,4] \times \left\{\frac{\pi}{2}\right\} \times [0,3] \times [0,4.5] \quad (27)$$

$$\eta = \text{diam}(\boldsymbol{\theta})/2^7 \quad (28)$$

where $\text{diam}(\boldsymbol{\theta})$ defines the length of each element of $(\boldsymbol{\theta})$.

The SIVIA algorithm is executed:

- without contractors (without step 1 in the algorithm). In this case the SIVIA function is called 13 543 times in 190 sec. The obtained outer enclosure $\overline{\mathbb{S}}$ is plotted in Fig.2.
- with the combined contractor (26) called at each step of the SIVIA algorithm (with step 1 in the algorithm). The SIVIA function is called 8 711 times in 296 sec. The obtained outer enclosure $\overline{\mathbb{S}}$ is plotted in Fig.3.

Moreover, the values at which the poles cross the imaginary axis correspond more or less exactly in both cased to the plot of Fig.4, which validates *a posteriori* that all the poles are inside the searching interval $\rho \in [0,4]$. In case some poles were touching the limit $\mathcal{R} = 4$, it would have been necessary to choose a bigger $\mathcal{R}$.

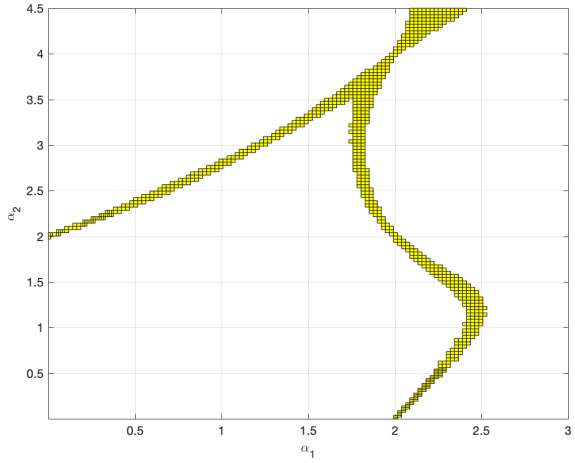

Fig. 2. First initialisation – Stability crossing sets obtained **without contractors**. Zeros of the characteristic function f which arguments equal $\frac{\pi}{2}$ are probably contained in the yellow boundary (outer enclosure $\overline{\mathbb{S}}$). The lower left region delimited by the yellow boundary represents the guaranteed stability region.

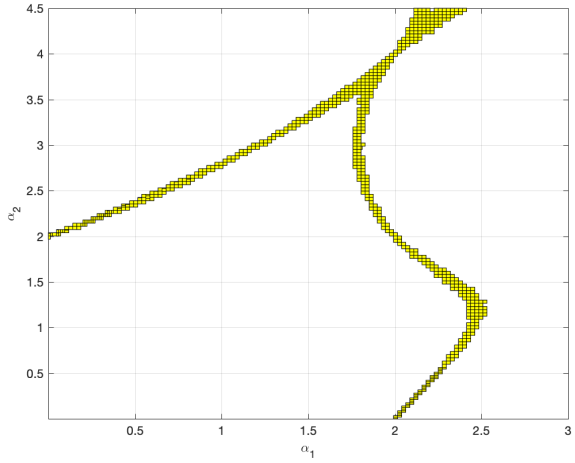

Fig. 3. The same as Fig.2, however **with contractors**.

As a conclusion, regarding this first initialization, the algorithm using the combined contractor is a little bit more precise for the same tolerance factor η. Execution speeds of both algorithms are comparable. The former as compared to the latter converges in a bigger number of iterations, however quicker, because the latter calls the contractor at each SIVIA iteration.

3) Second initialization: Let's search for the SCS by enlarging the searching domain. The initial box is now set to:

$$\boldsymbol{\theta} = (\rho, \theta, \alpha_1, \alpha_2)^T \in [0,4] \times \left\{\frac{\pi}{2}\right\} \times [0,15] \times [0,20] \quad (29)$$

The tolerance is defined as in (28), however applied to the new definition of the initial searching box.

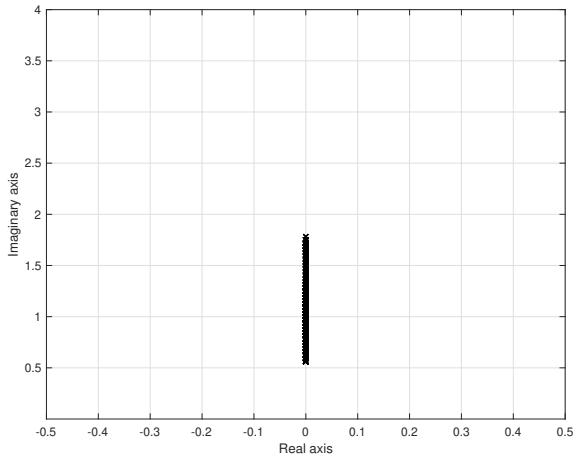

Fig. 4. First initialization – Zeros of the characteristic function $\bar{f}$ crossing the imaginary axis.

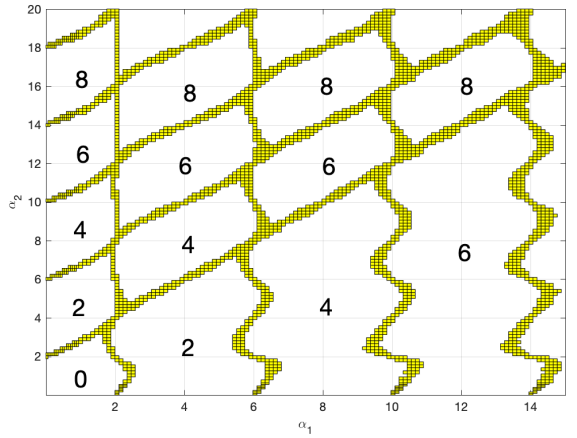

Fig. 5. Second initialization – Stability Crossing Sets (wider intervals as compared to Figs.2 and 3). The number of unstable poles is indicated in each region.

The SIVIA algorithm, without contractors, is called 73 037 times in 1 090 seconds. The obtained outer enclosure $\overline{\mathbb{S}}$ of the SCS is plotted in Figs 5, which indicates additionally the number of unstable poles, computed at integer values of the parametric points. Hence, all systems with parameters inside the different regions delimited by the SCS have the indicated number of poles. The intervals of poles look very much like the ones in Fig.4.

4) Third initialization: A major change is operated here. Instead of testing, the $\mathcal{CSP}$ defined in (12), a new $\mathcal{CSPN}$ is defined by enlarging the acceptable mapping of $\bar{f}(\rho e^{j\theta}, \boldsymbol{\alpha})$ to a square of size ϵ instead of a single point (the origine).

$$\mathcal{CSPN}: \begin{cases} -\epsilon \leq \mathscr{R}e\{\bar{f}(\rho e^{j\theta}, \boldsymbol{\alpha})\} \leq \epsilon, \\ -\epsilon \leq \mathscr{I}m\{\bar{f}(\rho e^{j\theta}, \boldsymbol{\alpha})\} \leq \epsilon, \\ 0 < \rho < \infty, \quad \theta \in \Theta, \\ 0 < \alpha_1 < \infty, \ 0 < \alpha_2 < \infty, \\ \epsilon = 0.1 \end{cases} \tag{30}$$

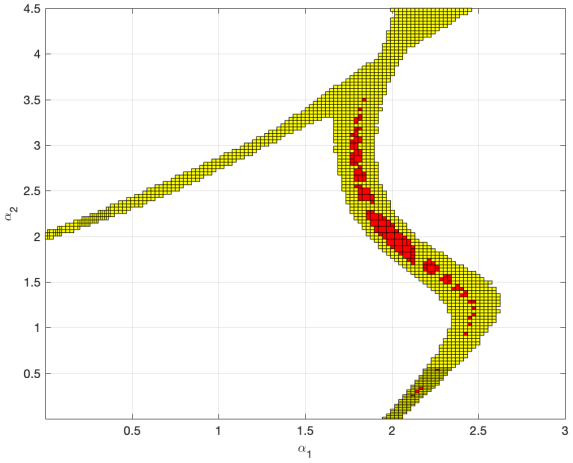

Fig. 6. Third initialization – Inner $\underline{\mathbb{S}}$ (in red), and Outer $\overline{\mathbb{S}}$ (in yellow) enclosures of the $\mathcal{CSPN}$ defined in (30)

Hence, instead of searching for the zeros of the characteristic function $\bar{f}$ in (22), the algorithm searches for intervals $[\boldsymbol{\theta}]$ that are mapped according to $\bar{f}$ inside a square of length ϵ. This is the usual way $\mathcal{CSP}$s are formulated. The same parameters and tolerance are chosen as in the first initialization in (27) and (28).

The results, obtained without contractors in 27 795 iterations and 443 sec, are plotted in Fig.9, where red and yellow parts indicate the inner and the outer enclosures $\underline{\mathbb{S}}$ and $\overline{\mathbb{S}}$ of (20).

It turns out not to be interesting to consider the $\mathcal{CSPN}$ (30) instead of the initial $\mathcal{CSP}$ (12), because it widens the feasible solution set as the square, of length ϵ, defining the admissible mapping gets wider.

5) Fourth initialization: In this part, the problem (P1) is solved. Hence, instead of looking for the stability crossing sets, let's look for all the zeros of $\bar{f}(\rho e^{j\theta}, \boldsymbol{\alpha})$ in the first quadrant. Consider the $\mathcal{CSP}$ in (12), and the following searching box:

$$\boldsymbol{\theta} = (\rho, \theta, \alpha_1, \alpha_2)^T \in [0, 4] \times \left[0, \frac{\pi}{2}\right] \times [0, 3] \times [0, 4.5] \tag{31}$$

When setting the tolerance to (28), the algorithm is stopped after an hour because of convergence issues. Then, the tolerance is augmented to:

$$\eta = \text{diam}(\boldsymbol{\theta})/2^4$$

The algorithm converges in 12 525 iterations and 194 sec. The obtained outer enclosure $\overline{\mathbb{S}}$ is plotted in Fig.7.

Apparently, the root-searching-domain in the first quadrant, is validated *a posteriori* in Fig.8: all the poles of the first quadrant are inside the searching domain, defined by $\rho \in [0, 4]$, when $(\alpha_1, \alpha_2) \in \times[0, 3] \times [0, 4.5]$.

Higher precision is definitely required to find out a better sketch of the stability region (in white).

However, this problem appears to be ill-posed as the $\mathcal{CSP}$ (12) evaluated for interval values of $[\boldsymbol{\theta}]$, can never be satisfied. A mapping of $[\boldsymbol{\theta}]$ with $\bar{f}$ is an interval that can never be a subset of $\{0\}$. Hence, in the instability region, the algorithm

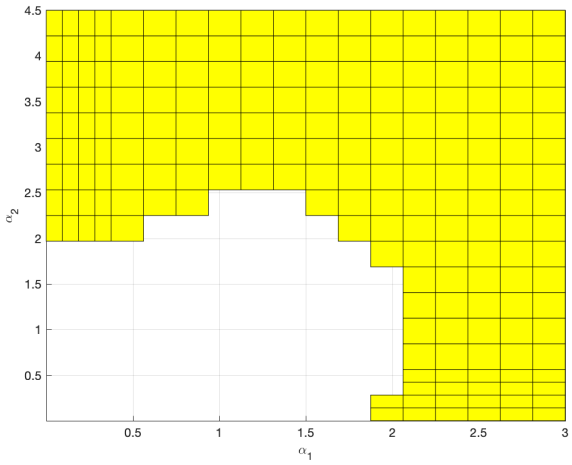

Fig. 7. Fourth initialization – Guaranteed stability in white and possible instability (outer enclosure $\overline{\mathbb{S}}$) in yellow

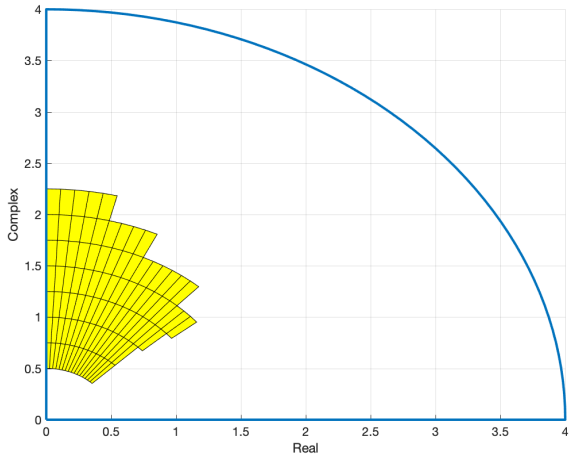

Fig. 8. Fourth initialization – Possible root location in yellow, searching domain boundary in blue

will keep bisecting, until reaching the precision η. It turns out that the time complexity of the SIVIA algorithm is higher than a brute-force search on boxes of elementary sizes η, which is not interesting.

As a conclusion of this part, it turns out that it is more interesting to solve the problem (P2) by looking for the stability crossing sets and deducing the stability regions.

III. Which norm for fractional systems?

This section of the paper contains results originally published in [2].

As mentioned previously, (4) is only a necessary condition. The system might be $\mathscr{L}_p$-stable and yet have an impulse response, f, with an infinite $\mathscr{L}_p$-norm $\forall p \in [1, \infty]$. The following theorem, proven in [2], states the existence conditions of the $\mathscr{L}_p$-norms.

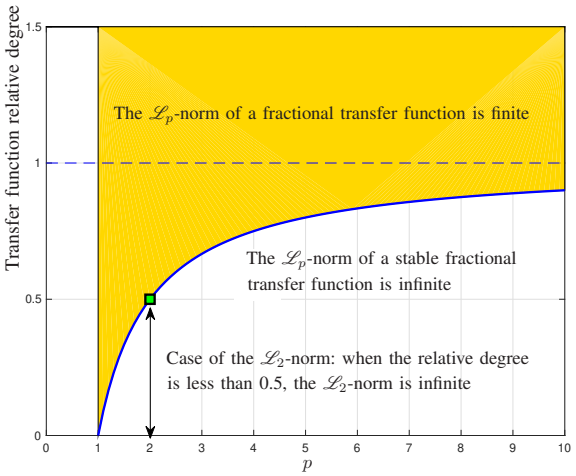

Fig. 9. Finiteness region of the $\mathscr{L}_p$-norm of fractional stable transfer functions in the relative-degree versus p plane. The border curve $(1 - \frac{1}{p})$ does not belong to the finiteness region.

Theorem 2. *Let a fractional transfer function as*

$$\tilde{F}(s) = \frac{F(s)}{s^{\mu}} \tag{32}$$

where $F(s)$, given by (1), is BIBO-stable and where $\mu \geq 0$. Numerator and denominator of $F(s)$ are assumed to be coprime (with no possible simplification between poles and zeros). Then, the $\mathscr{L}_p$-norm, $1 \leq p \leq \infty$, of the impulse response of $\tilde{F}(s)$ is finite if and only if the transfer function relative degree satisfies:

$$\mu + \alpha_N - \beta_M > 1 - \frac{1}{p} \tag{33}$$

and the integrator order satisfies:

$$0 < \mu < 1 - \frac{1}{p} \tag{34}$$

or

$$\mu = 0 \tag{35}$$

The yellow zone in Fig.9 shows finite combinations of $\mathscr{L}_p$-norms, in the plane relative-degree versus p. Similarly, the orange zone in Fig.10 shows finite combinations of $\mathscr{L}_p$-norms, in the plane integrator-order versus p.

Remarks:

- $\mathscr{L}_p$-norm finiteness conditions (33)-(34) are in accordance with the $\mathscr{L}_2$-norm finiteness conditions determined in [14].
- Equation (33) shows that all the $\mathscr{L}_p$-norms of rational systems, $\forall 1 \leq p \leq \infty$, are always finite because the relative degree is an integer at least equal to one (for a proper transfer function with no nonzero feedthrough gain). Additionally, (34) shows that the $\mathscr{L}_p$-norms, $\forall 1 \leq p \leq \infty$, are always infinite in presence of a rational integrator, with $\mu = 1$.
- A pure integrator $\frac{1}{s^{\mu}}$, $\forall \mu \in \mathbb{R}_{>0}$, has always an infinite $\mathscr{L}_p$-norm, $\forall 1 \leq p \leq \infty$, because conditions $\mu + \alpha_N -$

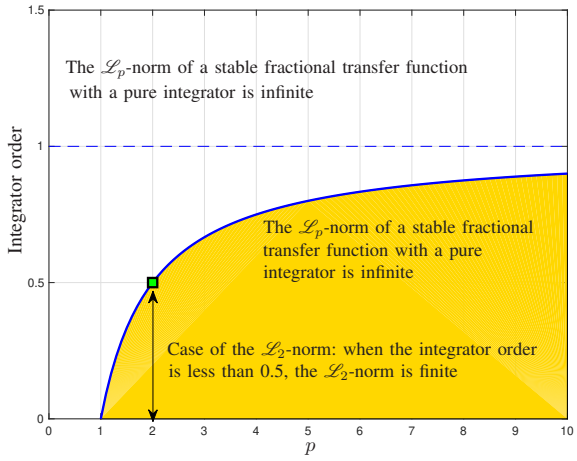

Fig. 10. Finiteness region of the $\mathscr{L}_p$-norm of fractional stable transfer functions in the integrator-order versus p plane. The border curve $(1-\frac{1}{p})$ does not belong to the finiteness region, except the point $(p=1, \mu=0)$ which does.

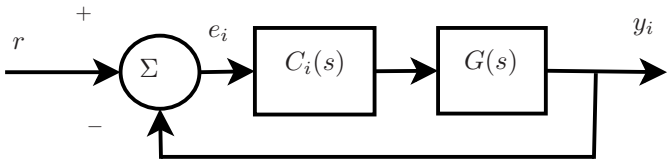

Fig. 11. A simple feedback control system structure

$\beta_M > (1-\frac{1}{p})$ and $\mu < (1-\frac{1}{p})$, cannot be satisfied simultaneously (here $\alpha_N = \beta_M = 0$) .

In the following example, the results are used to choose a proper criterion for evaluating performance of a feedback control loop.

IV. Example

This example is taken from [15, example 2]. Consider the simple feedback control system structure of Fig.11 and different fractional order PI controllers, with $i \in \{1,2,3,4\}$,

$$C_i(s) = K_{p_i} + \frac{K_{I_i}}{s^{\lambda_i}}, \tag{36}$$

which yield different closed-loop transfer functions:

$$T_i(s) = \frac{C_i(s)G_i(s)}{1+C_i(s)G_i(s)} \tag{37}$$

as reported in Table 1. Tavazoei (2010) evaluates numerically different integral performance indices among which the integral of absolute error (IAE) and the integral of squared error (ISE), on a step response. The IAE and ISE-indices are respectively the $\mathscr{L}_1$-norm and the $\mathscr{L}_2$-norm squared of the error signal $e_i(t)$ of Fig.11 (respectively $\|e_i\|_1$ and $\|e_i\|_2^2$) when the input $r(t)$ is a step:

$$E_i(s) = \frac{1}{s}(1-T_i(s)) \tag{38}$$

The $\mathscr{L}_2$-norm of $e_i(t)$ was also computed analytically in [14] and allowed to confirm the results announced in [15] regarding the ISE-index. In this paper, the $\mathscr{L}_4$-norm of $e_i(s)$ is additionally computed by numerical integration of the time-domain signals $e_i(t)$. The $\mathscr{L}_\infty$-norm is deduced easily.

Note that $E_1(s)$ has a proper integrator of order 0.2 and hence, according to (34), an infinite $\mathscr{L}_1$-norm and finite $\mathscr{L}_p$-norms for $p > 1.25$. Consequently, $\|e_i\|_2, \|e_i\|_4$, and $\|e_i\|_\infty$ are finite. $E_4(s)$ has a proper integrator of order 0.5 and hence infinite $\mathscr{L}_1$ and $\mathscr{L}_2$-norms. Additionally, [15] has evaluated other performance indices such as the *integral of time multiplied absolute error* (ITAE), the *integral of time multiplied squared error* (ITSE), and the *integral of squared of time multiplied error* (ITSE). All these performance indices were shown to be infinite for $E_4(s)$. No finite performance index has been proposed in [15] for evaluating the output feedback control law for $E_4(s)$. Theorem 2 and condition (34) show that the $\mathscr{L}_p$-norm is finite for all $p > 2$. Here, the $\mathscr{L}_4$-norm of the error signal can be used as a finite performance index of the output feedback control. For the remaining systems, $E_2(s)$ and $E_3(s)$ have no integrators, relative degrees greater than $(1-\frac{1}{p})$, stable $s^{0.5}$-poles, and hence finite $\mathscr{L}_p$-norms $\forall 1 \leq p \leq \infty$. Note that $\|e_i\|_\infty$ equals 1 for all i, because the step response always starts at $y_i(0) = 0$ and hence $\|e_i\|_\infty = e_i(0) = 1$. Consequently, the $\mathscr{L}_\infty$-norm is not, in this case, an interesting performance index.

V. Conclusions

This paper proposes an algorithm, based on interval arithmetics, for stability analysis of fractional transfer functions. Guaranteed stability region is determined in the parametric space. Two problems have been formulated and it has been shown that the problem of finding the parametric region for which the system is unstable is ill-posed because the bisection algorithm has a time-complexity worse than a brute-force search. However, the problem of finding stability crossing sets turns out to be very interesting, as it allows finding with a reasonable complexity, the stability crossing sets and hence deducing the whole stability region.

Having stable fractional transfer functions does not, however guarantee the existence of the $\mathscr{L}_p$-norms of its impulse response. Some additional conditions on its relative degree must be fulfilled. This helps choosing a performance criterion for feedback control loops.

The analytical computation of the $\mathscr{L}_2$-norm was proposed in [14] for commensurate systems only. A challanging task would be to extend this result to incommensurate systems.

References

[1] R. Malti, M. R. Rapaić, and V. Turkulov, "Stability analysis of incommensurate elementary fractional systems using interval arithmetics," in *International Conference on Fractional Differentiation and its Applications (ICFDA)*, Warsaw, Poland, 2021.

[2] R. Malti, "A note on L_p-norms of fractional systems," *Automatica*, vol. 49, no. 9, pp. 2923–2927, 2013. [Online]. Available: http://www.sciencedirect.com/science/article/pii/S0005109813003166

[3] K. Oldham and J. Spanier, "The replacement of Fick's laws by a formulation involving semi-differentiation," *Electro-anal. Chem. Interfacial Electrochem*, vol. 26, pp. 331–341, 1970.

[4] ——, *The fractionnal calculus - Theory and Applications of Differentiation and Integration to Arbitrary Order*. Academic Press, New-York and London, 1974.

i	$T_i(s)$	$E_i(s)$	$\|e_i\|_1$-IAE	$\|e_i\|_2^2$-ISE	$\|e_i\|_4^4$	$\|e_i\|_\infty$
1	$\frac{2s^{0.8}+1}{2s^{2.4}+s^{1.6}+s^{0.8}+1}$	$\frac{2s^{1.6}+s^{0.8}-1}{2s^{2.6}+s^{1.8}+s+s^{0.2}}$	∞	3.43	2.28	1
2	$\frac{2s^{1.6}+s^{0.8}+1}{2s^{2.4}+s^{1.6}+s^{0.8}+1}$	$\frac{2s^{1.4}-s^{0.6}}{2s^{2.4}+s^{1.6}+s^{0.8}+1}$	3.48	1.10	0.27	1
3	$\frac{s^{1.6}+s^{0.8}+1}{2s^{2.4}+s^{1.6}+s^{0.8}+1}$	$\frac{2s^{1.4}}{2s^{2.4}+s^{1.6}+s^{0.8}+1}$	3.32	1.11	0.35	1
4	$\frac{2s^{0.5}+1}{2s^{1.5}+s+s^{0.5}+1}$	$\frac{2s+s^{0.5}-1}{2s^{2}+s^{1.5}+s+s^{0.5}}$	∞	∞	0.27	1

TABLE I

$\mathscr{L}_1, \mathscr{L}_2, \mathscr{L}_4$, AND $\mathscr{L}_\infty$,-NORMS OF $e_i(t)$ FOR DIFFERENT OUTPUT FEEDBACK CONTROL SYSTEMS TAKEN FROM (TAVAZOEI, 2010, EXAMPLE 2).

[5] D. Matignon, "Stability properties for generalized fractional differential systems," *ESAIM proceedings - Systèmes Différentiels Fractionnaires - Modèles, Méthodes et Applications*, vol. 5, 1998.

[6] R. Malti, X. Moreau, F. Khemane, and A. Oustaloup, "Stability and resonance conditions of elementary fractional transfer functions," *Automatica*, vol. 47, no. 11, pp. 2462–2467, 2011.

[7] C. Hwang and Y.-C. Cheng, "A numerical algorithm for stability testing of fractional delay systems," *Automatica*, vol. 42, no. 5, pp. 825 – 831, 2006.

[8] J. Trigeassou, A. Benchellal, N. Maamri, and T. Poinot, "A frequency approach to the stability of fractional differential equations," *Transactions on Systems, Signals & Devices (TSSD)*, vol. 4, no. 1, pp. 1 – 25, 2009.

[9] C. Bonnet and J. Partington, "Coprime factorizations and stability of fractional differential systems," *Systems & Control Letters*, vol. 41, no. 3, pp. 167 – 174, 2000.

[10] R. Moore, *Interval analysis*. Englewood Cliffs, NJ: Prentice-Hall, 1966.

[11] L. Jaulin, M. Kieffer, O. Didrit, and E. Walter, *Applied interval analysis*. London: Springer-Verlag, 2001.

[12] L. Jaulin and E. Walter, "Set inversion via interval analysis for nonlinear bounded-error estimation," *Automatica*, vol. 29, no. 4, pp. 1053–1064, 1993.

[13] S. Rump, *Developments in reliable computing*. Kluwer academic publisher, 1999, ch. IntLab – Interval laboratory, pp. 77–104.

[14] R. Malti, M. Aoun, F. Levron, and A. Oustaloup, "Analytical computation of the H_2-norm of fractional commensurate transfer functions," *Automatica*, vol. 47, no. 11, pp. 2425–2432, 2011.

[15] M. Tavazoei, "Notes on integral performance indices in fractional-order control systems," *Journal of Process Control*, vol. 20, no. 3, pp. 285 – 291, 2010. [Online]. Available: http://www.sciencedirect.com/science/article/B6V4N-4XHC6CK-1/2/20d020ac73210cb2ce6f0f6ab89e92e2

Application of cascade control in the process of flue gas desulfurization of thermal power plant

Goran Kvascev, Zeljko Djurovic, Avram Avramovic

***Abstract*—The paper presents the use of cascade control for the needs of an efficient flue-gas desulphurization process in the thermal power plant TE KO Drmno. A system for reducing the content of sulfur oxides (SO2) in flue exhaust gases - desulphurization has been implemented within two thermal power plants units. The technological process, control structure, implementation of cascade control, and plant operation results are presented. By applying the proposed control structure, the efficient operation is achieved of the entire system in terms of the regulations of the European Commission in terms of emissions of sulfur oxides and particles, but also electricity consumption and energy efficiency. The goals that the plant was supposed to meet were achieved, as well as the economic justification of the entire project.**

***Index Terms*— Flue-gas desulphurization, thermal power plant, cascade control**

I. Introduction

In the Republic of Serbia, within the PE "Electric Power Industry of Serbia" (EPS), 34,896 GWh of electricity is produced annually, based on ten-year average. The electricity generation capacities owned by EPS have a total capacity of 7,855 MW and consist of 22 thermoblocks, 49 hydro units, and one reversible hydro power plant with 2 units. About 70% of production comes from thermal power plants and about 30% from hydropower plants. As fuel in thermal power plants, coal from surface mines is mostly used, i.e. lignite, whose average annual production ranges from 37 to 40 million tons of coal.

Lignite is a solid fuel that contains a high percentage of sulfur. Combustion of sulfur-containing fuel produces sulfur dioxide SO_2, as a dominant product of its oxidation, and sulfur trioxide SO_3 (in the amount of several percent of SO_2), as well as other oxides sulfur, which have no greater significance. Sulfur oxides SO_2 and SO_3 have been recognized as the most common and most dangerous gases of anthropogenic origin, with a serious negative impact on human health and vegetation, primarily creating acid rain. Therefore, it is of special interest to reduce the emission limit values (ELVs) of sulfur oxides to an acceptable level, which will not be harmful to the environment and the health of the population.

Goran Kvaščev is with the University of Belgrade, School of Electrical Engineering, Bulevar kralja Aleksandra 73, 11120 Belgrade, Serbia (e-mail: kvascev@etf.bg.ac.rs)

Željko Đurović is with the University of Belgrade, School of Electrical Engineering, , Bulevar kralja Aleksandra 73, 11120 Belgrade, Serbia (e-mail: zdjurovic@etf.bg.ac.rs)

Avram Avramovic is with the TE DRMNO - Kostolac, Serbia (e-mail: avram.avramovic@te-ko.rs)

In the Republic of Serbia, based on our conditions, ELVs are defined by several criteria:

- whether plants are fired by solid, liquid, or gaseous fuels,
- whether plants are small, medium, or large (in terms of power),
- whether plants are old or new.

In the Republic of Serbia, based on: "Uredba o graničnim vrednostima emisija zagađujućih materija u vazduhu iz postrojenja za sagorevanje" ("Sl. glasnik RS", br. 6/2016) [1], the emission limit values, ELVs, for sulfur dioxide are expressed in mg/normal m^3 as function of power of plant, and which are applied to old plants, are given in the Figure 1.

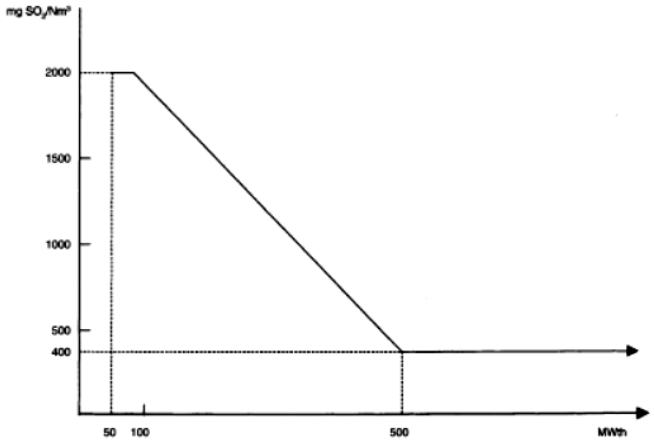

Fig. 1. Emission limit values, ELVs, for sulfur dioxide in mg/normal m3, which are applied to old plants as function of power of power plant

For plants with a thermal power of 100 to 500 MWth, the emission limit values for sulfur dioxide are calculated according to:

$$y = -4x + 2400$$

where: x - thermal power of the plant (MWth), y - emission limit value for SO_2 (mg SO_2/normal m^3).

For plants with a thermal power of more than 500 MWth, a desulphurization rate of at least 94% must be achieved.

On the other hand, observing the *National Plan for the Reduction of Emissions of Major Pollutants from Old Large Combustion Plants* [2] (*Nacionalni plan za smanjenje emisija*

glavnih zagađujućih materija koje potiču iz starih velikih postrojenja za sagorevanje), which clearly defines the maximum emissions of sulfur oxides, it is clear that these goals have not yet been achieved. If we take as an example the TE KO Drmno B1/B2 units, for which the maximum emission of 7,957.03 tons per year is defined according to the plan [2], and compare with the data that over 95,000 tons of SO_2 were emitted during the previous year, it is clear that it is necessary to provide a plant for processing sulfur oxides, i.e. flue-gas desulphurization system. Such a system has been put into operation during the past period. Tests, final adjustments of control loops, and obtaining the necessary approvals for work are in progress.

II. Flue-gas desulphurization TE KO Drmno

According to the conclusions of the Study "*Directions of optimal reduction of sulfur oxide emissions from thermal power plants of the Electric Power Industry of Serbia*" [3], TE KO Drmo B1/B2 was chosen as the first thermal power plant where the construction of such a plant is planned. The flue gas desulphurization plant in TE KO Drmno is the first desulphurization system in Serbia to be operational, and it started operating on October 23, 2020. Based on previously accepted analyzes, the wet limestone / gypsum process was defined as the reference desulphurization process.

Process Overview

The process of flue gas desulfurization consists of several chemical processes that are essential for understanding and applying the control system, which is presented in Figure 2:

- The SO_2 in the flue gas is absorbed into the circulating slurry
- Circulating slurry containing calcium sulfate ($CaSO_4$) and precipitated limestone
- Add some limestone into absorb to supply alkalinity and calcium ions (Ca ++) source
- Add air into absorb for Oxidized SO_2 to sulphate (SO_4).
- Solution sulfate ion and calcium ion reaction precipitated gypsum ($CaSO_4 * 2H_2O$)
- The precipitated gypsum is separated from the slurry water is removed. This results in solid by-product from the process. Slurry liquid return.

The process schematic is shown in Figure 3, which shows the thermal power plant that was upgraded by the flue-gas desulphurization subsystem, and which consists of three main parts:

- Absorber – within which the process of Absorption, Oxidation, and Neutralization (shown in Figure 2) takes place
- Absorbers preparation
- Gypsum dehydration

The most important process takes place in the Absorber, where the main control structures are located. It is necessary to control the flow of an absorber with the control valve in order to make chemical reaction to be successful and efficient. This can be achieved by adding limestone into the absorber to ensure alkalinity. Constant alkalinity produces a successful and efficient flue-gas desulphurization process. As the absorber system is large in volume, and the time constants are also large (on the order of 15 minutes), it is extremely important to accurately add limestone slurry. This is main task for the control system, to work efficiently and precisely. For this control structure, cascade control is proposed, with the outer loop according to alkalinity (with reference pH value), and an inner loop for control of a flow of limestone slurry.

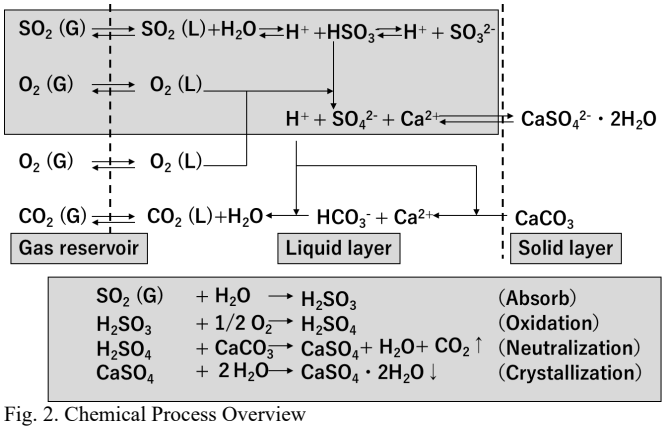

Fig. 2. Chemical Process Overview

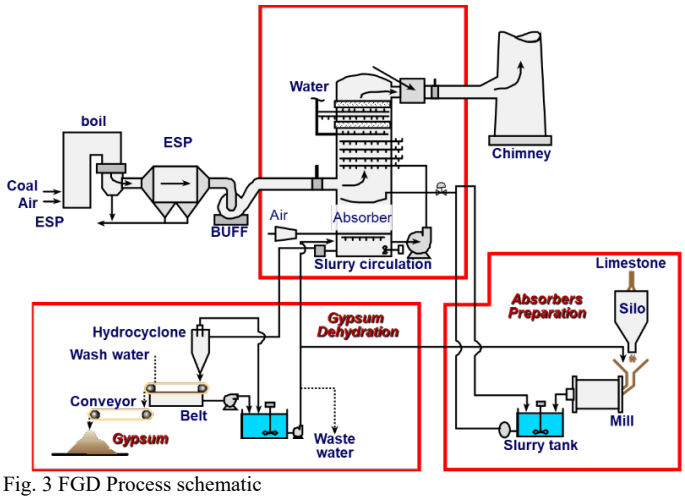

Fig. 3 FGD Process schematic

Figure 4 shows a process flow diagram (PFD):

- flue gases: when the flue gas system is running: VDG → ODG inlet valves → Buster fan → Absorber → New chimney
- flue gases: when the flue gas system is not working: VDG → Bypass valves → Old chimney
- air: when the air sealing system is running: Air sealing fan → Heater → Valve closed
- process water: when the process of flushing the absorber inlet with water in case of emergency is in progress: Process water tank → Flushing water pump in case of emergency → Flushing water tank → Flue gas duct spraying

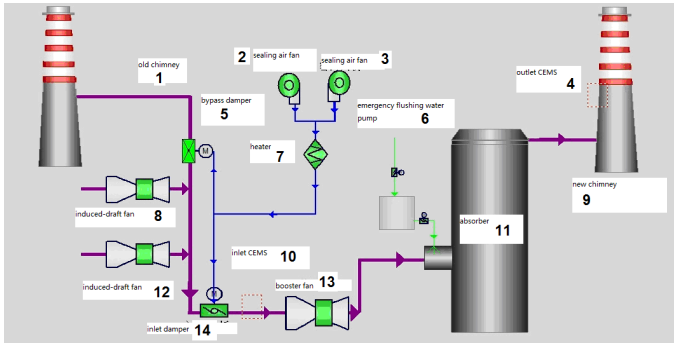

Fig. 4 Process flow diagram, 1-old chimney, 2,3-sealing fans, 4-outlet CEMS, 5-bypass damper, 6-emergency flushing water pump, 7-heater, 8,12-induced-draft fans, 9-new chimney, 10-inlet CEMS, 11-absorber, 13-booster fan, 14-inlet damper

III. CONTROL LOOPS

Figure 5 shows the simplified P&I diagram shown on DCS SCADA system - Absorber picture. Measurements, state of actuators (valves, pumps, and actuators), as well as controls within control loops are presented. Control valve (measured position: 2TJ39S001) is responsible for alkalinity (pH measurement marked as 2TD40A001 and 2TD40A002). The flow of liquid limestone slurry through this pipe is marked as 2TJ39F001. As the system for measuring the pH value needs to be maintained at regular time intervals, a double measurement is planned, so the value of one probe is taken as main and another as spare, which gives a regular measurement in full time.

Within this research, a cascade control structure was proposed, with the use of PI / PID controllers, shown in Figure 6. Simpler control procedures did not give satisfactory results, observing a testing period of 6 months.

Cascade control structure consists of two loops:

- The outer loop controls the alkalinity (pH value) of the PID controller - the pH value is controlled by setting the flow of the internal PI controller. Alkalinity measurements is achieved by sensors
- Internal PI control loop - controls the reference flow from the outer loop through control valve 2TJ39S001, and measured flow of limestone slurry – 2TJ39F001

PI/PID controllers are tuned using the SRT method [4], measuring the response in the open loop in the nominal mode of plant. In the first version, the control of the PID controller in the external loop was set without differential action, however, after testing, it was necessary to introduce significant differential action for two reasons: faster elimination of disturbances and problems due to jamming of the control valve due to longer periods without moving the actuator.

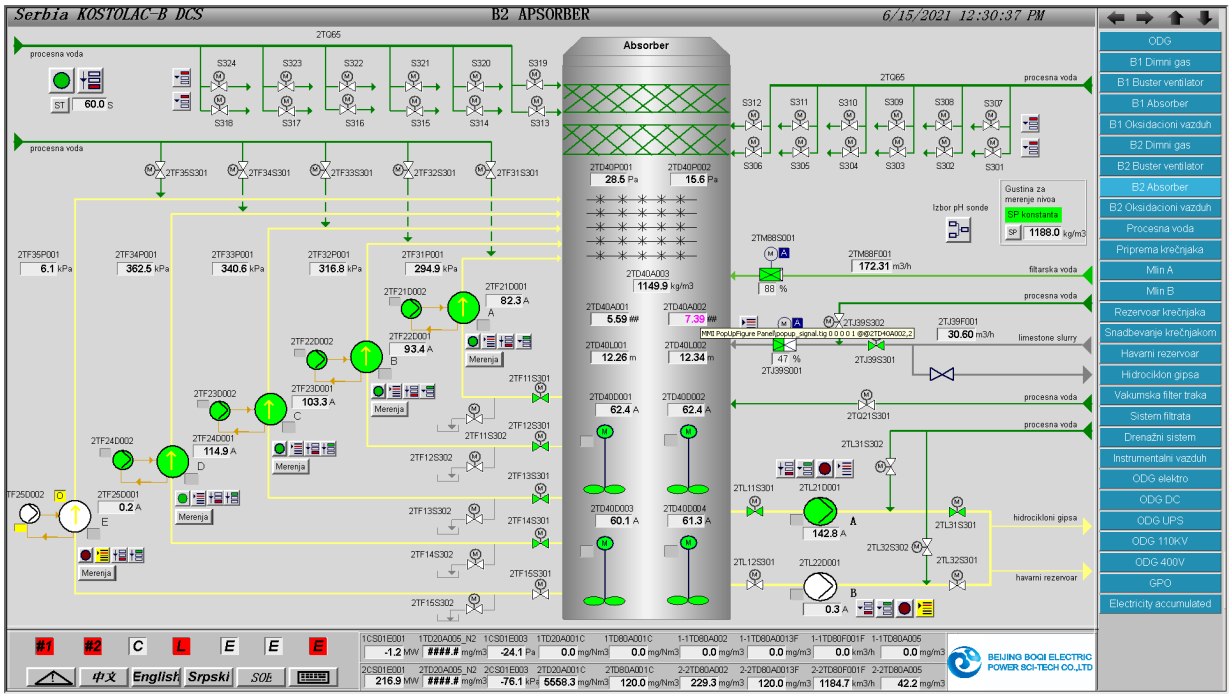

Fig. 5 SCADA control system – P&I diagram

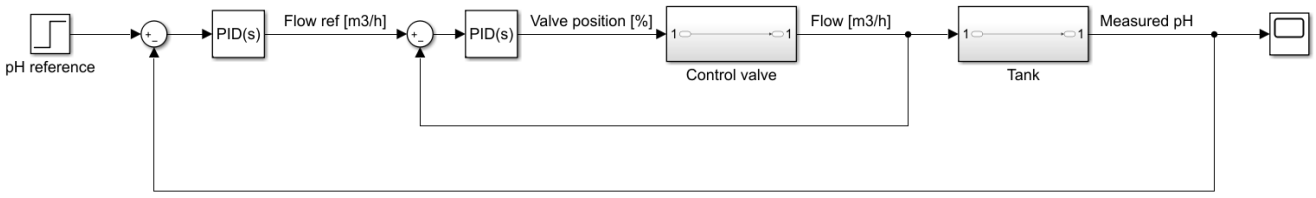

Fig. 6 Proposed cascade control structure

IV. Main Results

Figures 7 and 8 show the measurements from the plant after the final testing in the nominal regime. Figure 7 shows satisfactory results of control the alkalinity (pH value) with a rise time of about 10 minutes with a step change of the reference value. The measured flow in inner loop is almost same as flow reference.

Observing the measured values in the real environment, it can be concluded that the control of the plant operates within the specified standards. The emission of sulfur oxides SO_2 does not exceed the value of 250 mg/Nm^3, measured in 24 hours time range. Considering that the inlet concentration of SO_2 is in the range of about 5000mg/Nm^3, it can be confirmed that the efficiency of the desulfurization process is more then 99%.

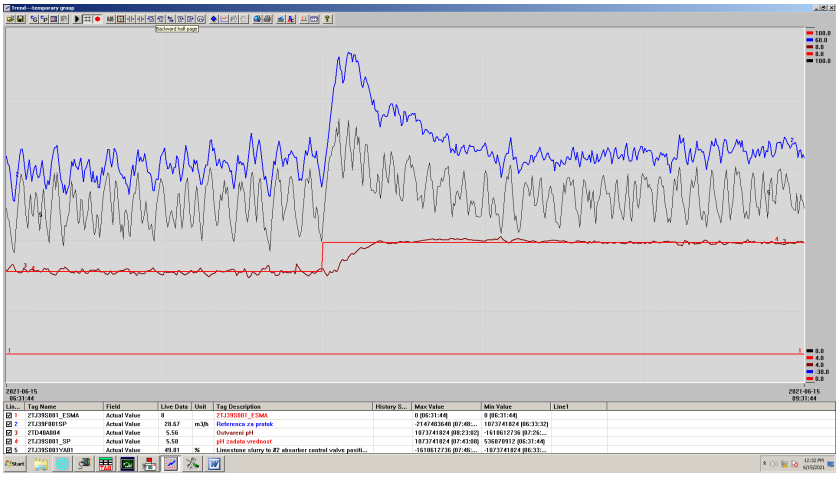

Fig. 7. Control performance pH control loops - 3h time scale: pH reference value – red color, pH measured value – brown color, flow reference – blue color, valve position – gray color

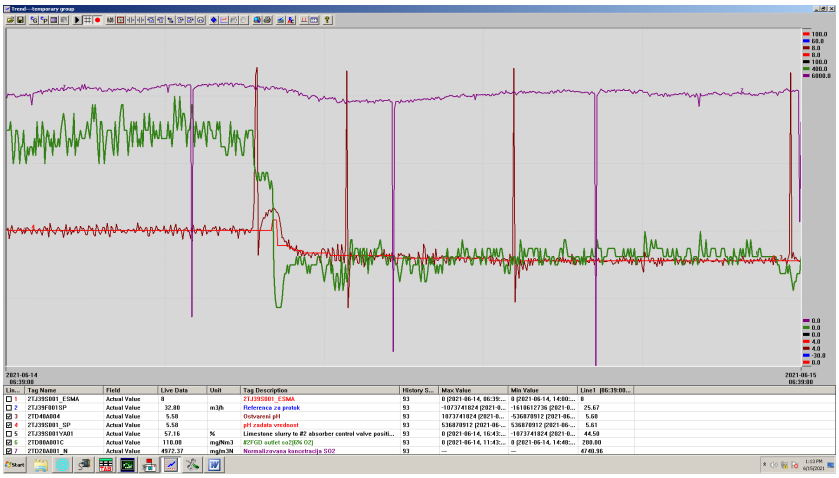

Fig. 8 Control performance of Absorber unit - 24hours time scale: pH reference value – red, pH measured value – brown, SO_2 inlet concentration [mg/Nm^3] – violet, SO_2 outlet concentration [mg/Nm^3] – green

V. Conclusion

The paper presents the application of the cascade control structure of desulphurization in the thermal power plant TE KO Drmno. By applying the proposed control structure, the efficient operation of the entire system was achieved in terms of meeting the regulations of the European Commission, which is shown through the data obtained in the actual operation of the plant. Possible improvements consist of the introduction of feedforward control depending on the boiler load, as well as the measured input values of sulfur oxide.

Acknowledgment

This research was supported by the Ministry of Education, Science and Technological Development of the Republic of Serbia.

References

[1] Uredba "*O graničnim vrednostima emisija zagađujućih materija u vazduh iz postrojenja za sagorevanje*", ("sl. Glasnik rs", br. 6/2016)

[2] Nacionalni plan za smanjenje emisija glavnih zagađujućih materija koje potiču iz starih velikih postrojenja za sagorevanje, "*Službeni glasnik RS*", broj 10 od 6. februara 2020.

[3] "*Pravci optimalnog smanjenja emisija sumpornih oksida iz termoelektrana EPS-a*" – studija, JP EPS, 2006

[4] M. R. Mataušek, G. S. Kvaščev „*A unified step response procedure for autotuning of PI controller and Smith predictor for stable processes*", Journal of Process Control, vol 13, pp. 787-800, 2003.